SUSTAINABLE SOLUTION TO RECYCLED CONCRETE: IMPROVING STRUCTURAL APPLICATIONS

A Dissertation
Presented to
The Academic Faculty

by

La Sasha Walker

In Partial Fulfillment
Of the Requirements for the Degree
Doctor of Philosophy in the
School of Civil and Environmental Engineering

Georgia Institute of Technology

May 2018

SUSTAINABLE SOLUTION TO RECYCLED CONCRETE: IMPROVING STRUCTURAL APPLICATIONS

Approved by:

Dr. Reginald DesRoches, Advisor
School of Civil and Environmental Engineering
Rice University

Dr. Susan Burns
School of Civil and Environmental Engineering
Georgia Institute of Technology

Dr. Kimberly Kurtis, Advisor
School of Civil and Environmental Engineering
Georgia Institute of Technology

Dr. Russell Gentry
School of Architecture
Georgia Institute of Technology

Dr. Larry Kahn
School of Civil and Environmental Engineering
Georgia Institute of Technology

Date Approved: March 28, 2018

ACKNOWLEDGEMENTS

I extend thanks to all my supporters throughout the many years of my educational journey. My journey is not complete—merely starting a new chapter. I thank my advisors, Dr. Kimberly Kurtis and Dr. Reginald DesRoches, for their direction and support. Throughout these past five years, their guidance has enlightened and pushed me to become a better researcher, scientist, and educator. I also thank my committee members, Dr. Susan Burns, Dr. Russell Gentry, and Dr. Kahn, for their support, time, and advice. Their insights made my research more diverse.

I gratefully acknowledge my funding. This research was funded by a National Science Foundation Graduate Research Fellowship under grant NO. DGE-1148903, and additional funds were provided by my advisors. I am thankful for the additional financial support of Georgia Institute of Technology.

I thank all my wonderful and strong undergraduate research assistants: Tamera Flowers, Sean Donovan, Suraj Sanghani, Ji Yoon Oh, Camila Bergamo, and James Rowe. They have put in many hours alongside me, making tons of concrete. I give a special thanks to Jeremy Mitchell. He gave me immeasurable guidance while working in the structures lab.

I acknowledge and thank the many past and present group members during these five years in the groups of both Dr. Kurtis and Dr. DesRoches: Dr. Nan Gao, Dr. Mehdi Rashidi, Dr. Elizabeth Nadelman, Dr. Behnaz Zaribaf, Dr. Bradley Dolphyn, Dr. Álvaro Paul, Dr. Chris Shearer, Dr. Nathan Mayercsik, Dr. Lisa Burris, Dr. Giovanni Loreto, Dr. Gun Kim, Dr. Jong-Su Jeon, Dr. Farahnaz Soleimani, Dr. Sujith Mangalathu, Prasanth Alapati, Natalia Cardelino, Cole Spencer, Qingxu ‘Bill’ Jin, Scotty Howard, Danial Benkeser, Leonidas

Emmenegger, Francesca Lolli, Ahmad Shalan, and unofficial group member Daniela Estrada. Special thanks to them for lending their ears and time, as well as their friendship. In addition, I thank them for the fun group outings of salsa dancing, watching movies, and trying international cuisines.

Finally, I thank my family. They supported me through thick and thin, including my many ups and downs during my PhD program. Without my family's support, I would not have made it this far. With their love and support, I know my next chapter will be better than the last!

TABLE OF CONTENTS

LIST OF TABLES

LIST OF FIGURES

LIST OF SYMBOLS AND ABBREVIATIONS

α_t	Approximate hydration of anhydrous cement
σ_i	Conductivity of charged species
A	Oven-dried aggregate weight
Al_2O_3	Aluminum oxide
AASHTO	American Association of State Highway and Transportation Officials
ACI	American Concrete Institute
ASR	Alkali-Silica Reaction
ASTM	American Society for Testing and Materials
B	Weight of aggregate at saturated surface dry conditions
b	Width of specimen
C	Weight of aggregate submerged in water
c	Chloride content
CaO	Calcium oxide
C&D	Construction and demolition
CH	Calcium hydroxide
CSH	Calcium silicate hydrate
d	Depth of specimen
Da	Apparent diffusion coefficient
DCP	Dehydrated cement paste
DTG	Differential thermogravimetric analysis
DVM	Direct volume replacement
DWM	Direct weight replacement

E	Modulus of Elasticity
EMR	Equivalent Mortar Replacement
EMV	Equivalent Mortar Volume
EPA	Environmental Protection Agency
f'c	Compressive strength of concrete
FA	Fly ash
FM	Fineness Modulus
FRCA	Recycled Concrete Aggregate Fines
GAB	Graded Aggregate Base
GDOT	Georgia Department of Transportation
H	Hydrogen
ITZ	Interfacial Transitional Zone
K_i	Constant based on temperature of porous medium, charge and concentration
L	Length of specimen
LA abrasion Test	Los Angeles abrasion test
M[i]	Molecular weight of compound i
MCFT	Modified compression field theory
MSA	Maximum size aggregate
NA	Natural Aggregate
NAC	Natural Aggregate Concrete
OPC	Ordinary Portland Cement
P	Maximum load
PA	Presoaked Aggregate
PSD	Particle size distribution

psi	Pounds per square inch
Qt	Cumulative heat of hydration at time, t
QP	Quartz powder
R	Gas constant
RA	Reactive aggregate
RAC	Recycled aggregate concrete
RCA	Recycled concrete aggregate
RCPT	Rapid Chloride Penetration Test
SiO_2	Silicon dioxide
SG_i	Specific gravity of specimen i
SCM	Supplementary cementitious materials
SSA	Specific surface area
SSD	Saturated surface dry
T	Absolute temperature
TGA	Thermalgravimetric analysis
TM	Triple mixing method
TSMA	Two-stage mixing approach
U	Activitation energy
w_i	Initial weight of oven-dried aggregate
w_c	Unit weight of concrete
W_f	Final weight of oven-dried “natural aggregate”
w_T	Weight at temperature, T
w/b ratio	Water-to-binder ratio
w/cm	Water-to- cementitious materials
XRD	X-ray Diffraction

SUMMARY

Construction and demolition (C&D) or debris concrete is an underutilized resource often landfilled or recycled as a non-structural fill material. This study's main objective is to examine the potential to expand reuse options for recycling concrete, specifically for use in structural applications. In 2014, the United States landfilled approximately 375 million tons of concrete, some of which could have been diverted to offset the 1 billion tons of stone aggregate produced that same year. Thus, expanding productive reuse options for debris concrete can be an important contribution to sustainability.

This study will address the knowledge gaps surrounding expanding utilization of recycled concrete in structural concrete by focusing on two main aspects: (1) use of recycled concrete aggregate (RCA) as replacement of coarse aggregate in structural concrete, and (2) use of recycled concrete fines as partial replacement of cement. On the structural scale, locally sourced recycled concrete was used as 100% of the coarse aggregate in the recycled aggregate concrete (RAC), and the influence of maximum size aggregate was assessed in shear and flexure. The durability of recycled aggregate concrete was assessed through measures of permeability, resistance to alkali–silica reaction, and service life modeling of structural elements in chloride-rich environments, all in comparison to companion concrete using natural coarse aggregate. The potential use of recycled concrete fines, smaller than 74μm, as a supplementary cementitious material or as filler at 20% by replacement of cement was explored. To increase the reactivity of recycled concrete fines, several techniques were used to activate the fines, including calcining and ball milling.

The recycled aggregate concretes produced exhibited comparable strength and durability comparable to natural aggregate concrete at 100% replacement of coarse aggregate. Recycled aggregate concrete in comparison to natural aggregate concrete at the same maximum size aggregate had -9% to 3%, -0.5 to 2.5%, -15% to 6.9% difference in compressive strength of 6 ksi at 28 days, flexural strength of 780 psi at 28 days, and shear strength of 800 psi at 28 day, respectively. Both natural aggregate concrete and recycled aggregate concrete had high to moderate permeability level. Maximum aggregate had negotiable effect on the performance of recycled concrete aggregate. Nevertheless, of the three maximum size aggregates tested in general 0.75-inch best structural performance. Thermogravimetric analysis show that recycled concrete fines do not exhibit pozzolanic reactivity and instead act as filler in cement systems. Activation techniques did enhance the reactivity of recycled concrete fines, as assessed through examination cement hydration kinetics and these improvements were linked to increases in surface area, reductions in impurities, and modified chemical composition. Of the methods explored calcining at 750°C produced the most reactive fines. This work demonstrates that, with proper mix design, recycled concrete can be used as coarse aggregate – at 100% rate of aggregate replacement – and as SCMs or fillers – at 20% rate of cement replacement – in structural concrete.

CHAPTER 1. INTRODUCTION

1.1 Motivation

The majority of construction and demolition (C&D) waste will not naturally decompose because it is inorganic. Therefore, a large amount of land is required to store the 1.5 Bt of C&D waste generated each year, which is unsustainable. C&D landfill material is composed of a combination of concrete, asphalt concrete, wood products, asphalt shingles, drywall and plaster, brick and tile, and steel and other metals. In the United States, prior to recycling, 70% of the C&D waste produced by mass is concrete [*1*]. In comparison, countries such as Japan, Taipei, and The Netherlands have nearly complete recycling of C&D concrete [*2*]. In the U.S., 95% of landfilled concrete comes from demolition, and only 5% is waste concrete from construction of roadways and bridges, roads, and other structures, including utilities and manufacturing infrastructures [*1*].

However, in the U.S., only 60% of the concrete debris is recycled, and of that percentage only 6% is incorporated in new concrete [*3*]. Recycled concrete aggregate accounts for 6%–8% of aggregate used in Europe and 5% in the U.S. [*2*]. Often, the new concrete is low-strength concrete, such as that used for pavements or driveways. There are several cases worldwide where RCA has been used in structural concrete, such as Germany Waldspriale high-rise residential complex in 1998 [2, 4] and Hong Kong Wetland Park in 2000 [5]. Hong Kong Wetland Park used 100% of RCA as coarse aggregate for low strength concrete and 20% RCA for high strength concrete. In 2014, the U.S. landfilled approximately 375 million tons of concrete, some of which could have been diverted to offset the 1 billion tons of stone aggregate produced that same year.

1.2 Background

The current usage of recycled concrete is mostly for roadway construction, e.g., road sub-base and surface, landscaping, and low-strength concrete [2, 6]. In fact, the majority of recycled concrete aggregate (RCA) is used in roadway construction, where it has advantages over virgin aggregate as a base or subbase material due to its self-cementing properties. In the United States, 41 of 50 states use recycled concrete as coarse aggregate, and primarily as road base material [2, 7]. However, only 11 states use RCA in concrete, and, of those 11 states, only 3 states use RCA in concrete pavements [7]. This limited usage is due to the potential for increased shrinkage and creep of recycled aggregate concrete (RAC).

1.3 Objective Statement

Research and application of RCA have been active since the 1950s, with investigations into the material characteristics, mechanical properties, durability of RAC, as well as preventative measures to enhance the performance of RCA. However, limited research has examined the impacts of maximum size aggregate as terms of mortar fraction on mechanical performance and durability of RAC or on the use of RCA fines (FRCA) for partial replacement of cement. Therefore, the contributions of this research effort to the field are toward expanding reuse options for recycled concrete aggregate by focusing on: (1) the potential use of fines, resulting from crushing debris concrete, as an alternative supplementary cementitious material (SCM) or filler; and (2) the potential use of recycled concrete as complete replacement of coarse aggregates in structural concrete. This research contributes to body of knowledge as the one of the first to study to investigate the effects

of MSA with local commercially manufactured RCAs in terms of mechanical and durability properties of RAC at 100% replacement of coarse aggregate for structural concrete. As well as, furthering the body of knowledge in terms of studying the cementitious nature of FRCA.

Throughout the next six chapters, the discussion focuses on potential uses of RCA in structural concrete. Chapter 2 presents the current literature on RCA, first examining the process of manufacturing RCA, then discussing the material properties of the RCA, followed by the impacts of RCA in concrete, and concluding with the reactivity of RCA fines. The next four chapters follow a similar pattern, presenting results and discussion regarding the material properties of RCA, the mechanical properties and durability of RAC, and the reactivity and properties of FRCA. The final chapter presents conclusions, recommendations, and suggested future work.

CHAPTER 2. LITERATURE REVIEW

This chapter examines the current literature involving recycled concrete aggregate. The first part of the literature review focuses on recycled concrete aggregate as a material, and the discussion includes manufacturing of RCA, physical and mechanical properties of RCA compared to natural aggregate (NA), current standards, and limitations. The second section focuses on RCA incorporated in concrete as partial or complete replacement of coarse NA. Furthermore, these sections include a discussion of the interfacial transitional zone (ITZ), mix design approaches, water absorption and workability, porosity and permeability, mechanical properties, durability, and sustainability. The final section discusses the potential uses for RCA fines as an alternative supplementary material.

2.1 Recycled Concrete Aggregate

2.1.1 Manufacturing of Recycled Concrete Aggregate

The production of RCA often involves several steps of crushing and monitoring for quality control. The quality of RCA depends on the production methods, as well as the initial material, and quantity of impurities, including but not limited to dirt, clay, wood, and metal. These impurities are often minimized by several screening and monitoring steps, such as use of magnetics to remove metals, air blowing to limit fines, and visual inspection. These screening, monitoring, and secondary crusher steps are often skipped with on-site crushers, i.e., mobile plants, and, as a result, on-site crushers often produce lower quality RCA. The mechanical operations occurring during the production of RCA (Figure 2.1) are similar to those for natural aggregate.

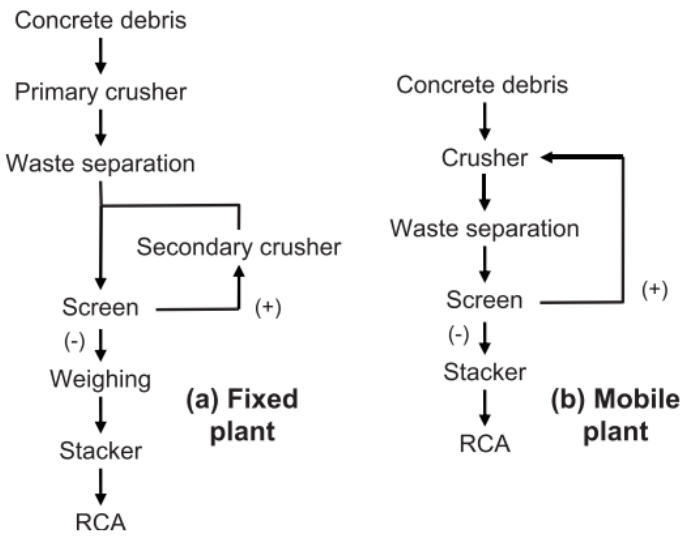

Figure 2.1: Diagrams of manufacturing processes for RCA (a) fixed plant, and (b) mobile plant [7]

Concrete recycling plants often have primary and secondary crushers and screens [8, 9]. During the manufacturing process, the RCA is sprinkled with water for dust control [10]. The primary crusher is frequently a jaw crusher that breaks large chunks of concrete pieces into surge aggregate, ranging between 4 and 12 inches and often used for erosion control. The preferred secondary crusher is an impact crusher [6], which is used to crush the surge-sized pieces into the desired sizes.

2.1.2 Physical and Mechanical Properties of Recycled Concrete Aggregate compared to Natural Aggregate

The primary difference between natural aggregate and recycled concrete aggregate is the attached mortar. The residual mortar makes the RCA more variable. RCA can contain up to 30%–40% of residual cement paste/mortar by volume [8, 11, 12]. The amount of

attached mortar after crushing is influenced by both the maximum size aggregate, the strength of the parent concrete, and the crushing methods [13]. In addition to the residual mortar, impurities such as dirt and other ceramic materials impact the quality of RCA. These are the key factors in determining the physical and mechanical properties of RCA and the resulting concrete.

Properties such as specific gravity, bulk density, porosity, water absorption, and wear resistance of coarse RCA are dependent on the amount of attached mortar and original natural aggregate [13, 14]. Nevertheless, compared to NA, RCA has higher water absorption and porosity, and lower density and wear resistance [8, 15, 16]. The density of RCA is lower than NA by 7%–17% [16], and it falls between normal aggregate and lightweight aggregate [8, 16]. In general, there is a reduction in wear resistance due to the attached mortar and crushing. The crushing during the recycling causes weak zones in the RCA. However, Zega et al. [14] found that quartzite aggregate had an increase in wear resistance, while all other aggregates in the study experienced a reduction in wear resistance. Other studies found the wear resistance in terms of the Los Angeles (LA) abrasion test was reduced by 4%–20% for RCA compared to NA [16, 17]. The water absorption of RCA typically is higher than that of NA due to increased porosity of RCA [16]. The water absorption of coarse RCA varies widely, but generally falls within 2%–10% [8, 18, 19].

2.1.3 Recycled Concrete Aggregate Quality and Standards

The quality of RCA is often measured by the percentages of mortar and natural aggregate present by mass. The amount of attached mortar is influenced by the amount of crushing

and the characteristics of the parent concrete. There is a negative correlation between the amount of crushing and the amount of attached mortar [20]. However, there is a tradeoff of additional crushing with higher cost and potential increased microcracking in the aggregate. RCA made from a low-strength parent concrete may have less attached mortar due to mortar fracture during the crushing process; the opposite is true for a high-strength parent concrete, which also typically has a greater paste fraction than weaker concrete [13, 20]. In addition, the maximum size aggregate (MSA) of the parent concrete has an inverse relationship to the amount of attached mortar [20].

Some international standards required RCA to be at least 90% of mortar and natural aggregate [6, 21]. RCA often meets the minimum requirements for aggregate, and therefore several international standards allow a small percentage replacement of coarse aggregate in concrete [21]. ASTM C33, for example, establishes minimum requirements for aggregate in concrete depending on the exposure and use of the concrete. ASTM C33 places limits on clay and friable particles, chert, the sum of clay and friable particles and chert, material finer than 75 μm, coal and lignite, abrasion, and magnesium sulfate soundness for coarse aggregate. Those requirements surrounding the amount of fines and abrasion resistance are among the more difficult for RCA to meet, depending on the production method used and the quality of the parent concrete [13, 20].

2.1.4 Limitations

RCA is not fully utilized due to several limitations. A few of these limitations are variability of RCA qualities, lack of standards and specifications for RCA, uncertainty of the benefits of the use of RCA, and the lower quality of the final product due to lack of knowledge in

designing RCA concrete [6]. The principal limitation is the variability due to the heterogeneous nature of RCA. In particular, the amount of attached mortar on RCA affects its structural integrity, which influences its quality and performance. As previously described, the amount of attached mortar is dependent on several factors, such as the method of crushing, the parent concrete of the RCA, and the coarse aggregate type. However, consistent aggregate can be produced with standard crushing procedures and known concrete and aggregate sources.

Compared to traditional or NA sources, RCA has a moderate compressive strength [15], but it often satisfies the fundamental requirements for aggregate for local and international standards [22]. Current research shows that coarse aggregate replacement ratios lower than 30% by volume do not negatively impact the concrete properties [23]. These variations in mechanical and physical properties between RCA and NA can have important effects on early and later age properties in concrete.

2.2 Recycled Aggregate Concrete

As mentioned, the main difference between natural aggregate and recycled concrete aggregate is the attached mortar, contributing to greater variability in RC properties. RCA can contain up to 30%–40% of attached mortar by volume [11, 12]. In addition to mortar, impurities such as dirt and other ceramic materials also impact the quality of RCA. These are the key factors in determining the material properties of RCA and the resulting concrete. Material properties such as water absorption of coarse RCA, and workability, porosity, and permeability of RAC are all major factors in determining the overall durability of concrete.

2.2.1 Mix Design Approaches

Use of RCA in concrete requires some special considerations during mix design due to differences between RCA and NA. In an evaluation of four common mix design methods in the 1990s, the American Concrete Institute (ACI) method produced higher strengths and lower strength differences than traditional concrete when compared to the Indian Standard method, Road Research Laboratory, and Surface and Angularity Index Method [24]. ACI method had higher strengths as the result of ACI method having a lower aggregate-to-cement ratio than the other three methods [24].

For modifying the mix design, some common methods are: adding extra cement, adjusting the w/b ratio, and accounting for the equivalent mortar volume (EMV). EMV, similar to equivalent mortar volume (EMR), takes into consideration the multi-phase material of RCA by accounting for additional mortar in calculating the mix proportion as the amount of mortar in the mix. Therefore, the mix design for RAC using the EMV method will require a reduction in cement and fine aggregate, and an increase in water [25, 26].

Fundamentally, there are several approaches to replace NA with RCA. These include the direct weight replacement method (DWM), the direct volume replacement method (DVM) and the EMR method [27]. These methods are visually represented in Figure 2.2. They consider 100% NA replacement with RCA for the cases of DWM and DVM; however, 100% RCA replacement for NA is not possible in the EMR method because of the nature of EMR.

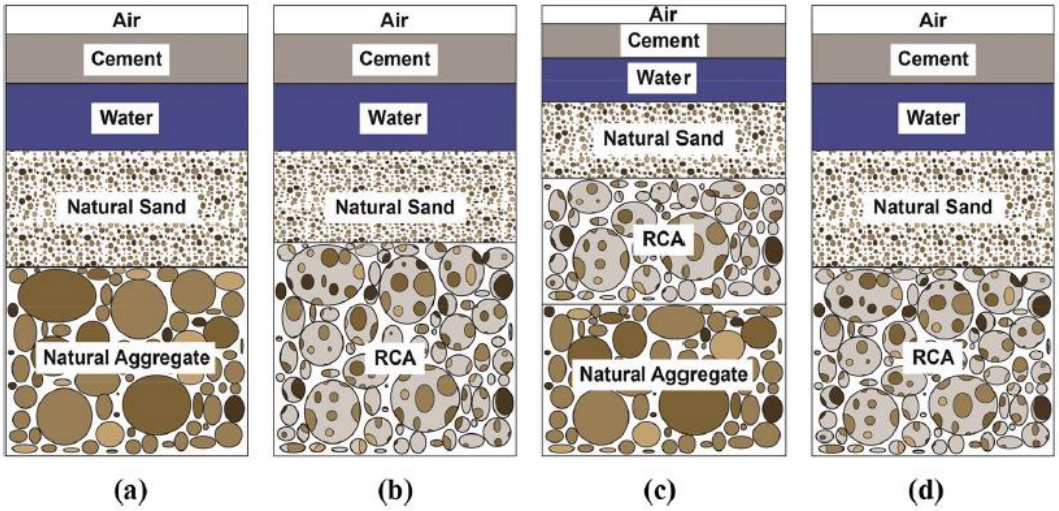

Figure 2.2: Mix design options: (a) traditional concrete with NA, (b) RAC with 100% Direct Weight Method, (c) equivalent mortar volume method, (d) RAC with 100% direct volume method [27]

In a comparison of traditional concrete with RCA concrete designed via direct weight replacement, there is an increase in coarse aggregate due to the lower density of RCA compared to the NA it replaces. When comparing concrete with a constant w/b ratio, Knaack et al. found workability is comparable to traditional concrete for RAC designed by DVM, while that designed by DWM had a small decrease in workability [28]. They found that the EMR method produced a significant decrease in workability due to the reductions in water and the cement additions. Furthermore, Knaack et al. determined that there is no significant difference between the different mix methods in their compressive strength and modulus of elasticity for w/b ratio of 0.44–0.45 [28].

To improve the properties of RAC, some preventative measures suggested including, but are not limited to, modifying the mixing techniques, using supplementary cementitious materials, and removing the surrounding mortar from the RCA.

There are a few unique mixing techniques that have been introduced for RAC including: two stage mixing approach (TSMA), triple mixing method (TM) (also known as stone enveloped with pozzolanic powder) and presoaking aggregate (PA) [12, 28]. PA involves soaking the aggregate in water before mixing.

Another method to improve RAC mix design is through incorporating SCMs. A variety of SCMs have been added to RAC to improve the properties of RAC, with fly ash, slag and silica fume among the most common. Incorporating SCMs reduces the amount of cement, as well as in general improves the durability of RAC.

Other proposed methods for improving RCA include additional crushing, cleaning, acid treating, and heating of RCA [12]. These approaches address the removal of old mortar surrounding the RCA and improve RAC by eliminating or minimizing the first ITZ, densifying aggregate, or decreasing water absorption and porosity. However, these measures often require extra energy, materials, and cost. In addition, they have a potential to introduce contaminants into the concrete [12].

2.2.2 Workability

The absorption of RCA influences fresh and hardened RAC properties. RAC has comparable workability to traditional concrete, with a proper mix design. However, workability issues can arise with the increase of recycled fines. The increased percentages of recycled fines causes higher water absorption and increases water demand. Therefore, a maximum allowable limit on fine material of 20 - 30% is proposed ASTM C33 to minimize reduction in workability and compressive strength [7]. It is suggested that the RCA is washed to prevent excess fine particles [7]. Also, the water absorption of RAC increases

with increase of RCA, but at 30% replacement of coarse aggregate it is less than 3% and can be classified at low water absorption [29]. At 80% replacement, the water absorption was slightly greater than two times than the control concrete [29].

2.2.3 Interfacial Transitional Zone

The interfacial transitional zone is often identified as a weak area of concrete because it contains a greater proportion of pores and microcracks than the bulk paste [12, 30]. ITZ properties can impact the mechanical properties of RAC, since it results in two ITZs [31]. The RCA ITZ is located between the original NA and mortar (which becomes the RCA), and the RAC ITZ is situated between the new mortar and the RCA in RAC. In both cases, the quality of ITZ is initially impacted by a combination of factors, including water-to-binder (w/b) ratio, binder particle reactivity and size distribution, and age, as well as aggregate properties, including their type, size, and roughness [31]. In the case of RAC, the quality—and specifically the degree of microcracking in the RCA ITZ—can be influenced by the processing methods. In RAC, the width of the RAC ITZ has a positive correlation to the percentage of RCA [23].

2.2.4 Porosity and Permeability

Due to the two types of ITZs, porosity is greater in RAC than in traditional concrete. Porosity of concrete is important because, when interconnected, it increases permeability of concrete and can lead to reduced service life [32]. García-González et al. found that total porosity is greater than NAC but deceases with an increase of replacement of RCA at a w/c of 0.55 at 28 days, therefore 50% replacement had higher porosity than 100% replacement. [33]. In addition, the RAC had greater percentages of smaller pores less than 0.1μm and

that should affect mechanical and durability properties [33]. Kou et al. found after 5 years of curing in water tank that RAC, 100% recycled concrete, had lower porosity than traditional concrete at w/c 0.55 [32]. In general, the permeability of RAC increases with the increased replacement of NA with RCA [29, 34, 35]. Over time, permeability decreases due to increasing cement hydration, and RAC and traditional concrete permeability converge at a lower water-to-cementitious materials (w/cm) ratio [32].

2.2.5 Mechanical Properties

2.2.5.1 Compressive and Tensile Strength

At coarse aggregate replacement ratios of coarse aggregate greater than 30%, typically the compressive strength of RAC decreases with the increasing percentage of RCA [8, 23]. At 100% replacement the compressive strength is reduced by 12 – 25% [8]. The reduction in compressive strength is due to several factors including increased porosity and weak interfacial transition zone between the aggregate and matrix. However, a desirable compressive strength can be achieved by decreasing the water-to-cement ratio [8]. Kou et al 2011 found that the strength gains from 28 days to 5 years are higher than in traditional concrete. They propose that this is due to long-term improvement of the RCA interfacial properties as a result of the self-cementing properties in RAC [32, 36]. In some cases, RAC can exhibit higher compressive strength than traditional concrete of similar design if the parent concrete is stronger than design RAC performance level [16].

Comparatively, splitting tensile strength is less impacted by replacement by RCA. Studies have found comparable or higher strengths in RAC than companion traditional concrete [16, 37]. This is attributed to enhanced bond between RCA and cement matrix [37]. Others

indicate the improvement of tensile strength is due to the lower w/cm ratio employed in RAC and the use of higher strength parent concrete sources [16]. However, other studies have reported that both splitting and uniaxial tensile strengths reduce with increases in RCA content [38]. For example, up to 31% lower uniaxial tensile strength was found with 100% RAC replacement, and splitting tensile strength decreased by 20%–30% with 100% RAC replacement [8].

2.2.5.2 Modulus of Elasticity

The modulus of elasticity (E) of RAC typically found to be lower than traditional concrete [28, 35, 38, 39]. E is also negatively correlated to the percentage of RCA, with values for E at 100% RCA decreased by as much as 45% [28, 35, 38, 39]. The reduction of E is due to lower E and inherent microcracking due to processing and the RCA ITZ of RCA. The reduction of E depends on the parent concrete and attached mortar of RCA [13, 38, 39] However, the reduction in E contributes to the ability of RAC to deform more than traditional concrete [16].

2.2.5.3 Shear and Flexural Strength

Shear capacity can be significantly impacted by the percentage of RCA [38, 39]. At 100% replacement, the shear strength of beam can be reduced from 17–30% compared to traditional concrete [28, 38, 39]. Due to the influence of RCA, the current codes are unconservative for RAC beams without stirrups, and therefore researchers have proposed modification of shear capacity equations to account for the RCA percentage [28, 38, 39]. However, RCA beams with stirrups exhibited comparable shear performance at serviceability and ultimate limit states [38]. The RCA percentage also increases the

maximum mid-span deflection. However, the failure modes are similar to traditional concrete [28, 38, 39].

Shear transfer capacity across a crack influences the shear capacity of deep beams, corbels, and shear walls due to the interactions of aggregate interlock, dowel action, and crack surface friction [38, 39]. Xiao et al found that ultimate shear load was impacted by RCA replacement, at lower than 30% replacement is was similar to NAC, and reduced 15% lower than NAC at higher replacements. Furthermore, RAC had similar shape and performance of shear stress-slip curve, crack propagations, and shear transfer [31].

ACI method defines slender beams as shear span to depth ratio > 2.5. Shear stress decreases as crack widths increase and MSA decrease or more aggregate crossing creak cleaves [40]. Modified compression field theory (MCFT) is used to predict shear performance due to size effect by limiting the capacity of large cracks to transfer shear stresses [40]. Sherwood et al. found that positive correlation with MSA and shear strength, and larger effect on deeper members due to larger MSA increase the aggregate interlock capacity. They found that the ACI method did predict the performance of their beams; however, they recommend using simplified MCFT since the ACI method can overestimate shear capacity of deep beams without stirrups.

The RCA replacement ratio had negligible influence on flexural strength [8]. RAC beams showed similar crack patterns and shape of failure as NAC. RAC beams had no influence on bearing capacity, though there was a slight increase in deflection and reduction in stiffness [28]. At 100% RCA, the deflection increase by 10-24% [28]. However, the

flexural performance of RAC slabs are influenced by the RCA percentage. Both the cracking load and ultimate load decreases with increase of RCA content [38].

2.2.5.4 Creep and Shrinkage

Concerns regarding increased creep and shrinkage are another reason that the use of RCA is not used in structural concrete. Both creep and shrinkage increase with increased replacement of RCA [38, 39, 41, 42]. Domingo-Cabo et al found that at 100% RCA there was increase of 51% and 70% at 180 days of creep and shrinkage, respectively. The increase in shrinkage maybe due to lower restraining capacity of RCA [38]. However, both shrinkage and creep of high quality RCA can have similar to NAC [38]. The increase creep is due the of stress levels[38].

2.2.6 Durability

2.2.6.1 Chloride Penetration

RAC has lower resistance to chloride penetration than NAC, but meets minimum requirements [38]. The chloride penetration resistance decreases with the increase of RCA content [38]. According to ACI C1202, RAC with less than 50% RCA it measured at low, while greater than 50% it measured at medium [8]. Zega et al found that chloride diffusion with RAC depends on aggregate types; granitic or basaltic aggregates caused an increase, while quartzite and river gravel caused a decrease in chloride diffusion compared to NAC.

2.2.6.2 Alkali-Silica Reaction

Alkali-silica reaction (ASR) reactivity increases with the increase replacement of RCA [3]. ASR reactivity also depended on the amount of mortar. As the amount of mortar increased, the amount of natural aggregate decreased, causing a lower reactivity [43]. In addition, maturity and amount of pervious ASR on the original NA may impact the reactivity by reducing the amount of available reactive silica. Therefore, studies as described in Adams et al have found that RCA had lower ASR reactivity than NA. However, Shehata found that RCA with 12 years of exposure can have comparable expansion as original aggregate [3]. Furthermore, RAC requires more SCMs to mitigate expansion, compared to NAC [43].

2.2.6.3 Other Durability Concerns

In terms of freeze-thaw resistance, RCA has almost no influence at low cycles about 50 cycles. However, at higher cycles about 200 cycles, RAC had a slower mass loss and dynamic modulus of elasticity loss but a faster strength loss in comparison to NAC [8]. The freeze-thaw resistance can be increased with the use of air-entrainment and reduction of water to cement ratio [8]. Debieb et al found that RAC had good resistance to freeze-thaw with less than 1% loss of mass [44]. Carbonation depth is dependent on amount of RCA at high replacement rates carbonation of RAC decreases due to available alkalinity[35]. Carbonation depth for RAC had increased up to 62% with 60% of recycled concrete aggregate [8], whereas above 70% replacement there was a reduction in carbonation depth [45]. However, during an accelerated carbonation test, it was found to carbonation rate increased by 10% to NAC [46]. Contaminated RCA with chlorides should be soaked in water for two weeks, otherwise it could cause corrosion of reinforcement [44].

2.2.7 Sustainability: Life Cycle Assessment of Recycled Aggregate Concrete

The recycling of concrete debris is encouraged/enforced by governmental agencies to promote sustainability. The United States Environmental Protection Agency (EPA) wants to decrease the landfill waste by promoting increased "reduce, reuse, and recycle" of C&D waste. To encourage the use of debris materials, there are many incentives, including tax credits and credits of green construction certificates. The sustainability of RCA is dependent on several aspects, such as manufacturing, avoiding landfills and use of natural resources, adding extra cement, and transporting the material [9, 47, 48]. Since the manufacturing process of RCA is similar to NA, they have similar emissions and environmental impacts in terms of manufacturing. However, there are minor differences in on-site crushing and concrete recycling plants. The key benefits in terms of sustainability are the reduction of landfilled material and limiting the use of natural resources. The key hindrance in terms of sustainability is the use of additional cement. Cement is the highest producer of CO_2 emissions in concrete due to the production techniques. Thus, increasing the amount of cement to have comparable strengths at high replacement ratios of RCA will result in either a minimum or negative impact in sustainability compared to the use of NA [9, 47, 48].The other key aspect in terms of sustainability is transportation of the RCA [9, 47, 48]. The transportation of RCA can either be a benefit or hindrance to lifecycle assessment. If the RCA manufacturer is closer to the jobsite than the NA manufacturer, then there is a reduction in emissions and improvement of sustainability indicators. However, if the reverse is true then there is an increase in emission and deduction in sustainability indicators. As a result, there is a breakeven point in terms of transportation of the RCA when it is no longer a benefit to use RCA.

2.3 Recycled Concrete Aggregate Fines

Recently, RCA studies have focused on using fine RCA with particle sizes smaller than 150 μm as partial replacement of cement due to challenges with the disposal of these finer particles produced during crushing and due to interest in the potential for RCA to exhibit self-cementing properties. Kim et al determined that 100% replacement of cement with RCA fines of less than 75 μm had negligible recementation reactivity due to the dominant mineral being $CaCO_3$ and the inability to form new C-S-H [49]. Florea et al. found at 10% replacement, fine RCA had a filler effect, but a higher replacement ratio had a detrimental effect on both flexural and compressive strength [50]. On the other hand, dehydrated cement paste (DCP) at 800°C had gained 60% of the compressive strength of original Portland cement paste [51]. DCP with replacement of silica fume or fly ash has shown to enhance the performance of compressive strengths [51]. Therefore, fine RCA with heat treatment has a potential for use as an SCM; however, inert fines, such as sand and bricks, have a negative effect on strength development [50-52].

CHAPTER 3. MATERIAL PROPERTIES OF RECYCLED CONCRETE AGGREGATE

This chapter focuses on the material properties of the RCA used in this study. The RCA from this study was sourced from a recycling plant for C&D materials located in Atlanta, Georgia, USA. The first section of this chapter provides an overview of the manufacturing process and summarizes the Georgia Department of Transportation (GDOT) specifications for RCA. The second section compares the physical properties of RCA in terms of aggregate gradation, bulk density, specific gravity, and absorption to those of natural aggregate. The final section evaluates the amount of residual mortar surrounding the RCA by MSA.

3.1 Recycled Concrete Aggregate Properties

RCA properties are dependent on several aspects, including parent concrete, impurities, and manufacturing process. The RCA used in this study was sourced from a local C&D waste recycling plant, MetroGreen Recycling. This manufacturer accepts all types of concrete from any source. Thus, the parent concrete is unknown, but the majority of the original NA was granitic gneiss, which is the most common coarse aggregate in the region. This study used both graded aggregate base (GAB) and size #57 for coarse aggregate as defined by ASTM C33 (i.e., #57 stone). GAB, also known as 'crusher run', is regulated by GDOT by aggregate sizes ranging from 1.5 inch up to 15% finer than 2.95×10^{-2} inch. As defined by ASTM C33, #57 stone has aggregate sizes of 1 inch to 9.29×10^{-3} inch (#8 sieve). Prior to use, the aggregate was sieved to get the appropriate size fractions for

the three types of size numbers and to obtain fines passing the 0.187 inch (#4 sieve) by removing that fraction from the bulk material.

3.1.1 MetroGreen Recycling Facilities

MetroGreen Recycling has two sites in the metro Atlanta area. MetroGreen Recycling II is the smaller facility and primarily focuses on recycling concrete. This facility accepts all types of concrete. MetroGreen Recycling II is located on 2490 Marietta Road NW only 8 miles from the research laboratory used in these studies. MetroGreen Recycling products are #34, #57, GAB, and Surge recycled concrete. Their primary customers are pipeline and construction fill contractors because the RCA is 15% lighter than the NA and possesses additional compacting properties beneficial in those applications [10]. During the site visit, the manufacturer was only producing three of its four product lines. The availability is limited due to a combination of factors, including illegal dumping of debris concrete, constructors opting to use on-site crushers, and local competitors [10]. Nevertheless, the tipping fee (i.e., fee for dropping off materials) is less than for conventional C&D landfills [10].

3.1.2 Manufacturer Quality Assurance

This manufacturer regularly tests their products for quality and assurance. Their GAB is type 2 Class A, approved for use by GDOT. The GDOT Supplemental Specification sets the following requirements for aggregates based on AASHTO, ASTM, and GDOT standards: material passing the No. 200 sieve; sulphur content; potential for weathering; petrographic analysis; soundness (by magnesium sulfate testing); abrasion resistance (by LA abrasion test); aggregate gradation; reactivity; and presence of schist or phyllite, flat

and elongated particles, and friable particles. Based on recent testing of the aggregate, the LA abrasion loss average is 38.1% and the magnesium sulfate soundness loss average is 4.42%, both of which are below the maximum allowable of 65% and 15%, respectively, as regulated by the GDOT Supplemental Specification [53].

3.1.3 MetroGreen Recycling Manufacturing Process

The manufacturing procedure this producer uses for recycling the concrete is similar to processes used at many traditional concrete recycling plants and includes initial crushing followed by primary and secondary procedures. The initial crushing breaks down larger debris concrete into smaller pieces to fit onto the initial conveyor belt. Then, the primary procedure starts with screening for metals using a magnet and dirt. This is followed by crushing using a jaw crusher. The primary procedure is shown in Figure 3.1.

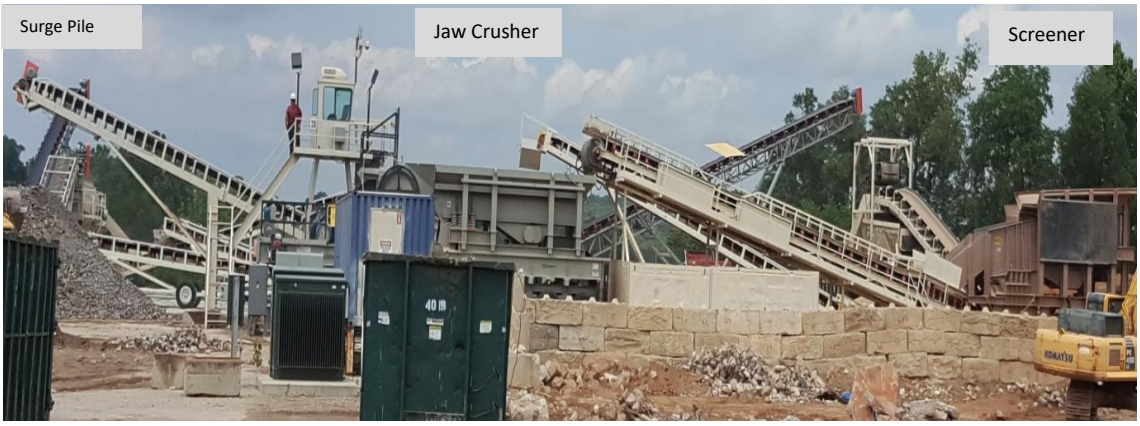

Figure 3.1: Primary procedure at the manufacturer site in Atlanta, GA

The result of the primary procedure is the 'surge aggregate.' The surge aggregate sizes are regulated and are around the size of an average adult fist. Some of the surge aggregate is sold as-is, and the other part goes into the secondary procedure for additional processing.

The secondary procedure starts with screening for metal and visual inspection for deleterious materials. The screening steps are shown in Figure 3.2a.

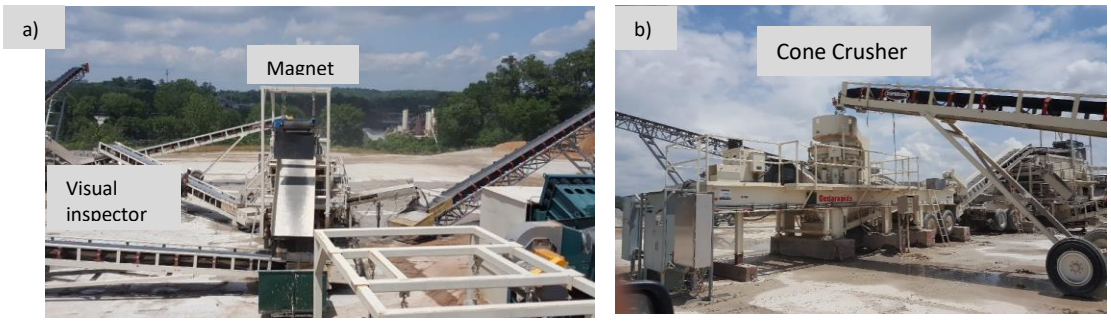

Figure 3.2: a) Screening for metal and conveyer belt for visual inspector and b) cone crusher

Next, the material is fed into the cone crusher to produce either #57 stone or GAB with a MSA of 1.5 inch, shown in Figure 3.2b. Figure 3.3 show the final products: #57 stone and GAB, with a dollar bill as a reference scale.

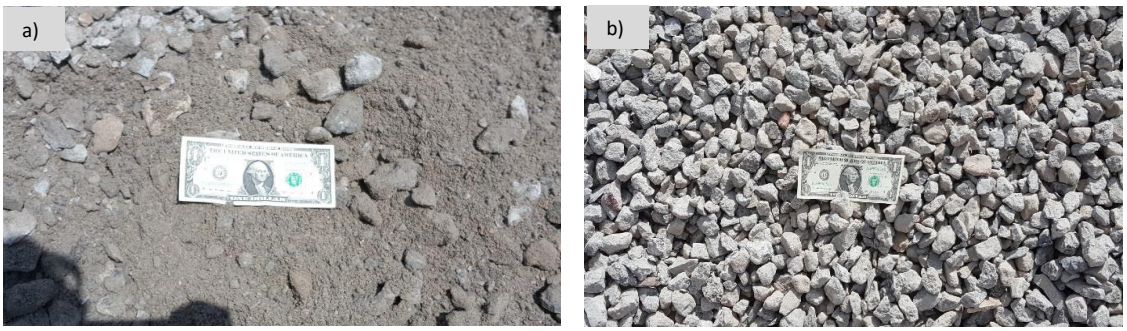

Figure 3.3: Picture of RCA GAB (a) and #57 (b)

The main difference between the GAB and #57 stone is the GAB has a higher percentage of fines and wider particle size range than #57 stone. As seen in Figure 3.3a, GAB is a mixture of fine and coarse aggregate with MSA 1.5 inches and no limit on minimum size.

Whereas #57 stone has a more uniform graduation with only coarse aggregate. The #57 stone has MSA of 1 inch and minimum size of $9.29x10^{-2}$ inch, which conforms with the ASTM C33 gradation specifications.

3.2 Physical Properties

After both #57 and GAB RCA was received on May 2016 initial aggregate physical properties were determined. The physical properties studied includes aggregate gradation, bulk density, specific gravity and absorption by the following ASTM C136, ASTM C29, and ASTM C127 procedures, respectively.

3.2.1 Aggregate Gradation

The aggregate gradations of the GAB and the #57 stone were determined using ASTM C136 [54]. Since the MSA was 1 inch, 22 lb of material were tested in three to four batches due to the 8-inch diameter of the sieves. The material was randomly removed from the bucket, then placed into an oven at 110°C until a constant mass was obtained. Then, the material was placed into the mechanical sieve shaker for a minimum of 5 minutes.

Finally, the material in each sieve was carefully removed and weighed. Figures 3.4 and 3.5 show the resulting gradations of the GAB and the #57 stone.

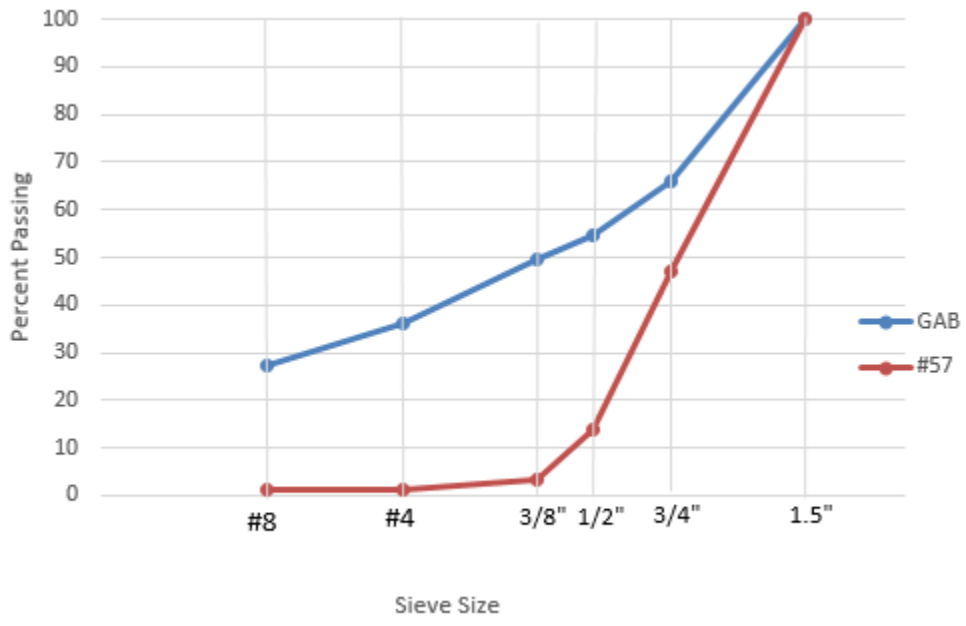

Figure 3.4: Average gradation curves of GAB and #57 sieve sizes 1.5” - #8

The average percents passing for #8 sieve was around 1% and 27% for the #57 stone and GAB, respectively. The #57 stone passes the ASTM C33 requirements of limit the percent finer than #8 to be less than 5% [55]. As stated in GDOT Supplemental Specification, the GAB type 2 limit is 25 – 45% passing #10 sieve. Therefore, RCA GAB also meets the requirement for GAB type 2. Figure 3.5 shows the gradation curve for sieve sizes of #16 - #325. Figure 3.5 was adjusted based on percentage of fines that passed #8 sieve. However, the fineness modulus (FM) was calculated passed on the total weight of the material collected. FM was determined by the summation of cumulative percent retained on the following sieves: #100, #50, #30, #16, #8, #4, ⅜ inch, ¾ inch and 1.5 inch divided by 100. FM for the #57 stone and the GAB was 7.42 and 4.86, respectively. GAB has a lower FM

than #57 stone therefore; it is finer average particle size which agrees with the visual observation.

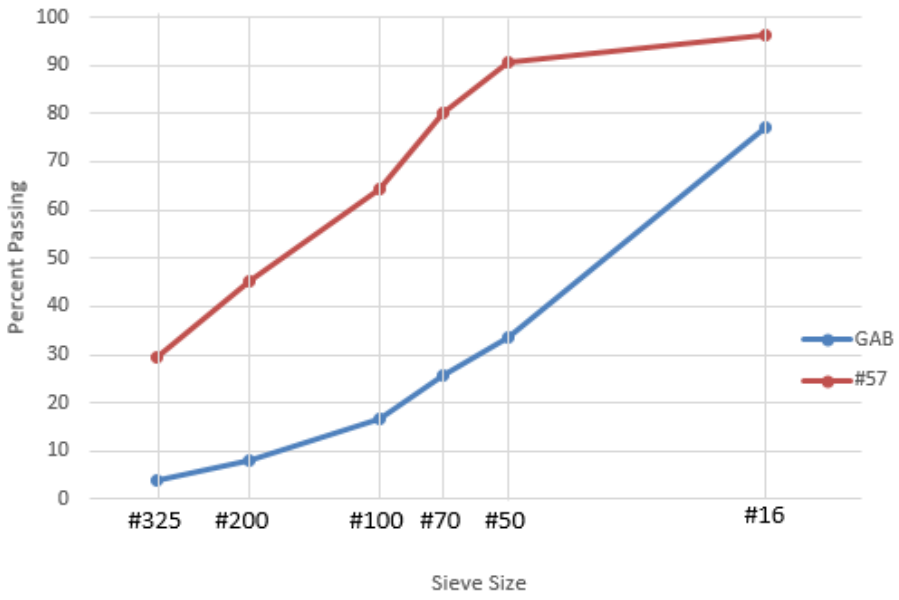

Figure 3.5: Average gradation curves of GAB and #57 sieve sizes #16 - #325

Based on the total weight of the sample, the average percentage of particles passing the #200 and #325 sieve was 2.24%, 1.07% and 0.59%, 0.38% for GAB and #57 stone, respectively. The percent passing #200 sieve for #57 stone aggregate is lower than 1% limit for coarse aggregate in concrete in ASTM C33 for deleterious substances [55].

The GAB and the #57 stone were sorted into three size numbers based on the MSA of 1 inch, ¾ inch, and ½ inch by sieving. The aggregate was placed into a large sieve shaker and was operated for approximately 5 to 12 minutes depending on the amount of material placed into the sieve shaker. Afterwards the as-is gradations were determined. Based on the three MSA, size numbers #57, #67, and #87 for coarse aggregate was selected. The

coarse aggregate grading requirements are shown in Table 3.1 for the three selected size numbers.

Table 3.1: Grading requirements for coarse aggregate [55]

Size Number	% Passing by mass						
	1.5”	1”	¾”	½”	3/8”	#4	#8
#57	100	100 - 90	-	25 - 60	-	0 - 10	0 - 5
#67	-	100	90 - 100	-	20 - 55	0 - 10	0 - 5
#87	-	-	100	90 - 100	40 - 70	0 - 15	0 - 5

The RCA was graded to conform to ASTM C33 based on Table 3.1.

The coarse aggregate NA is granite gneiss, also referred to as granite in industry, which is locally manufactured. The NA for this study is manufactured and distributed by Vulcun Materials Company. It is manufactured with a similar crushing process as RCA, but produced in a larger range of size numbers. The NA was received in three selected size numbers. Granite is a common coarse aggregate used throughout Georgia; therefore, it can be assumed that the majority of RCA original coarse aggregate is the same as the granite gneiss NA selected for this study. Throughout this study the specimens will be labeled with size number and ‘R’ for recycled or ‘G’ for granite gneiss, e.g., the MSA of 1-inch RCA would be labeled #57R. Figures 3.6 – 3.8 show the graduation curves RCA of the three different MSA compared to NA.

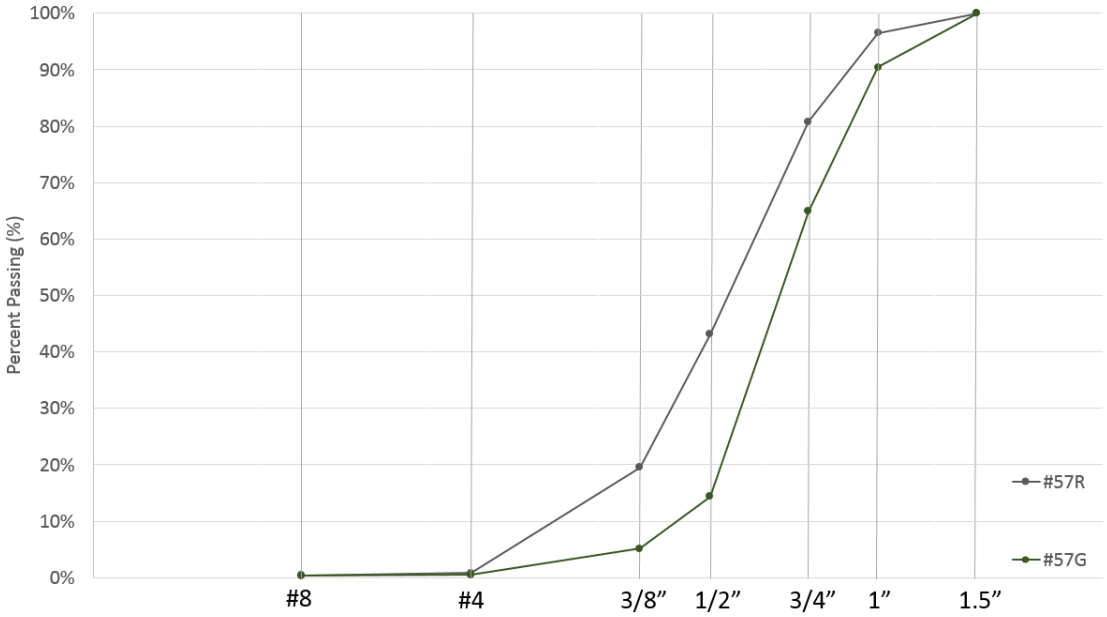

Figure 3.6: Gradation curves of MSA of 1”

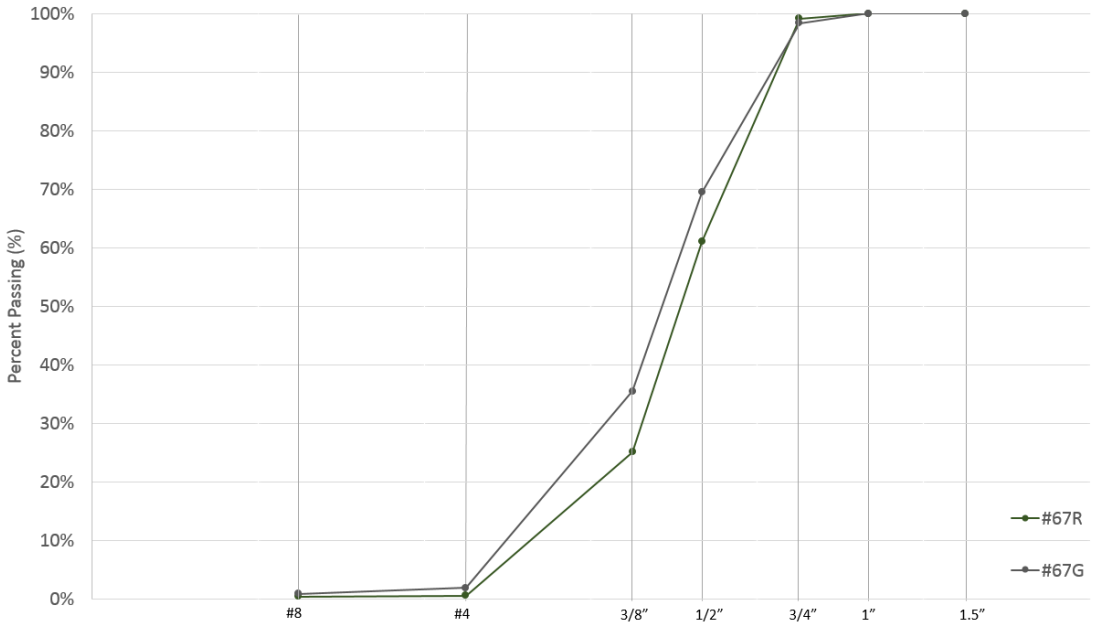

Figure 3.7: Gradation curves of MSA of ¾”

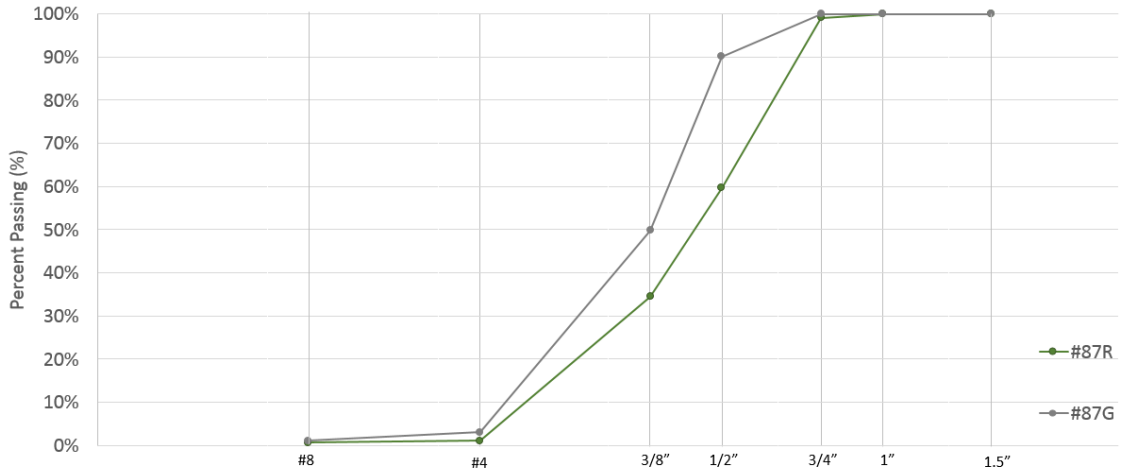

Figure 3.8: Gradation curves of MSA of ½"

The aggregate was randomly selected from sorted aggregate barrels. As seen in Figure 3.8, only #87R did not meet the gradation specification of ASTM C33. In each of the graduation curves obtained for the different MSA, the RCA tend to be slightly coarser than the NA. Table 3.2 shows the gradation data for both as-received and processed RCA compared to as-received NA.

Table 3.2: Percentage passing by mass of size number for both as-received (AR) and processed RCA compared to as-received NA

Size Number	% Passing by mass							
	1”	¾”	½”	3/8”	#4	#8	200	325
#57R$_{AR}$	--	47.15	13.85	3.47	1.38	1.31	0.59	0.38
GAB$_{AR}$	--	65.9	54.8	49.8	36.1	27.3	2.24	1.07
#57R	96.5	80.8	43.2	19.6	0.82	0.33	--	--
#57G$_{AR}$	90.5	65.9	14.4	5.19	0.53	0.38	--	--
#67R	100	99.1	61.0	25.1	0.53	0.40	--	--
#67G$_{AR}$	100	98.4	69.4	35.4	1.92	0.85	--	--
#87R	100	99.1	59.7	34.5	1.09	0.69	--	--
#87G$_{AR}$	100	100	100	49.8	3.08	1.13	--	--

Figures 3.9 – 3.11 show the gradation of RCA by percentage of mass passing sieve with the upper and lower bonds of the gradation based on ASTM C33. For the sizes ASTM C33 did not specified a straight line was drawn to connect the pervious specified size, for example ASTM C33 does not specify an upper or lower bond for ¾ inch for #57.

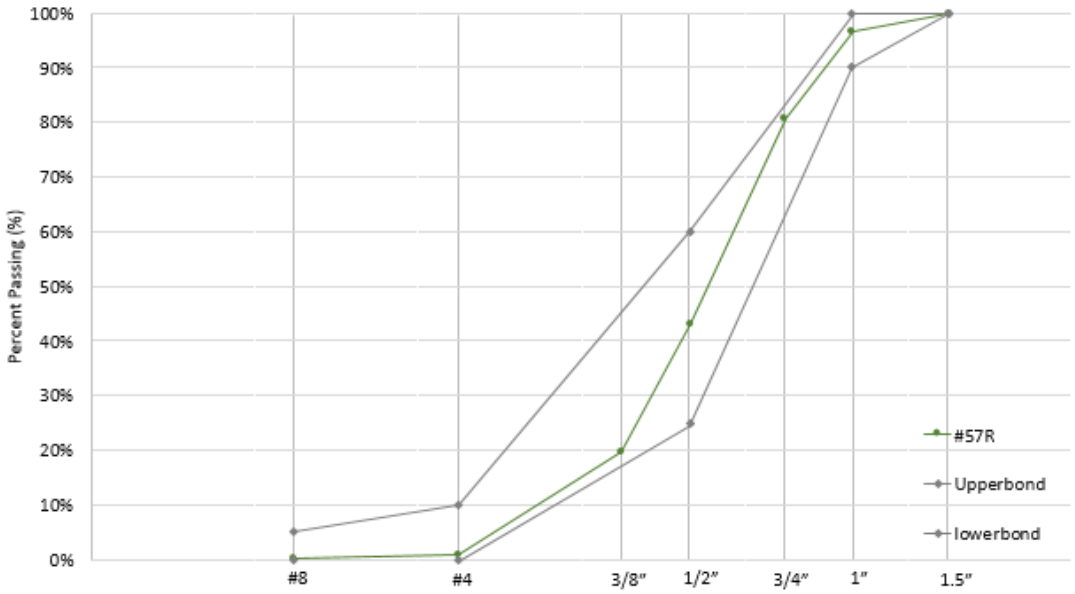

Figure 3.9: Graduation curve of #57R with upper and lower bonds per ASTM C33

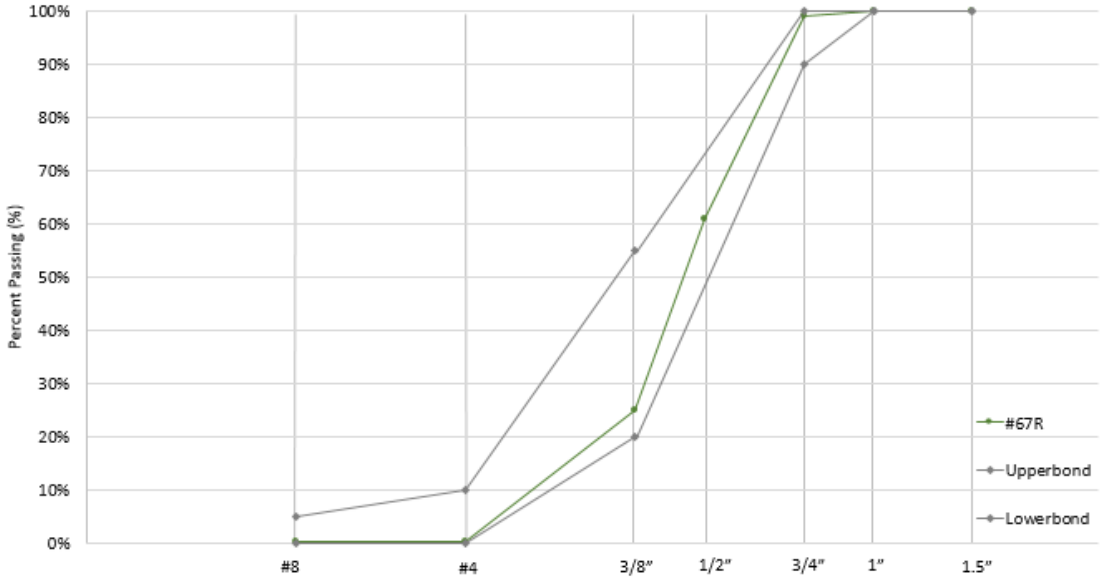

Figure 3.10: Graduation curve of #67R with upper and lower bonds per ASTM C33

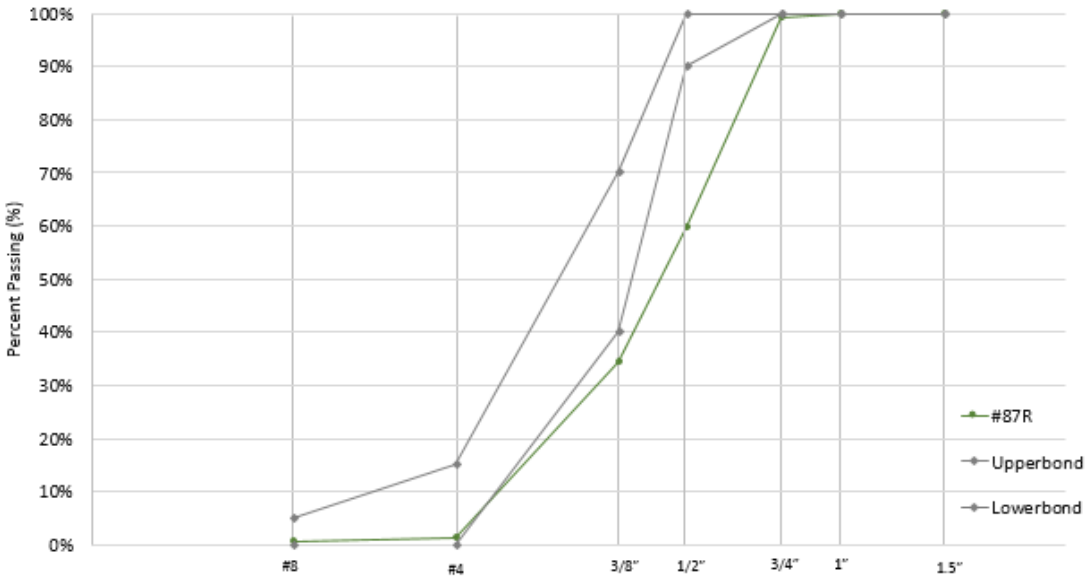

Figure 3.11: Graduation curve of #87R with upper and lower bonds per ASTM C33

The graded RCAs tend to favor the lower bonds at lower sizes and shift towards the upper bonds higher sizes. Therefore, the graded RCAs has an overall coarse grading.

3.2.2 Bulk Density

The bulk density was measured per ASTM C29 specifications [56]. The aggregates both RCA and NA were dried to a constant mass at 110ºC. The measure a standard bucket of 1 ft^3 was filled with the aggregate to a third of bucket followed by rodding 25 times and leveling, these steps was repeated two more times until the bucket was full. Then, the mass is measure and aggregate is weighted. Finally, the dry-rodded unit weight was calculated by dividing weight of aggregate minus the bucket by volume of bucket [56]. The calculated dry-rodded unit weights are shown in Table 3.3.

Table 3.3: Dry-rodded unit verse RCA weight of NA

MSA (inch)	NA (lb/ft^3)	RCA (lb/ft^3)	Δ (%)
0.5	94.0	87.1	7
0.75	95.0	84.7	12
1.0	96.0	87.9	10

The bulk density of the RCA was lower the NA by 7 – 12%. The RCA's lower dry-rodded unit weight is potentially due to the surrounding mortar and other materials in it, such as clay and voids. The measured bulk density agrees with previous studies that observed an decrease in density with increased RCA content [8, 15, 16].

3.2.3 Specific Gravity and Absorption Capacity

ASTM C127 was used to measure the bulk specific gravity at saturated surface dry (SSD) and absorption capacity of RCA and NA. The aggregates were dried to a constant mass at 110ºC, then soaked in water for 24 hours. The aggregate was rolled into absorbent cloth to remove the visual water film on the surface of the aggregate. Then, the SSD aggregate was weighted to determined B (see Equations 3.1 and 3.2). The aggregate is submerged in water and weigh to obtain C. Finally, the aggregate is then placed back into the oven until it reaches a constant mass the cooled in air for at 1–3 hours. The oven-dried aggregate is weighted to determine A. The following equations are used to determine specific gravity and absorption capacity of aggregate [57].

$$\textbf{Relative Density (specific gravity):}\ \frac{A}{B-C} \tag{3.1}$$

$$\textbf{Absorption capacity, \%:}\ \left[\frac{B-A}{A}\right] * 100 \tag{3.2}$$

Table 3.4: Absorption capacity and specific gravity at SSD of NA and RCA

MSA (inch)	NA		RCA	
	Absorption (%)	Specific Gravity at SSD	Absorption (%)	Specific Gravity at SSD
0.5	0.91	2.65	4.3	2.39
0.75	0.63		3.83	2.33
1.0	0.6		4.0	2.43

The absorption of RCA mainly fell within the ranges 4 – 10% measured by other studies [8, 18]. The absorption of RCA is four to six times greater than of the NA. The bulk specific gravity at SSD of the RCA was approximately 10% lower than NA. The increase absorption and lower specific gravity of RCA is due to residual mortar, as well as other materials.

3.3 Residual Mortar Content

Residual mortar is the remaining mortar surrounding and bonded to the natural coarse aggregate particles after the crushing the debris concrete, as shown in Figure 3.12.

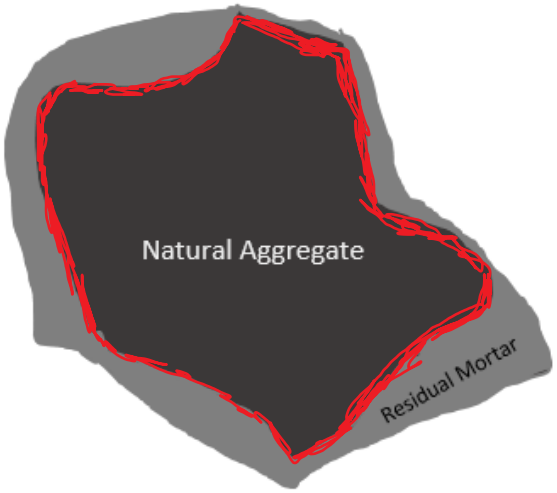

Figure 3.12: Model of RCA

The residual mortar is a combination of cement paste and fine aggregate. The residual mortar can account for 30 – 40% by volume or 10 – 50% by weight of the RCA [11, 12, 58]. The interface of residual mortar and the coarse aggregate is the RCA ITZ, as shown (not to scale) in red in Figure 3.12. This ITZ is one of the two found in RAC. These boundary layers are weaker zones and more porous regions in the aggregate. The residual mortar has lower density than coarse aggregate therefore resulting in overall lower unit weight, depending on the amount of residual mortar. The amount of residual mortar depends on the several factors, including the manufacturing process, original concrete strength, type of aggregate, and maximum size aggregate of original and new aggregate [13, 14]. When incorporating RAC into new concrete the amount of residual mortar impacts multiple properties including absorption of water, permeability, unit weight, and strength [8, 15, 16]. Thus, it is important to determine the approximate amount surrounding mortar on RCA.

There are several ways to approximate the amount of residual mortar including acid treatment, freeze-thaw cycles, additional crushing, mix design/specific gravity, heat treatment, image techniques, and combination of these methods [52, 58]. A few limitations of these methods are inaccuracy, time consuming, and/or costly. These methods tend to underestimate or overestimate the amount of attached mortar. The time requirements range for few minutes to a week. Many of these methods requires additional resources and energy.

In this study two methods used to approximate the residue mortar content was Abbas 2007 method and specific gravity methods [58]. The Abbas 2007 method is a combination of sodium sulfate solution exposure and freeze thaw cycling. The method starts with oven drying about 2 kg of each type of as-received aggregate at 105°C for 24 hours, and then weighing the aggregate and submerged into 26% sodium sulfate solution for another 24 hr. Then, the submerged aggregate is subjected to five daily cycles of freezing and thawing. The aggregates are washed over a #4 sieve and dried in the oven for another 24 hours at 105°C. Finally, the oven dried weight of the resulting aggregate is determined. During the freeze thaw cycle, the submerged aggregate in 26% sodium sulfate in placed in a freezer for 16 hours at -12°C (1.4°F) and then placed in the oven for 8 hours at 80°C. The residual mortar content is the percent change from the initial oven-dried weight of the RCA to the final oven-dried weight of "natural aggregate." Equation 3.3 is used to calculate the percentage of residue mortar of RCA.

$$RMC_{ABBAS} = \frac{W_i - W_f}{W_i} * 100 \quad (3.3)$$

The procedure for determining mortar fraction size specific gravity method is determining the specific gravity of both the RCA and natural aggregate, based on ASTM C127. Then, the values are compared using percent difference. Similar models to this take into the account the cement mortar specific gravity if the concrete mix design is known [52].

$$RMC_{SGM} = \frac{SG_{RCA} - SG_{NA}}{SG_{cement\ mortar} - SG_{NA}} * 100 \quad (3.4)$$

Here, the specific gravity of cement mortar was assumed to 2.16 and specific gravity of natural aggregate (granitic gniess) assumed to be 2.69, which is typical for coarse aggregate in metro Atlanta area. Table 3.5 show the results of the residual mortar calculations.

Table 3.5: Approximate Residual Mortar per MSA

MSA (inch)	ABBAS et al Method (%)	Specific Gravity Method (%)
1	18.5	20.8
0.75	26.6	37.5
0.5	15.4	26.2

Based on Table 3.5, there are no direct correlations with MSA to the amount of residue mortar. #67 stone had the highest residual mortar in both cases. The specific gravity method gave higher percentages of residual mortar. The difference between the test methods are potentially due to use of different set of aggregate for each test method or attributed to the limitations of specific gravity method. The main limitations of the specific gravity method

are the initial assumptions of specific gravity of both the cement mortar and original natural aggregate and it doesn't account for foreign particles or irregularity of natural aggregate types. Specific gravity method requires background knowledge of the RCA sources, to be more accurate. These limitations are addressed in ABBAS method, since the residue mortar is chemical/physically removed. However, ABBAS method requires additional time and resources. Figure 3.13 shows the before and after photos of ABBAS method.

Figure 3.13: Before and after photo of ABBAS method for RCA

As seen in Figure 3.13, the ABBAS method visually removed most attached of the residual mortar. Nevertheless, both methods give reasonable approximation of residue mortar surrounding RCA. Since both methods are suitable to estimate the residue mortar, it is recommended based on energy consumption and ease of testing to use specific gravity method.

Table 3.6 presents a summary of the physical properties of RCA and NA. Although, residual mortar impacts the physical properties of RCA there is no direct correlation. Therefore, other factors play a role into the changes of physical properties including variability of RCA.

Table 3.6: Summary of physical properties of RCA and NA

Size Number	RMC_{Abbas}	RMC_{SG}	DRUW	Absorption Capacity (%)	Specific Gravity SSD
#57R	18.5	20.8	87.9	4.0	2.43
#57G	-	-	96.0	0.60	2.65
#67R	26.6	37.5	84.7	3.83	2.33
#67G	-	-	95.0	0.63	2.65
#87R	15.4	26.2	87.1	4.3	2.39
#87G	-	-	94.0	0.91	2.65

The variability of RCA based on visual inspection shows that RCA had about 5% of different types of NA original coarse aggregate, such as rounded river gravel, in comparison to angular granitic gneiss. As well as 1% of other materials including plastic, wood, dirt, ceramics, clay and metal. However, majority of the additional materials was removed during grading process of RCA to obtain proper size number.

CHAPTER 4. DESIGNED PROPERTIES OF RECYCLED AGGREGATE CONCRETE

This chapter focuses on concrete mix design and physical and mechanical properties of RAC. The first section is a walkthrough of the mix design and the modified mix design based on aggregate properties. The next section explains the mixing procedures for mixes. The third section discusses the fresh concrete properties, such as slump, unit weight, and air content. The following four sections discuss the compressive strength, modulus of elasticity, shear strength of short beams, and flexural strength results.

4.1 Mix Design

The mix design for concrete is based on the performance criteria for the resulting concrete. Concrete mix design are often a balance of economy and performance. Performance criteria for concrete, includes workability, strength, and/or durability requirements, is project depended. This study focus is on the use of RCA in structural concrete. Structural concrete projects have a range of applications but often have a requirement of 3 – 7 ksi for compressive strength. Aside for compressive strength, there are no standard performance requirement for structural concrete. Most requirements are application based i.e. beams in marine environment require lower permeability levels for higher durability. These requirements were considered when determining the mix design based on ACI absolute volume method.

4.1.1 Mix Design by ACI Absolute Volume Method

The mix design for this study was based on the ACI 211.1-91 reapproved in 2009 for the absolute volume method. The target slump for the mixes was 3–5 inches for considering structural elements such as beams and columns. The MSA ranges were selected based on availability of RCA and guidelines suggested by ACI 211.1 equations. Based on the suggested equations, the largest MSA for the formwork and reinforcement scheme was 1.2 inches. The water and air contents were estimated using Table 4.1.

Table 4.1: Approximate mixing water and air content requirements for different slumps and nominal maximum size of aggregates [59]

Water, lb/yd^3 of concrete for indicated nominal maximum sizes of aggregate								
Slump, in	3/8 in	½ in	¾ in	1 in	1-½ in	2 in	3 in	6 in
	Non-air-entrained concrete							
1 to 2	350	335	315	300	275	260	220	190
3 to 4	385	365	340	325	300	285	245	210
6 to 7	410	385	360	340	315	300	270	--
More than 7	--	--	--	--	--	--	--	--
Approximate amount of entrapped air in non-air-entrained concrete, percent	3	2.5	2	1.5	1	0.5	0.3	0.2

The values for this study is boxed are blue for water demand and gold for entrapped air. Based on Table 4.1, both the water demand and entrapped air increases as MSA decreases, due to need for more cement paste to surround the aggregates. Next, the w/cm ratio of 0.45 was selected, and, thus, the estimated compressive strength was 5.5 ksi. The cement content was determined based on the w/cm ratio and water demand. The estimated coarse aggregate

was determine using Table 4.2, using the DRUW of the coarse aggregate and fineness moduli of the fine aggregate, 2.75.

Table 4.2: Volume of coarse aggregate per unit volume of concrete [59]

Nominal Maximum size of aggregate, in	Volume of oven-dry-rodded coarse aggregate* per unit volume of concrete for different fineness moduli of fine aggregate+			
	2.40	2.60	2.80	3.00
3/8	0.50	0.48	0.46	0.44
1/2	0.59	0.57	0.55	0.53
3/4	0.66	0.64	0.62	0.60
1	0.71	0.69	0.67	0.65
1 1/2	0.75	0.73	0.71	0.69
2	0.78	0.76	0.74	0.72
3	0.82	0.80	0.78	0.76
6	0.87	0.85	0.83	0.81

Since the fineness moduli of the fine aggregate was 2.75, linear interpolation was used to determine the values for volume of coarse aggregate per unit volume of concrete. Finally, the fine aggregate content was determined by subtracting to total volume of 27 ft^3 by the volume of air, cement, water and coarse aggregate. The paste fraction includes the cement, water, fine aggregate and the air content. The final mix proportions are listed in Table 4.3 below.

Table 4.3: Mix proportions based on ACI absolute volume method

	Materials	lb/yd^3	ft^3/yd^3	% total volume
Mix Design for MSA 0.5”	Water	365.00	5.69	21.1%
	Cement	811.11	4.01	14.9%
	Coarse Aggregate	1424.53	7.92	29.4%
	Fine Aggregate	1452.91	8.70	32.2%
	Air	-	0.68	2.5%
	Paste	-	18.40	68.1%
Mix Design for MSA 0.75”	Water	340.00	5.30	19.6%
	Cement	755.56	3.74	13.8%
	Coarse Aggregate	1603.13	8.92	33.0%
	Fine Aggregate	1420.45	8.51	31.5%
	Air	-	0.54	2.0%
	Paste	-	17.54	65.0%
Mix Design for MSA 1.0”	Water	325.00	5.06	18.7%
	Cement	722.22	3.57	13.2%
	Coarse Aggregate	1731.38	9.63	35.7%
	Fine Aggregate	1390.41	8.33	30.9%
	Air	-	0.41	1.5%
	Paste	-	16.96	62.8%

4.1.2 Modified Mix Design

After examining the mix proportions based on ACI 211, multiple parameters were changing with the change of MSA. Therefore, in order to limit the number of changing variables, a modified mix design was developed to have constant volume of paste and coarse aggregate fractions. Keeping the constant volume of paste per mix would allow for direct comparisons of three MSAs by ignoring the influence of paste fraction. A constant mortar fraction allowed for the water and cement percentages to fluctuate based on MSA per ACI 211.1-91 recommendations to provide enough paste adequately surrounding the

available surface area of the aggregate. Based on the ACI mix design, the paste and coarse aggregate fraction was set to 66% and 34%, respectively. Table 4.4 shows the modified mix design. In comparing Table 4.3 and Table 4.4, the main difference is the amounts of fine and coarse aggregate per mix.

Table 4.4: Modified Constant Volume Mix Design

		lb/yd^3	ft^3/yd^3	A/cement	% Total volume
Mix Design for MSA 0.5”	Water	365.00	5.69	1.42	21.1%
	Cement	811.11	4.01	1.00	14.9%
	Coarse Aggregate	1650.20	9.18	2.29	34.0%
	Fine Aggregate	1243.35	7.45	1.86	27.6%
	air		0.68	0.17	2.5%
	paste		17.15	4.27	66.0%
Mix Design for MSA 0.75”	Water	340.00	5.30	1.42	19.6%
	Cement	755.56	3.74	1.00	13.8%
	Coarse Aggregate	1650.20	9.18	2.46	34.0%
	Fine Aggregate	1376.74	8.25	2.21	30.5%
	air		0.54	0.14	2.0%
	paste		17.28	4.63	66.0%
Mix Design for MSA 1.0”	Water	325.00	5.06	1.42	18.7%
	Cement	722.22	3.57	1.00	13.2%
	Coarse Aggregate	1650.20	9.18	2.57	34.0%
	Fine Aggregate	1465.79	8.78	2.46	32.5%
	air		0.41	0.11	1.5%
	paste		17.42	4.88	66.0%

The RCA replaced at direct weight replacement of the coarse aggregate, therefore, due to the lower density of the RCA there was a slight increase percentage of coarse aggregate over the initial calculated mix design. Prior to mixing, the coarse and fine aggregates and

water weights was adjusted to account for the current moisture content of the aggregate. The moisture content of the coarse and fine aggregate were measured prior to mixing.

4.2 Mixing Procedure

Both RAC and NAC was mixed according to ASTM C192. The mixing procedure is as follows seven main steps. The mixing procedure follows seven steps: (1) dampen the 3 ft^3 drum concrete mixer and mixing tools; (2) place all coarse aggregate into mixer with a small amount of mix water, and start mixer; (3) while mixer is rotating, pour fine aggregate into mixer, followed by cementitious material and water; (4) allow for the concrete to mix for 3 minutes; (5) stop and cover mixer to let concrete rest for 3 minutes; (6) start mixer and mix concrete for additional 2 minutes; (7) measure slump; if the slump is smaller than 3 inches, add superplasticizer and remix for additional 3 minutes [60].

Due to limitation of concrete mixer's 3ft^3 volume, this study was broken into two series. Series 1 was cast in three duplicate batches per mix in the months January–March 2017. Series 1's focus was shear strength of reinforced concrete short beams. Series 2 was casted in one batch per mix in June – July 2017. Series 2 focused on flexural strength of concrete beams. Furthermore, two specialty cases were select to measure the influence of recycle concrete fines on RAC. The specialty cases had a 15% replacement of cement with either FRCA, #67R-15%FRCA, or fly ash, #67R-15%FA for RAC concrete mix with MSA of 0.75. The specialty cases were investigated in both series. In both series concrete fresh properties, compressive strength and modulus of elasticity was measured for consistence.

4.3 Concrete Fresh Properties

The fresh concrete properties measured were slump, temperature, unit weight, and air content, according to the following standards: ASTM C143, ASTM C1064, ASTM C138, and ASTM C231. For Series 1 testing, three duplicate mixes were cast. Only one set of specialty cases, #67R-15%FRCA and #67R-15%FA, was tested due to limited availability of FRCA.

The nomenclature for the labels are as follows: the first three slots denote the size number, for example #67R1 is MSA of 0.75 inch; the fourth slot denotes coarse aggregate type, i.e., recycled, R, versus granite, G, aggregate; and the last slot denotes which repetition. Table 4.5 shows the resulting properties of fresh concrete mixes.

Table 4.5: Fresh Properties of Concrete Mixes for Shear Beams

Mix	Slump Average (in)	Temperature (^{o}F)	Unit Weight Average (lb/ft^3)	SD
67G	6.2	74	144.9	0.889
67R	6.8	77	143.4	2.18
67R-15FRCA	2*	-	144.6*	-
67R-15FA	7*	80	143.1*	-
87G	8.6	68	144.3	1.69
87R	8.2	68	142.8	0.902
57G	5.6	80	145.0	3.15
57R	4.5	79	144.3	1.96

* values are not averages since only one batch was made

Table 4.6: Fresh Properties of Concrete Mixes of for Flexural Strength

Mix	Slump (inch)	Superplasticizer (oz/100 lbs of cement)	Temperature (^{0}F)	Unit Weight (lb/ft$^{3)}$
67G	4.5	1.6	83.3	144.0
67R	4.125	4.7	83	145.1
67R-15FRCA	5		84	139.3
67R-15FA	3.25	3.2	81	139.9
87G	7.5		82	147.1
87R	9	3.7	-	140.6
57G	3.5	0.83	84	148.1
57R	3.25	2.5	79	142.4

The slump of the mixes ranged from 2 – 9.5 inches, mainly without any admixtures. The lower slumps were due to increased fineness of particles with the addition of FRCA, as well as the high water absorption of FRCA. Moreover, the higher slump might be a result of the modified mix design. Figure 4.1 and 4.2 show a trend shows that the slump increased as the MSA decreases.

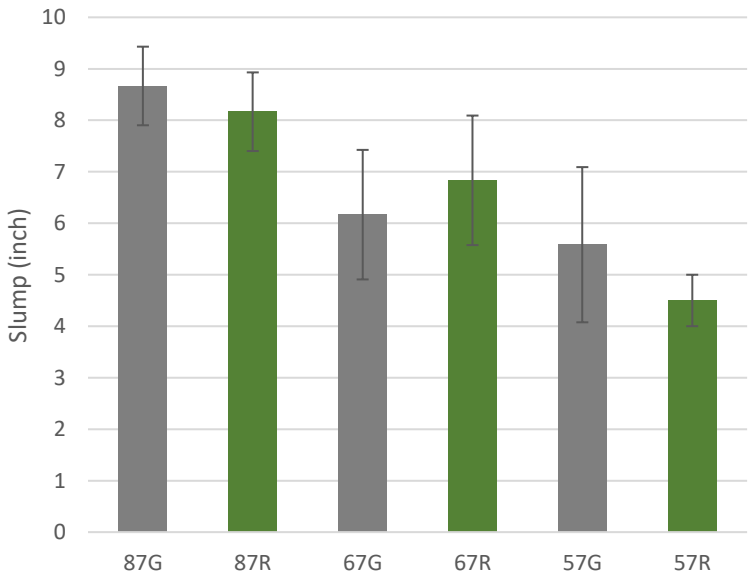

Figure 4.1: MSA versus average slump for shear beams

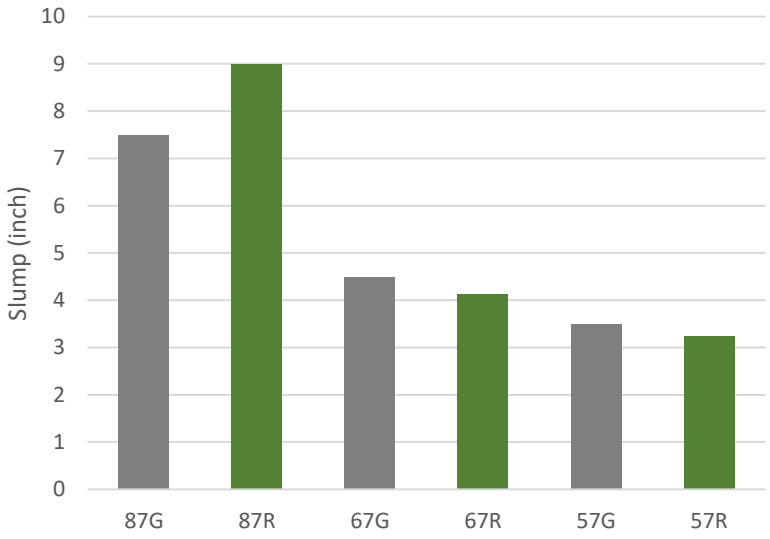

Figure 4.2: MSA versus slump for flexural beams

Nevertheless, the slumps of the RAC were similar to those of the NAC. The unit weight of the mixes' averages ranged from 142.8 – 145.0 lb/ft^3, which correspond traditional concrete

density value of 140-150 lb/ft^3 [61]. In general, the RAC has slightly lower unit weights then NAC and higher standard deviations. The lower unit weight of RAC averages might be due to higher air content percentages and lower specific gravity of the aggregate. The average air content ranged from 1.9 – 4%. This range was slightly higher than expected. However, the air content was not affected by the RCA, i.e., no trends in air content and RCA content were found.

4.4 Compressive Strength

Compressive strength is an important factor for concrete since there are many strength-based standards. The compressive strength depends on several factors including materials, mix properties curing conditions, and testing parameters. The materials are important in terms of the porosity of the concrete. Key materials and mix parameters to consider are type of cement, water-to-cement ratio, aggregate type and size, and admixtures. The curing conditions including type of curing, age, and temperature determine the degree of hydration of the concrete and as a result its porosity. The testing parameters include specimen size, moisture state and testing load rate impacts the measured strength.

The compressive strength was measured according to ASTM C39 in both series of the study. The compressive strength per mix shown in the Table 4.7- 4.8 and Figure 4.5-4.8 are the average of five 4”x8” cylinder per mix at each age. The cylinders were cured in a fog room kept at room temperature, i.e., 73.4°F, and relative humidity of 70% until testing. Prior to testing, the cylinders’ tops and/or bottoms layers were hand-ground to have a level surface. Then, they were placed into a metal testing caps with neoprene bearing pads.

Finally, the cylinders were placed into the testing apparatus and loading at a constant rate of 35 ± 7 psi/s until failure [62].

4.4.1 Influence of Maximum Size Aggregate

Table 4.7 shows the compressive strength results for Series 1 and 2 for 7, 28 and 91-days. Series 1 show the average compressive strength per mix of three batches. Series 2 was done in one batch, so it is only compressive strength per mix.

Table 4.7: Compressive strength per MSA

Concrete Age (days)	7		28		91	
	f'c (ksi)	σ	f'c (ksi)	σ	f'c (ksi)	σ
Series 1						
#87G(AVG)	4.13	0.069	6.35	0.874	-	-
#87R(AVG)	4.73	0.197	5.98	0.332	-	-
#67G(AVG)	5.07	0.282	7.00	0.101	-	-
#67R(AVG)	4.04	0.193	5.59	0.304	-	-
#57G(AVG)	4.93	0.292	6.14	0.287	-	-
#57R(AVG)	4.58	0.327	5.66	0.442	-	-
Series 2						
#87G	5.19	0.174	6.53	0.120	7.27	0.175
#87R	5.34	0.108	6.16	0.245	7.26	0.271
#67G	5.17	0.412	6.58	0.526	7.00	0.337
#67R	4.97	0.368	6.53	0.120	7.29	0.227
#57G	4.70	0.315	6.02	0.203	7.38	0.256
#57R	4.56	0.116	5.63	0.347	6.04	0.036

Based on Table 4.7, the averages of all mixes reached the estimated 28-day strength of 5.5 ksi for 0.45 w/c ratio as defined in the ACI absolute volume method. Figure 4.3 show the failure modes of compressive strength specimens.

Figure 4.3: Failure modes of compressive strength specimens of #57G (top) and #57R (bottom) at 28-day

As since in Figure 4.3, the failure modes of the compressive strength specimens were similar for both RAC and NAC. Based on visual observation, the failure modes were comparable for different MSAs. In addition, the RAC had more fractures through the aggregate than NAC. More fractures through the aggregate could be attributed to better bond with RCA to new mortar as well as RCA being weaker potentially than NA due irregularity of RCA original NA, as seen in Figure 4.4.

Figure 4.4: Close-up of the failed compressive strength specimens

Figure 4.5 shows the overall compressive strength results for 7 and 28-day according to ASTM C39 completed for Series 1.

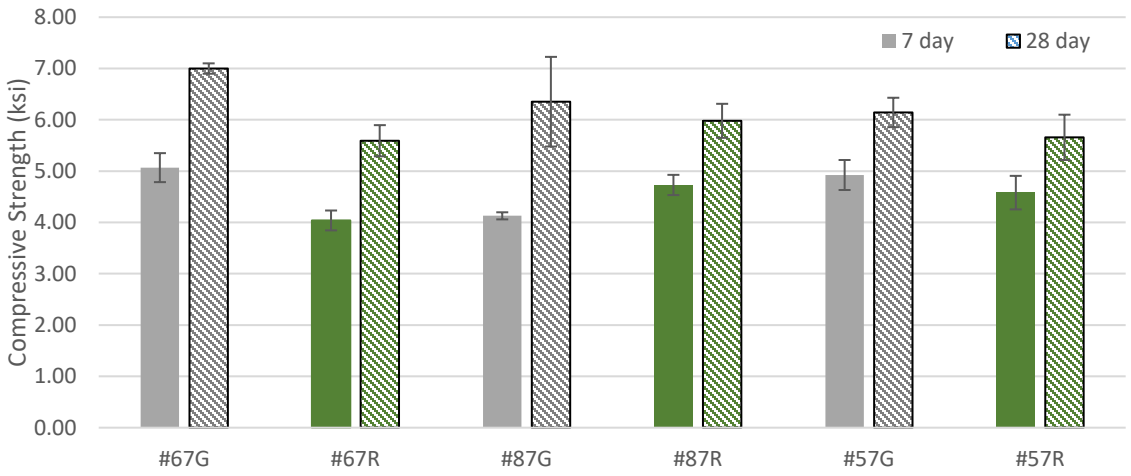

Figure 4.5: Average compressive strength per MSA for series 1

Based on Figure 4.5, the RAC mixes compared to NAC had lower average compressive strengths and higher standard deviation. The strength difference between RAC mixes compared to NAC ranged only from -20% to 15%. On average RAC mixes had around 8% reduction of strength in Series 1 as compared to NAC, which is lower than what was found in previous studies with the range of 12 – 30% [8, 23, 63].

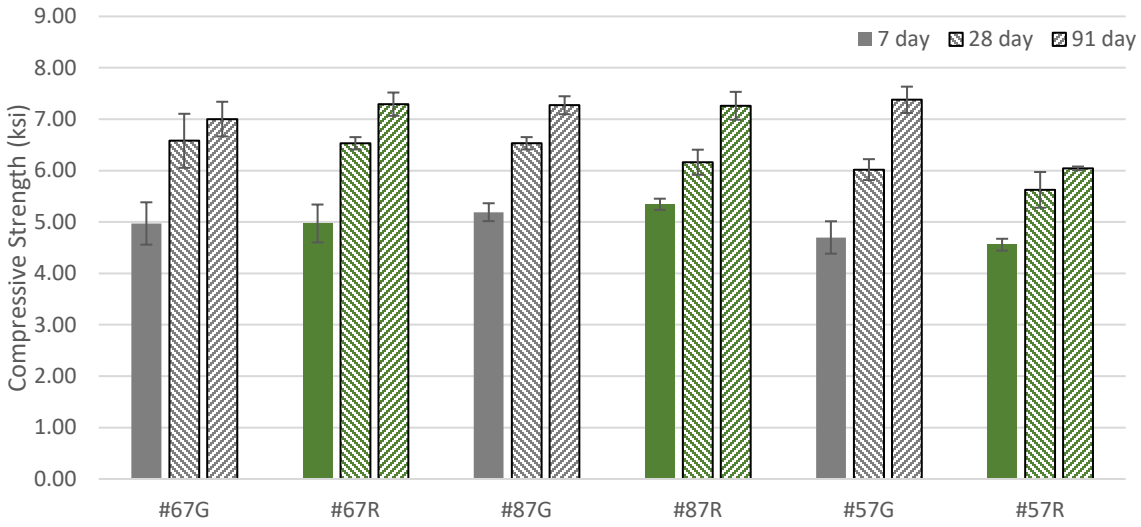

Figure 4.6: Average compressive strength per MSA for series 2

Series 2 of the project shows similar trends to series 1 with lower compressive strength of the RAC mixes than the NAC. In addition, the strength between each mix was closer in Series 2 than Series 1 ranging between 0.15% - 18%. On average, the RAC mixes had around 3% reduction of strength in Series 2 as compared to NAC. At 91-day, both #67R and #87R had higher compressive strength than the NA counterpart. The strength gain between 28 days and 91 days for both #67R and #87R was twice the amount of the NA, while #57R had one-third of the strength gain compared to #57G. This may be due to the RCA releasing excess water in the residual mortar layer that was absorbed during mixing, therefore increasing the degree of hydration and densifying surrounding external ITZ via internal curing.

4.4.2 Influence of Recycled Fines

To study the influence of fines in regard to the RAC, 15% of the Portland cement was replaced by mass with either fine recycled concrete aggregate or Class F fly ash (FA). The #67 size number was selected to study the influence of fines. Series 1 showed lower early age compressive strength; therefore, Series 2 was expanded to 91 days to observe the effect of pozzolanic reaction of fly ash and potentially FRCA. Table 4.8 shows the compressive strength of #67 MSA with 15% replacement by mass of cement.

Table 4.8: Compressive strength of #67 MSA with/without 15% replacement of Portland cement

Concrete Age (days)	7		28		91	
	f'c (ksi)	σ	f'c (ksi)	σ	f'c (ksi)	σ
Series 1						
#67G(AVG)	5.07	0.282	7.00	0.101	-	-
#67R(AVG)	4.04	0.193	5.59	0.304	-	-
#67R- 15%FRCA	4.21	0.231	5.43	0.179	-	-
#67R- 15%FA	3.70	0.144	4.93	0.229	-	-
Series 2						
#67G	5.17	0.412	6.58	0.525	7.00	0.337
#67R	4.97	0.368	6.53	0.120	7.29	0.227
#67R- 15%FRCA	3.66	0.132	4.87	0.222	5.37	0.080
#67R- 15%FA	4.46	0.188	5.72	0.092	7.00	0.096

Due to the delayed pozzolanic reaction of fly ash and partial replacement of cement, both #67R-15%FRCA and #67R-15%FA resulted in lower compressive strengths than both #67R and #67G. Figures 4.5 and 4.6 show the effect of including fines for Series 1 and 2.

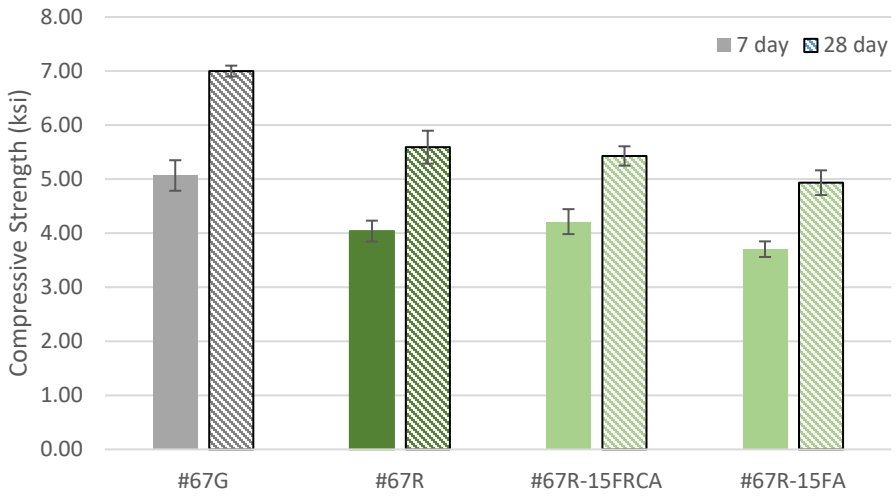

Figure 4.7: The effect of fines for Series 1

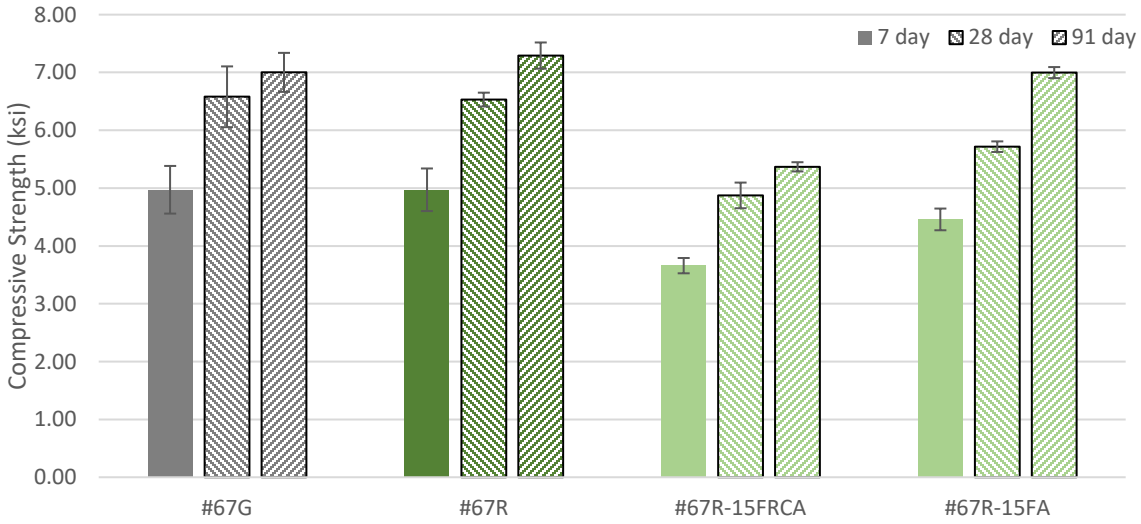

Figure 4.8: The effect of fines for Series 2

The difference between Series 1 and Series 2 results are that #67R-15FA shown higher strength in Series 2 than Series 1 and the opposite is true for #67R-15FRCA. As expected, in Series 2 the delay pozzolanic reaction observed with #67R-15FA.

4.5 Modulus of Elasticity

The modulus of elasticity is the measure of stress to reversible strain [30]. Since concrete is heterogeneous material, the modulus of elasticity of concrete is a combination of each constituent and affected by the formation of the bond between constituent. The modulus of elasticity depends on several components, including aggregate, cement paste matrix, interfacial transition zone, moisture conditions, and loading rate [30]. The porosity of both aggregate and cement paste matrix are important factors of the E. Porosity impacts the overall stiffness; thus, porosity has a negative correlation to E. Finally, testing conditions such, as moisture and loading rate, also effect the measured modulus of elasticity.

Static modulus of elasticity was measured according to ASTM C469. The compressive strength was measured using average of five 4- by 8-inch cylinders. The static modulus was measured with three 6- by 12-inch cylinders. The cylinders were loaded to 40% ultimate load at a loading rate was 35 ± 7 psi/s [64]. Figure 4.9 shows the testing schematic for modulus of elasticity.

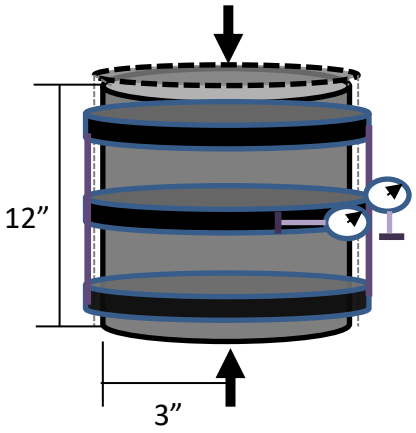

Figure 4.9: Modulus of elasticity schematic

The modulus of elasticity of measured in both series of study. In Series 1, the modulus of elasticity is the average of three sets of three cylinders. In Series 2, the modulus of elasticity was the average of one set of three cylinders.

4.5.1 Influence of Recycled Concrete Aggregate

Figure 4.10 shows the measured static modulus of elasticity for both series at 28 days.

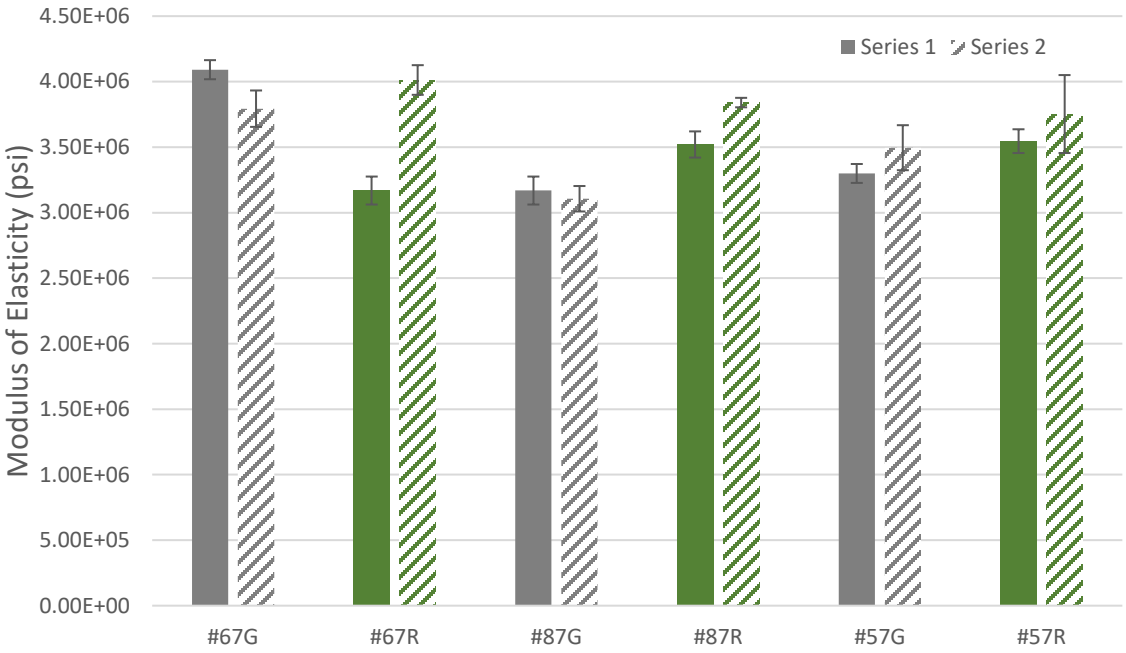

Figure 4.10: Modulus of elasticity of concrete cylinders in Series 1 and 2 at 28 days

The measured static modulus of elasticity ranged from 3.11–4.43 x 10^6 psi. In both series, the RAC had a range percent difference of -20% to 19% static modulus of elasticity compared to the NAC. In general, the RAC was greater than the NAC with the exception is #67 in Series 1. These findings disagree with previous studies, which state the with RCA lowers the modulus of elasticity in comparison to NAC [28, 39] . However, agreed with the findings Ho et al that found the modulus of elasticity to be statically the same for NAC and RAC at different replacement level of coarse aggregate [22]. In addition, the #67 had the highest E out of the group of MSA. The static modulus of elasticity was higher for recycled aggregate potentially due to enhanced bond of aggregate-to-cement matrix due to absorption of the mixture, reducing the porosity of the external ITZ [23]. Furthermore, the increased amounts of coarse aggregate in the RAC could have led to an increase of modulus of elasticity.

4.5.2 Influence of Recycled Fines

Figure 4.11 represents measured static modulus of elasticity at 28 days with 15% replacement of cement with fines.

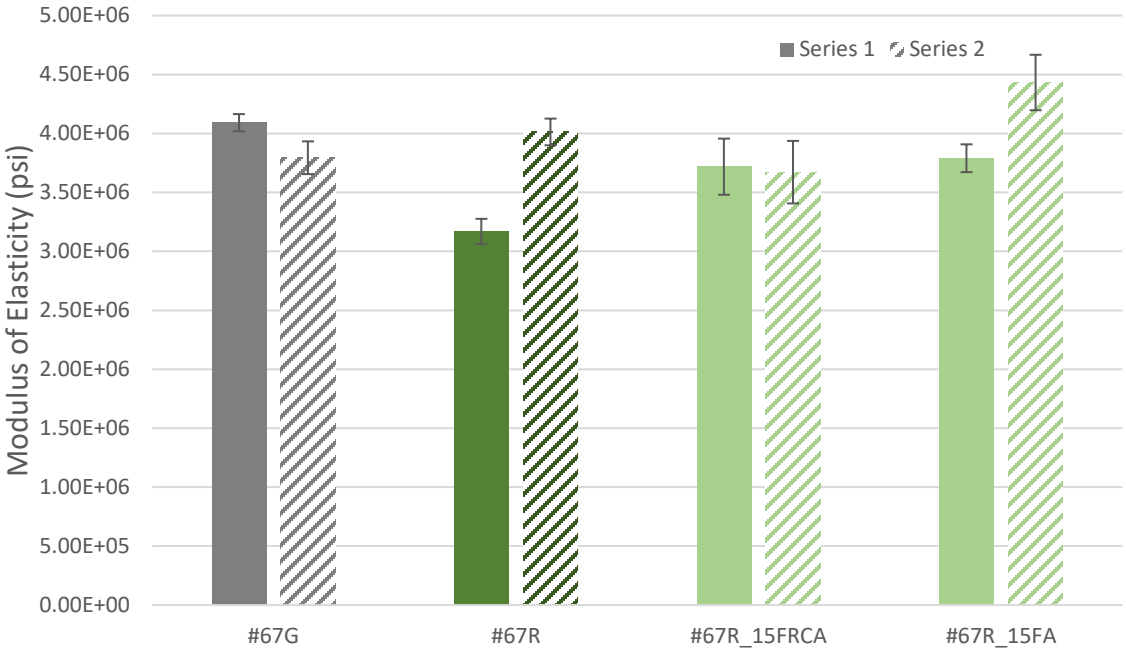

Figure 4.11: Modulus of elasticity of concrete cylinders with/without fines in Series 1 and 2 at 28-day

As seen in Figure 4.11, the modulus of elasticity increased in Series 1 for both #67R_15FRCA and #67R_15FA in comparison to #67R, but it was lower than #67G. In both series, #67R_15FRCA had a similar static modulus of elasticity around $3.7x10^6$. However, #67R_15FA in Series 2 was greater than both #67R and #67G. The higher performance of the could be attributed to the pozzolanic reaction of FA and filler effect of

both FRCA and FA, since it will help densify and refine the concrete paste matrix; lowering the porosity of concrete and enhancing the modulus of elasticity.

4.5.3 Comparison of Measured to Estimated Modulus of Elasticity by Compressive Strength

In the concrete industry, the modulus of elasticity of concrete is often estimated based on the compressive strength. The American Concrete Institute (ACI) has several equations to make such an estimate, which are developed based on empirical data. Two common equations are ACI 363 for high-performance concrete and ACI 318 for normal concrete, where w_c is the unit weight of the concrete and f'_c is the compressive strength [65, 66].

$$E_{ACI363} = 4000\sqrt{f_c'} + 1 * 10^6 \qquad 3000 \text{ psi} < f'_c < 12000 \text{ psi} \qquad (4.1)$$

$$E_{ACI318} = 33 * {w_c}^{1.5}\sqrt{f_c'} \qquad 94 \text{ lb/ft}^3 < W_c < 156 \text{ lb/ft}^3 \qquad (4.2)$$

ACI 318 tends to overestimate modulus of elasticity for compressive strengths over 6,000 psi. Therefore, ACI 363 is recommended for high strength concrete. Table 4.9 shows the comparison of measured to estimated modulus of elasticity for Series 1.

Table 4.9: Comparison of measured to estimated modulus of elasticity for series 1

MSA	UW (lb/ft^3)	f'c (psi)	E_m (PSI)	$E_{ACI\ 363}$	$E_{ACI\ 318}$
#67G(AVG)	144.9	6999.1	4.09E+06	4.35E+06	4.82E+06
#67R(AVG)	143.4	5591.7	3.80E+06	3.99E+06	4.24E+06
#87G(AVG)	144.3	6352.9	3.17E+06	4.18E+06	4.56E+06
#87R(AVG)	142.8	5980.2	3.52 E+06	4.09E+06	4.35E+06
#57G(AVG)	145.0	6143.5	3.30 E+06	4.14E+06	4.52E+06
#57R(AVG)	144.3	5658.2	3.55 E+06	4.01E+06	4.30E+06

As shown in Table 4.9, equations for modulus of elasticity tends to overestimate the measured modulus of elasticity. Since, most of the compressive strengths was over 6 ksi, ACI 363 was the more conservative compared to ACI 318.

4.6 Shear Strength of Short Beams

As discussed previously, shear strength of a reinforced concrete beam is dependent on three key components including interactions of aggregate interlock, dowel action, and compression zone. In this study, dowel action can be assumed to remain constant since the rebar remains constant and the compressive zone are similar. Therefore, the main influence on the shear strength of these beams is the aggregate interlock. As seen in previous studies, there is a positive correlation between increase of MSA and aggregate interlock in deep beams [40]. This study's focus is on the shear strength of short beams. Short beams have a span-to-depth ratio of 1–2.5 and behave similarly deep beam where it fails within the D-region, as seen in Figure 4.12.

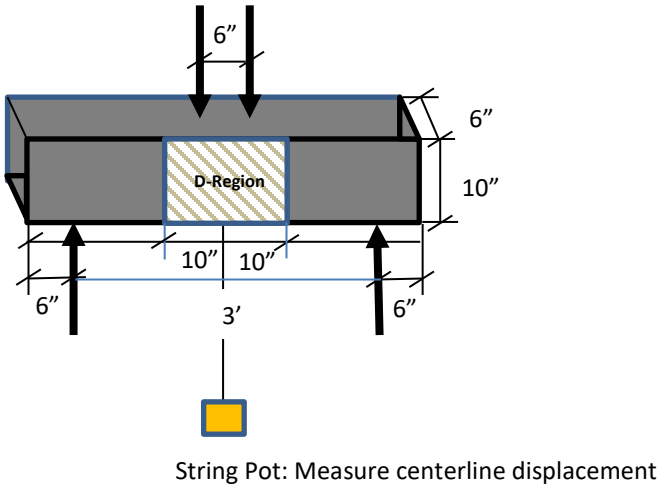

Figure 4.12: Schematic of shear strength test with short beam

Therefore, shear strength of short beams is increased due to arch actions, and traditional shear equations tends to be conservative. Nevertheless, the failure modes of shear beams are similar. The failure of shear beams can be cause by either bond failure, splitting failure, or dowel failure along the tension reinforcement.

The short shear beams were 6- by 10- by 48-inch rectangular cross-section. The span-to-depth ratio of the beams was 1.9. The beams were loaded into 4-point bending incrementally using an electric pump, which loaded the beam approximately 1 kip per pump during the test. The beam was inspected for cracks after each pump until it was close to failure. The mid-point displacement was measured using a string pot attached at the bottom center of the beam. The load was measured using a load cell, which was calibrated prior to use.

4.6.1 Influence of Maximum Size Aggregate

Table 4.10 shows the results of the shear beams in terms of maximum deflection and shear strength.

Table 4.10: Average maximum load and deflection of short beams

	Δ (inch)	**Vu (kip)**	**Vu (psi)**
#67G(Avg)	0.63	50.22	837.0
#67R(Avg)	0.58	45.50	758.3
#67R-15FRCA	0.63	49.64	827.4
#67R-15FA	0.95	50.79	846.6
#87G(Avg)	0.35	47.23	787.2
#87R(Avg)	0.56	50.59	843.2
#57G(Avg)	0.50	49.68	827.9
#57R(Avg)	0.53	42.85	714.1

Figure 4.13 and 4 .14 shows the average shear strength and max deflection of short beams. The short beams failed a 3 times higher shear strength than estimated by traditional shear strength equations in ACI 318-14. This is due to additional, arching actions of short beam often mentioned as size effect. In general, the RAC shear beam deflected more than NAC and failed at lower strengths. One expectation is #87R, and #87R, which had the largest shear strength average overall- even greater than its NAC counterpart. Nevertheless, statically, the NAC and RAC performed the same.

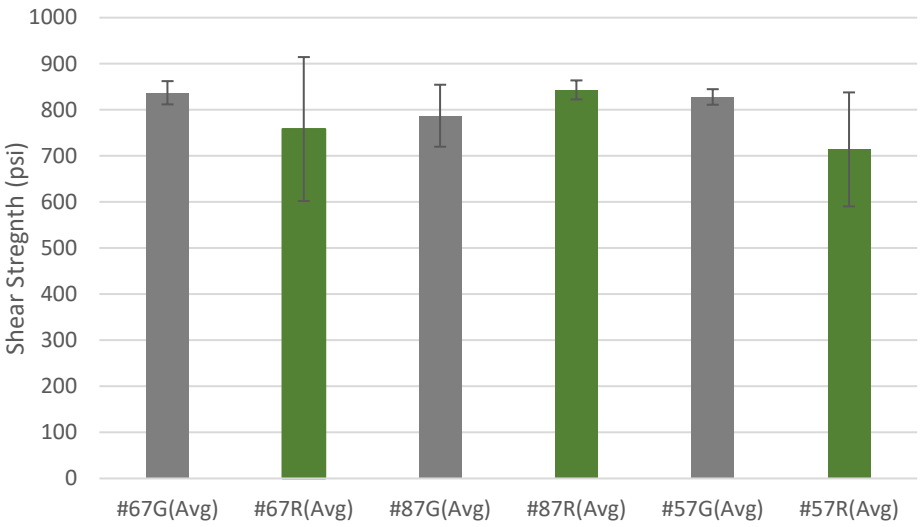

Figure 4.13: Average shear strength of short beam

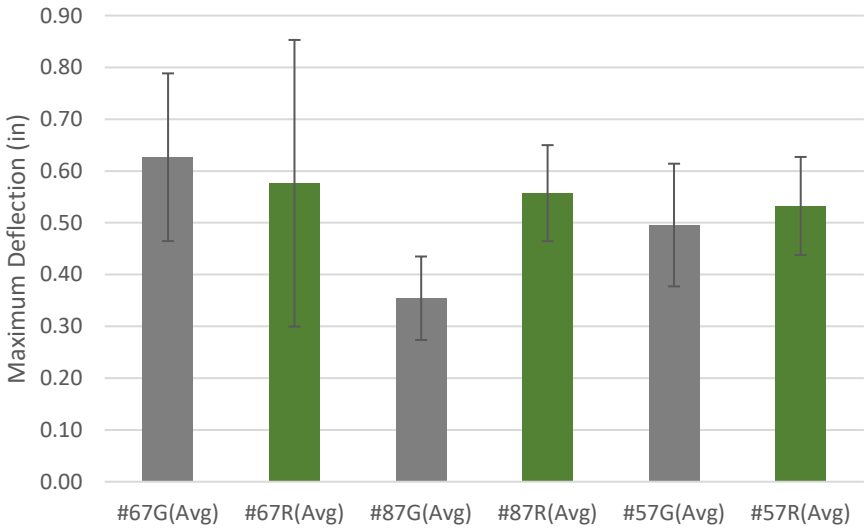

Figure 4.14: Average maximum deflection of short beam

The RAC shear strength increase with a decrease of MSA; however this trend does not hold true for the NAC. Shear strengths were measured after 28 days. The shear strength -

deflection curves and failure modes were similar for NAC and RAC. Figures 4.15–4.17 show the load deflection curve of #67, #87, and #57.

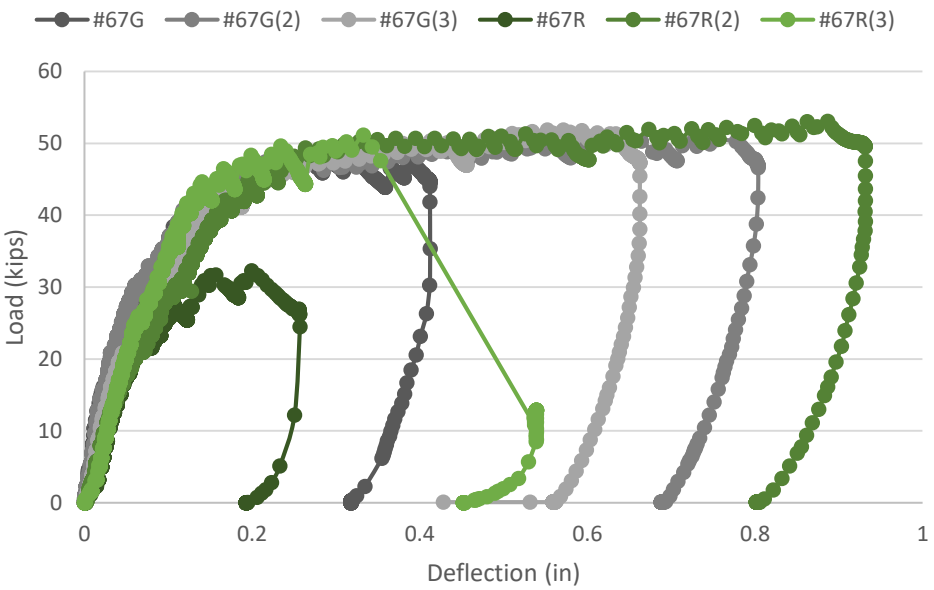

Figure 4.15: #67 load verses deflection curves

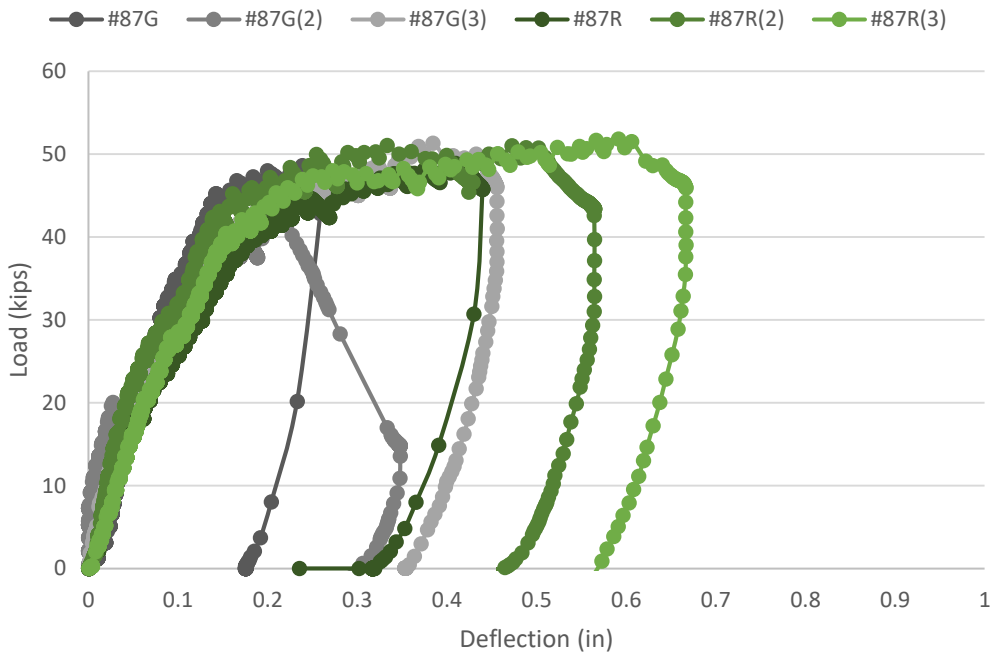

Figure 4.16: #87 load verses deflection curves

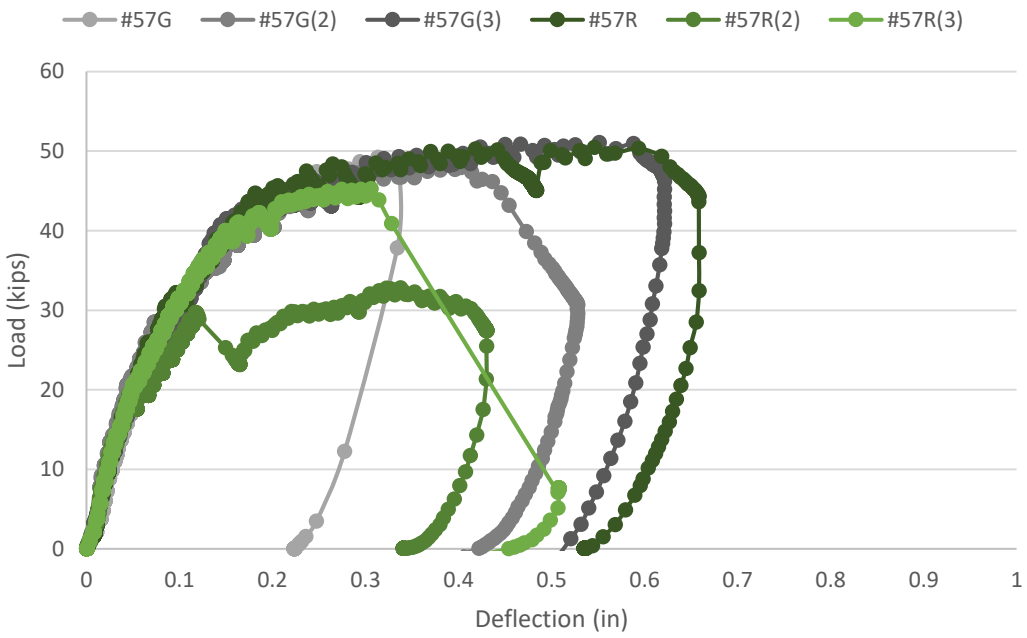

Figure 4.17: #57 load verses deflection curves

The load verse deflection curves show that MSA #67 absorbed more energy prior to failing. In general, the following is the order of energy absorption by size number: (1) #67, (2) #57, and (3) #87, as seen in Table 4.11.

Table 4.11: Average energy absorption the area under the curve of load – deflection graph

	Energy Absorption (kip-in)
#67G(Avg)	25.82
#67R(Avg)	21.65
#87G(Avg)	11.26
#87R(Avg)	21.16
#57G(Avg)	17.89
#57R(Avg)	17.60

In general, the NAC tend to absorb more energy than RAC, except in the case of #87, for which RAC had double the amount absorbed energy. The dips in load – deflection graphs show formation of large cracks or sudden failures of the beam. In addition, the cracking pattern for RAC and NAC are similar, starting with small flexure cracking and then developing large shear cracking that extend to top and bottom of the beam. The shear failure shown the development of compression struts. Example crack pattern for short shear beams are shown, below in Figure 4.18 and 4.19.

Figure 4.18: Failure crack pattern of #87G (left) and #87R (right)

Figure 4.19: Failure along reinforcement

Due to weaker concrete on top, a few of the beams failed by crushing at the top of the beam in the compression zone, along with large diagonal cracking. Two beams seem to have failure along the reinforcement, as seen in Figure 4.19, which is due to the rebar splitting. The majority of the beams failed due to splitting along the compression strut.

4.6.2 Influence of Recycled Fines

The inclusion of the FRCA and FA had a slight improvement over the average shear strength of #67R, as seen in Table 4.10 and Figure 4.20.

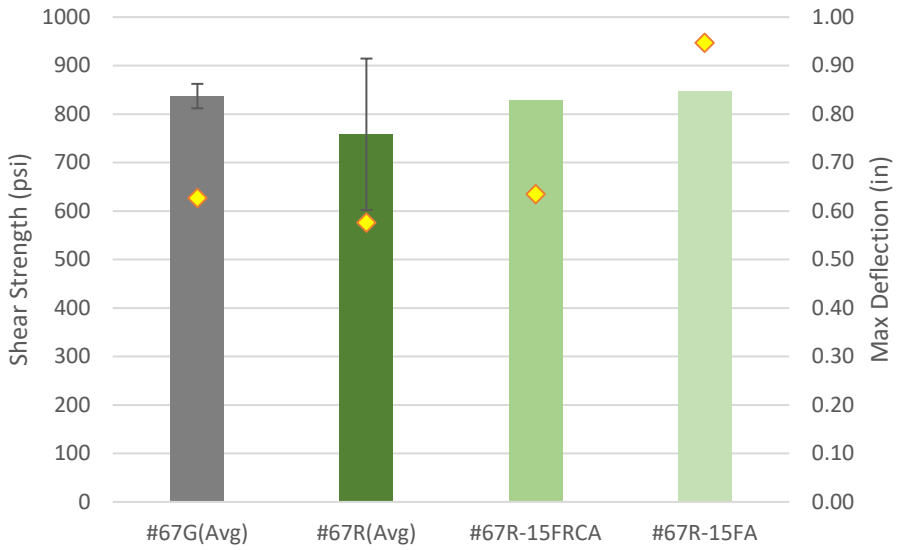

Figure 4.20: Shear Strength and Max Deflection of #67 with/without fines

In addition to the increase in shear strength, the maximum deflection also slightly increased. Figures 4.21 shows the load deflection curve of #67 with the inclusion of FRCA and FA.

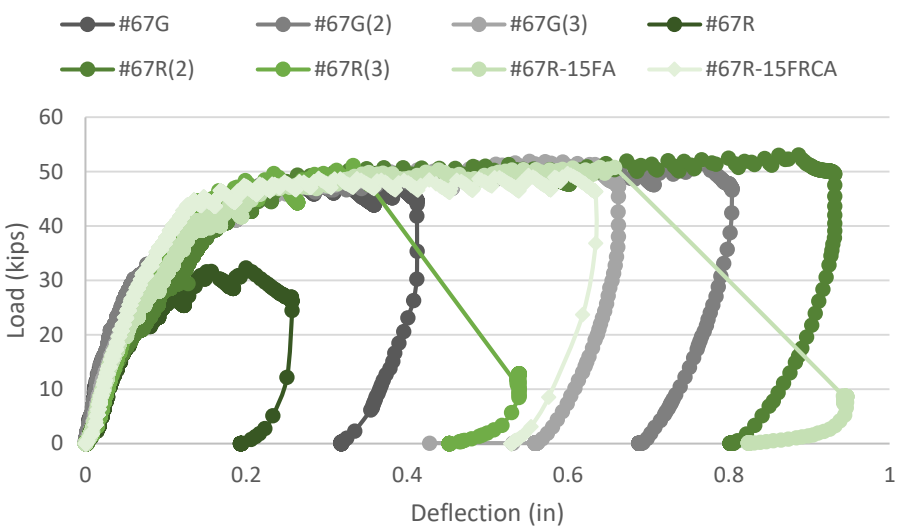

Figure 4.21: #67 load verses deflection curves

In comparing load deflections curves, the fines increased absorbed energy. Whereas, #67R-15FA had highest energy absorption of with 36.6 kip-in and failed suddenly similar to #67R(3). Nevertheless, the beams had similar failure pattern as the NAC.

4.7 Flexural Strength

The flexural strength is an indirect measure of tensile strength. The tensile strength depends on the propagation of cracks. Concrete is weak in tension; it can carry approximately one-tenth of its compressive strength [30]. The flexural strength is measured by the modulus of rupture. Depending on the strength of the concrete, the modulus of rupture can overestimate the strength by 1.5 to 2 times the direct tensile strength [30]. This inaccuracy is due to how it is tested in three-point bending. Despite three-point bending often overestimating tensile strength, it is relevant for concrete that experiences more bending modes, such as

pavements. The tensile strength depends on the compressive strength and is affected by similar factors, whereas, both shear and bond strengths depend on tensile strength.

The flexural strength specimens were tested according to ASTM C78. For each mix, four 6- by 6- by 24-inch beams were cast. The beams were fog cured until 28 days then tested in three-point bending. The beams were loaded at a constant rate of 1,200 lb/min until failure [67]. Figure 4.22 shows the sketch of flexure test schematics.

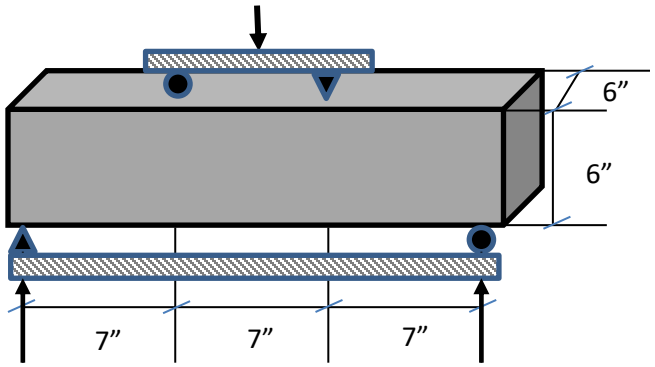

Figure 4.22: Flexural strength test schematics

The modulus of rupture, R, was calculated using Equation 4.3, where P is the maximum load, L is the length, b is the width, and d is the depth of specimen, as shown in Figure 4.22 [67].

$$R = \frac{PL}{bd^2} \tag{4.3}$$

4.7.1 Influence of Maximum Size Aggregate

Figure 4.23 shows the measured flexural strength of concrete specimens per change of maximum size aggregate. The average flexural strength ranged of the concrete mixes are 750 – 820 psi.

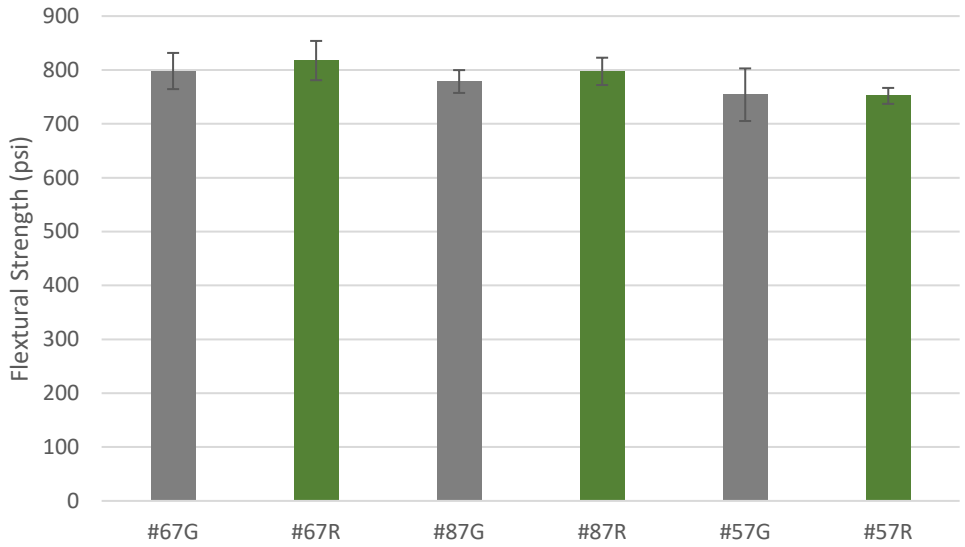

Figure 4.23: Flexural strength of concrete specimens

In general, the flexural strength of RAC was comparable to NAC. This results confirm previous research where RCA has negligible influence on flexural strength [8]. The difference between flexural strength of RAC and NAC are within the variation of ASTM C78. The flexural strength was highest for #67, followed by #87 and then #57, similar to the pattern shown in compressive strength. Figure 4.24 show the comparison of flexural strength to compressive strength.

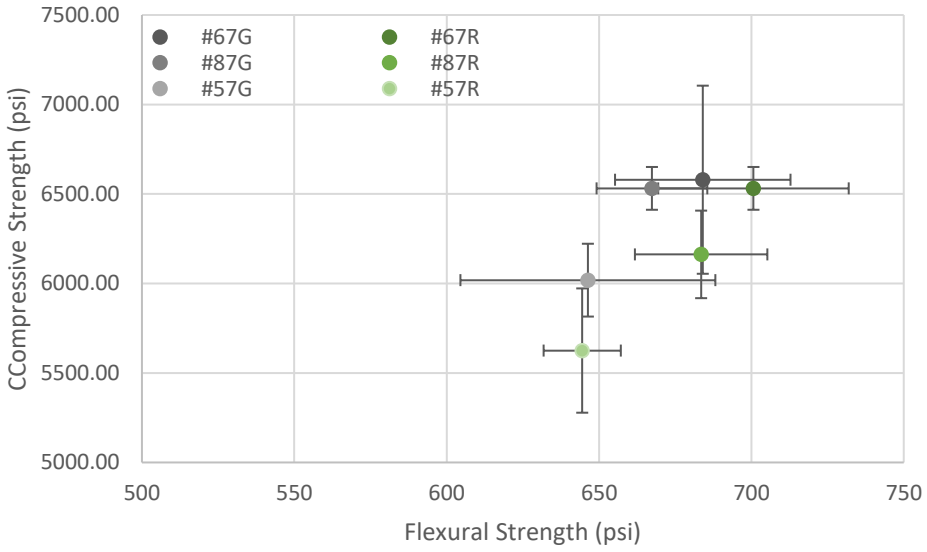

Figure 4.24: Flexural strength versus compressive strength at 28 days

The flexural strength and compressive strength of Series 2 at 28 day correlates well, as seen in Figure 4.24. The R^2 for all the mixes was 0.592, the RCA mixes was 0.987, and NA mixes was 0.863. In general, the flexural strength increased as compressive strength increased for both NAC and RAC.

4.7.2 Influence of Recycled Fines

Figure 4.25 shows the measured flexural strength of concrete specimens for #67 with inclusions of fines.

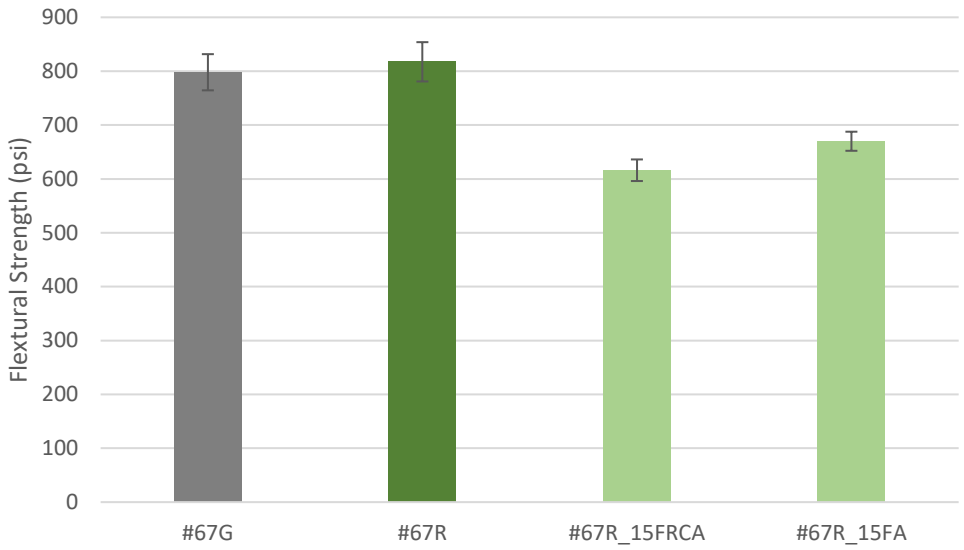

Figure 4.25: Measured flexural strength of #67 concrete specimens with inclusion of fines

At 28 days, #67R with fly ash and with recycled fines had 20% or 28% lower flexural strength than #67R, respectively. This is due to the slower acting pozzolanic reaction of fly ash and the reduction of cement. The flexural strength and compressive strength of Series 2 at 28 days correlates well with the inclusion of fines, and the R^2 is 0.944.

CHAPTER 5. DURABILITY OF RECYCLED AGGREGATE CONCRETE

This chapter focuses on the effect of the maximum size aggregate of the recycled concrete aggregate on the durability of the recycled asphalt concrete. Permeability, resistance to chloride penetration, and expansion due to alkali–silica reaction were assessed. Based on previous studies, as mentioned in the literature review in Chapter 2, the RCA content tends to increase both permeability and chloride penetration of concrete [8, 14, 29, 34, 35, 39]. In terms of ASR, previous studies showed inconsistent performance of the RCA in terms of expansion [3, 43]. Permeability was measured using the rapid chloride penetration test (RCPT) and resistivity, according to ASTM C1202 and AASHTO 358-17.

5.1 Permeability

5.1.1 Rapid Chloride Penetration Test

The RCPT is the measure of electrical current that passes during a 6-hour period. The RCPT was used to measure permeability on cylinders moist cured for 28 and 91 days on a set of four 2-inch-thick and 4-inch-diameter cylinder cuts. Figure 5.1 shows the average

RCPT results measured at 28 days for Series 1. The colored dashed lines on Figure 5.1 show the recommended guidelines for penetrability level based on ASTM C1202 [68].

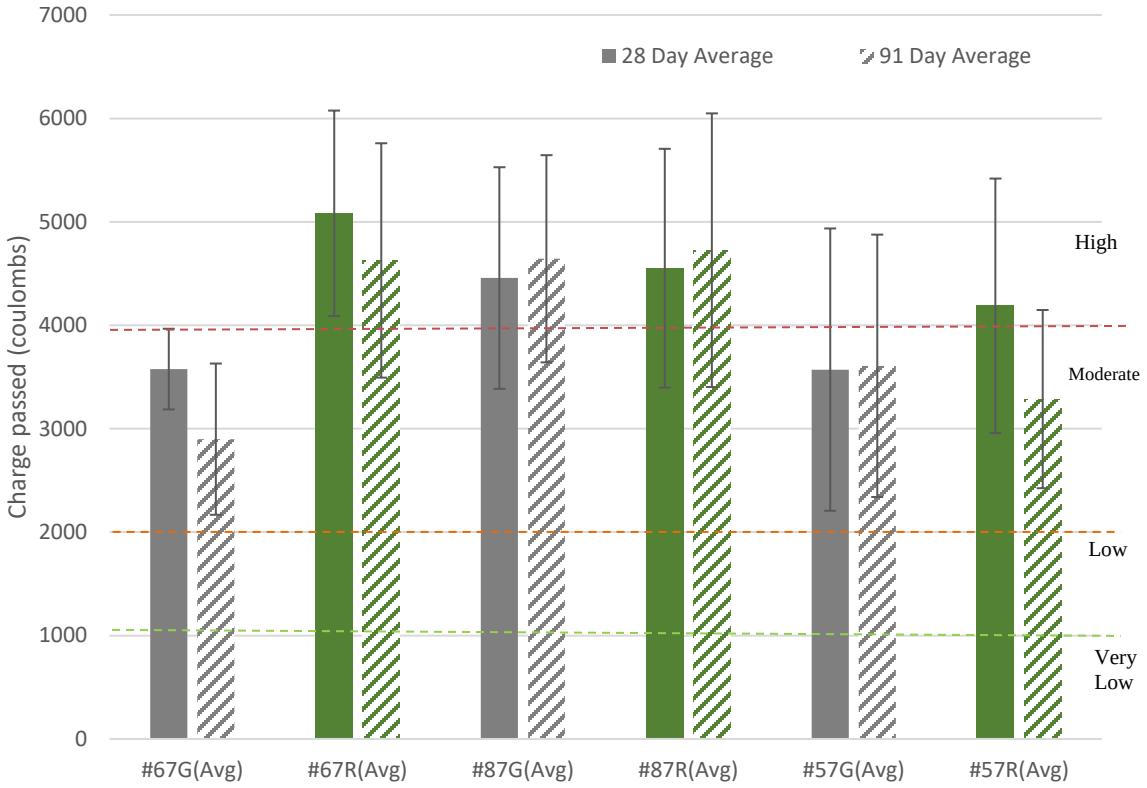

Figure 5.1: 28-day and 91-day average RCPT results for Series 1

The RCPT results show that all mixes except for #67G and #57G had high permeability level at 28-days, while #67G and #57G had moderate permeability. In general, the RCPT was higher for the RAC mixes than the NAC. The exceptions #87R which had negligible difference from the #87G. Furthermore, as the MSA increased, the charged passed decreases. The RCPT results in Series 1 showed #67G, #57G, and #57R had moderate permeability level at 91-days, and all others have high permeability. It is interesting to note, approximately one-half of the 91-day results had a greater charge passed than 28-day

results, although it would be expected that the RCPT results would remain the same or decrease due to further hydration of the cement particles. Unlike in Series 1, all specimens in Series 2 showed a reduction in charged passed between 28 and 91-day, as shown in Figure 5.2.

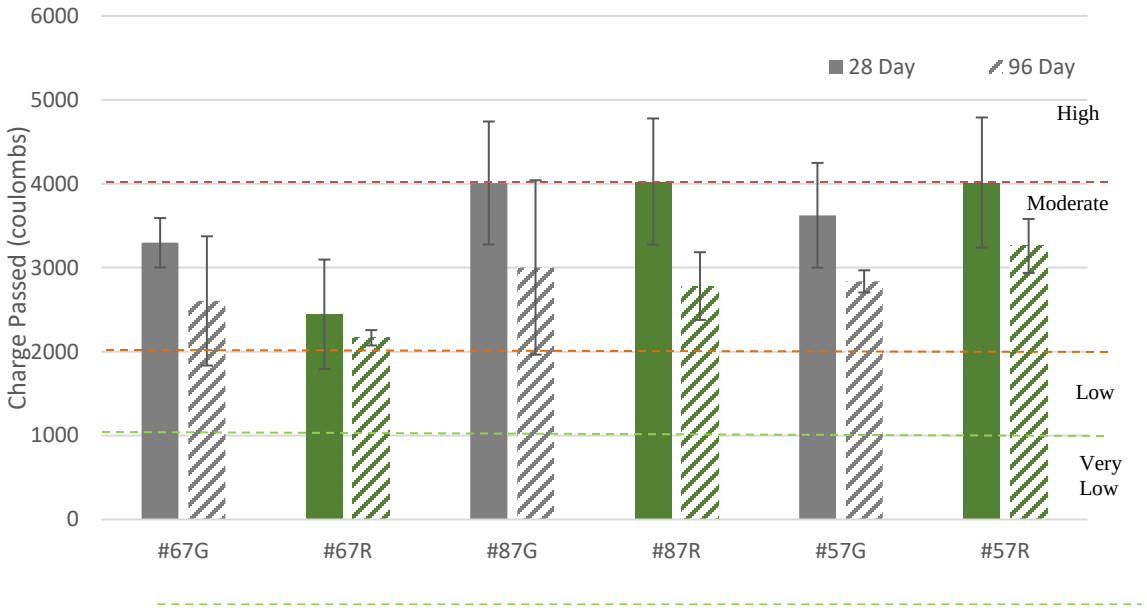

Figure 5.2: 28-day and 91-day average RCPT results for Series 2

In Series 2, there was no trend on the impact of MSA on RCPT results, and both NAC and RAC had comparable permeability as measured by RCPT.

Figure 5.3 shows influence of addition of fines on #67 in both Series 1 and 2. The permeability was measured by the RCPT at 91-day to observe slow reacting pozzolanic reaction. As shown in Figure 5.3, the charge passed was reduced by nearly one-half of 28-day result from high to moderate permeability level at 91 day in Series 1 as the result of pozzolanic reaction of fly ash.

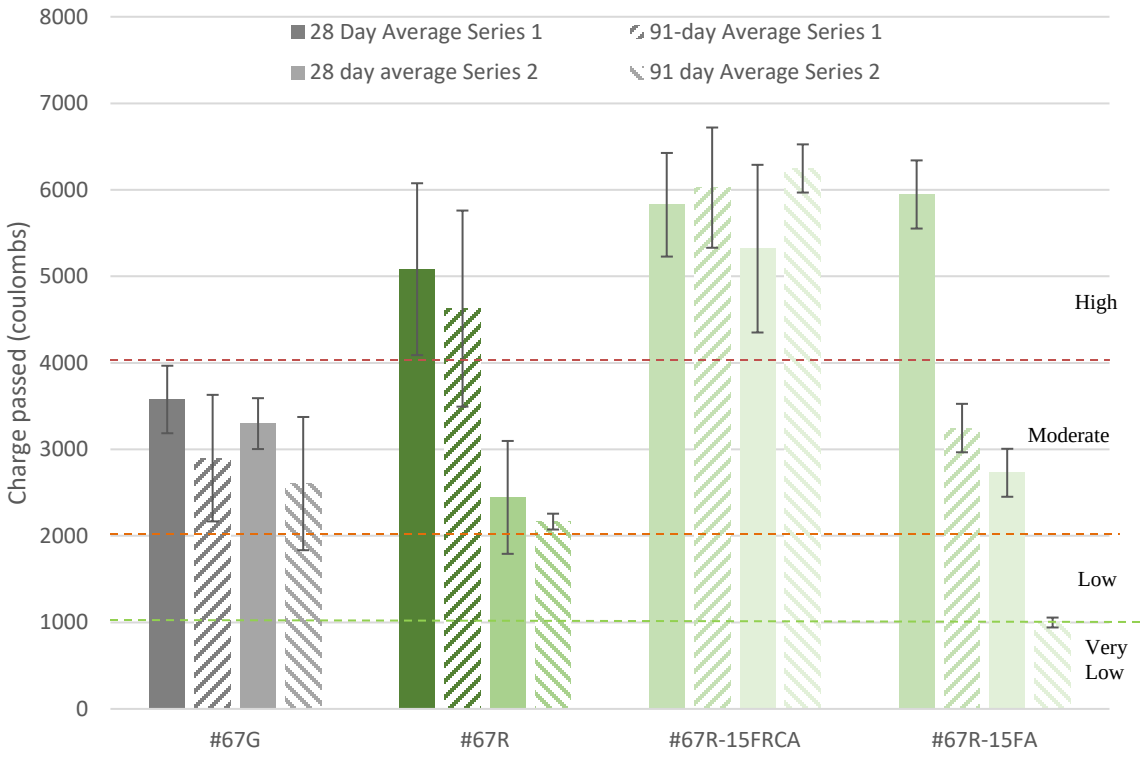

Figure 5.3: 28-day and 91-day RCPT for #67 with/without fines results for Series 1 and 2

Figure 5.3 show that the RCPT results in Series 2 indicated #67R-15FRCA had a high permeability level at both 28 and 91-day and all other specimens in Series 2 have moderate permeability. Similar to Series 1, #67R-15FA had a reduction of more than one-half of 28-day charged passed to 91-day as it moved from moderate to very low permeability level. In addition, #67R-15FRCA had the highest amount of charge passed in both parts and increase in charged passes between 28 and 91 days.

5.1.2 Surface Resistivity

Surface electrical resistivity is the measure of the concrete's surface ability to resist electrical charge. The surface resistivity can be used as an indicator of the concrete

permeability as well as the chloride penetration resistance. In addition to factors affecting permeability, including porosity and pore network connectivity, surface resistivity measurements are affected by other factors including pore solution chemistry, cure conditions, temperature, and humidity [69]. Oftentimes, the surface resistivity correlates well with RCPT results of above R^2=0.9 [69, 70]. Table 5.1 shows the recommended permeability limits for both RCPT and surface resistivity from AASHTO 358-17.

Table 5.1: Permeability levels for RCPT and Surface Resistivity [69]

Permeability Level	**Charge Passed (coulombs)**	**Surface Resistivity (kΩ-cm)**
High	> 4,000	< 12
Moderate	2,000 – 4,000	12 - 21
Low	1,000 – 2,000	21 - 37
Very Low	100 – 1,000	37 - 254
Negligible	< 100	> 254

The test setup for both tests are as follows: One cylinder per mix was used to measure resistivity. The cylinder was cured in a fog room, and was measured on four locations along the length of the cylinder at 90° around the circumference of the cylinder. The surface resistivity was taken at three different time intervals during the curing process: early age, 1–7 day: measured once daily; adolescence, 7–28 day: measured three times weekly; and mature, above 28 days: measured once weekly. Figures 5.4–5.7 show the measured surface resistivity of all the mixes, the mixes' averages, and each of the averages per MSA. The

outliers, i.e., defined data points outside of the 95% confidence interval, were removed from the figures.

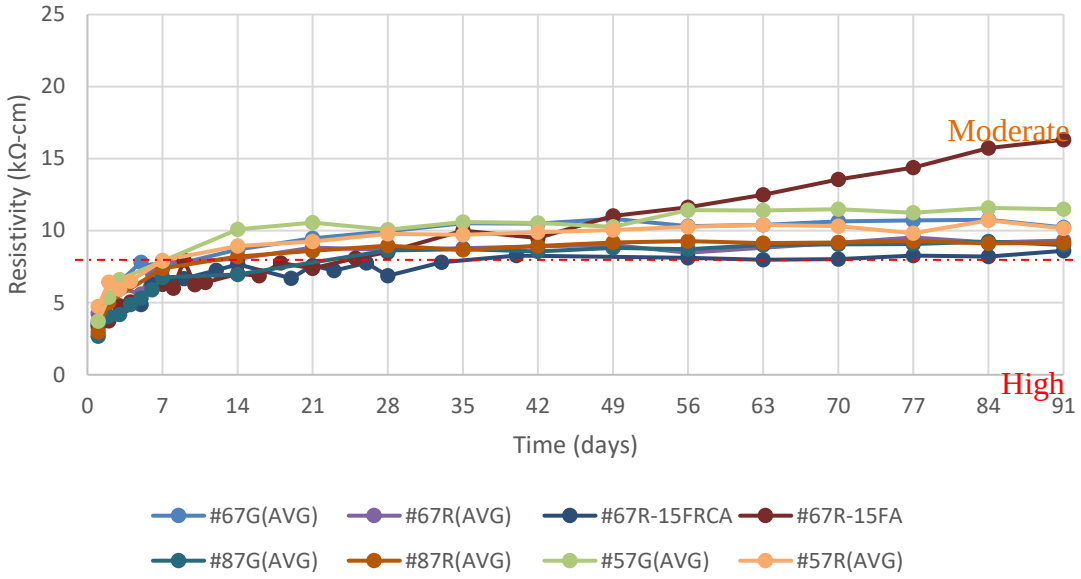

Figure 5.4: The average surface resistivity per MSA to 91 days for Series 1

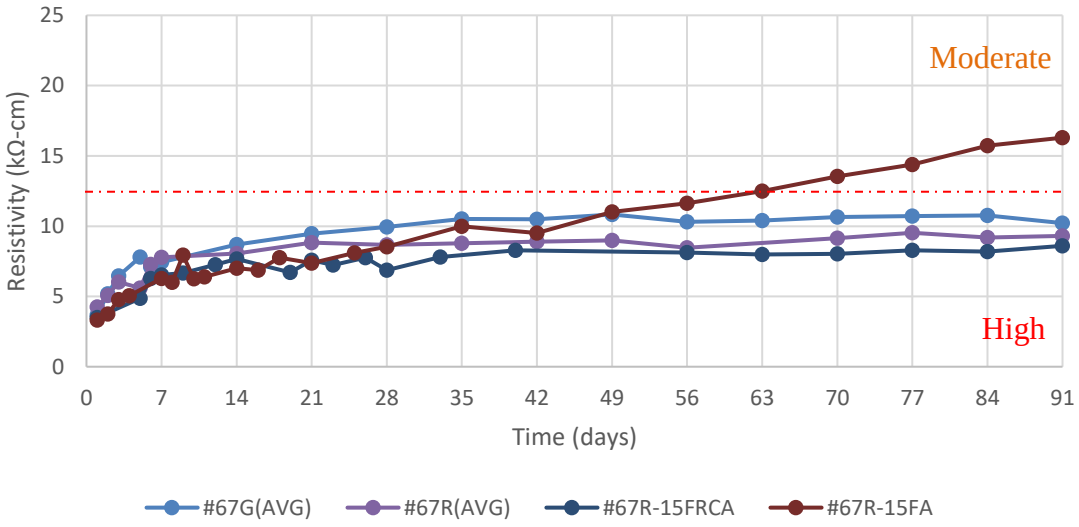

Figure 5.5: The average surface resistivity of MSA #67 to 91 days for Series 1

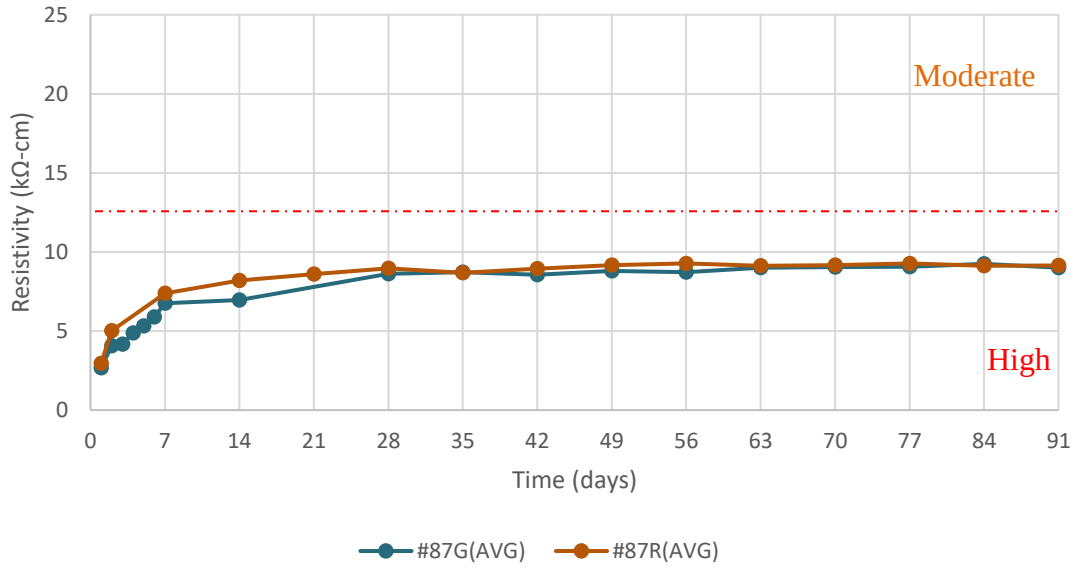

Figure 5.6: The average surface resistivity of MSA #87 to 91 days for Series 1

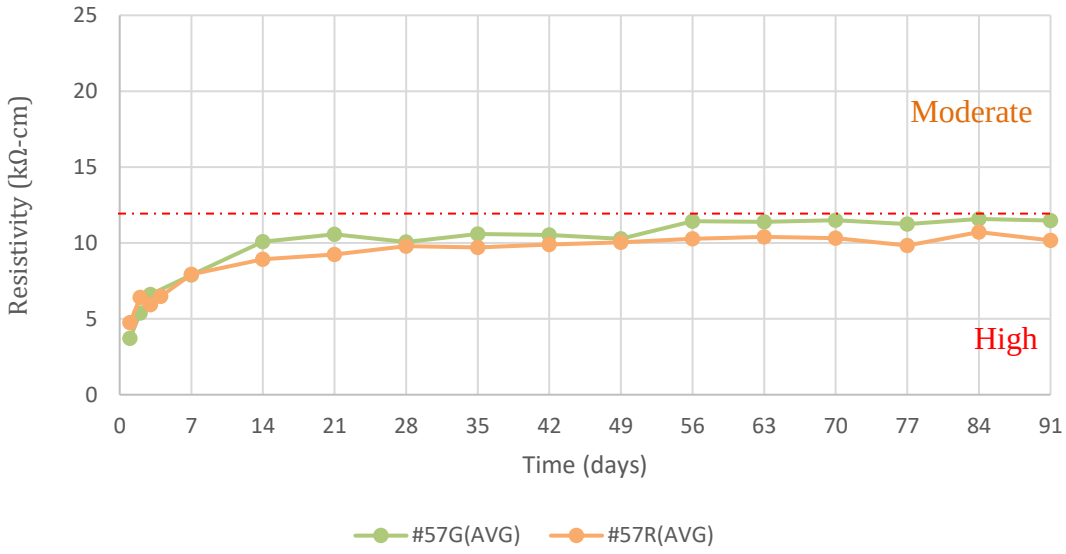

Figure 5.7: The average surface resistivity of MSA #57 to 91 days for Series 1

The surface resistivity of all the mixes were within high permeability level at 28 days. In general, all the mixes had a similar performance, and the difference between RAC and NA is negligible as seen in Figures 5.5 – 5.7. The average surface resistivity was around 10 kΩ-cm.

MSA had negligible effect on the surface resistivity. However, there was positive correlation between MSA and surface resistivity. Similar trends were seen in Series 2. Figures 5.8 -5.11 show the surface resistivity of the eight mixes for Series 2.

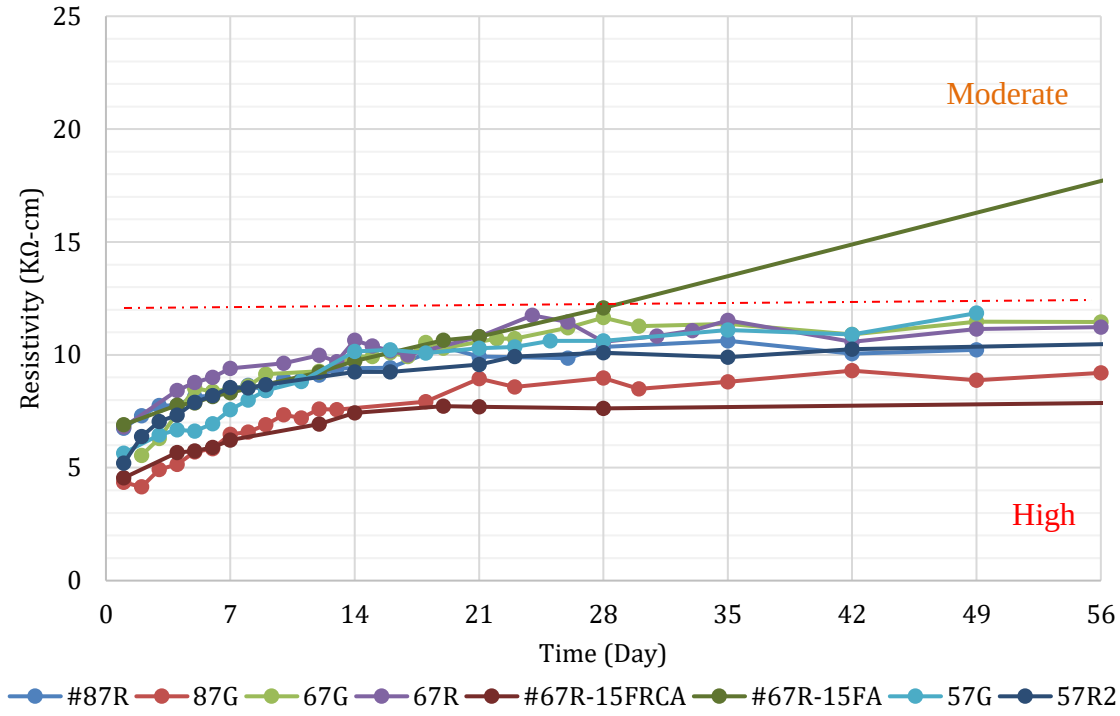

Figure 5.8: The average surface resistivity of mixes to 49 days for Series 2

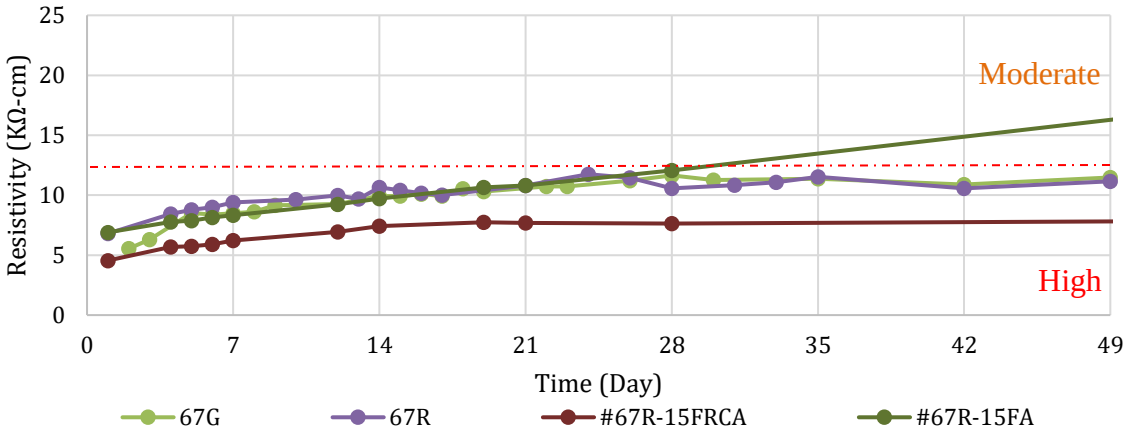

Figure 5.9: The average surface resistivity of MSA #67 to 49 days for Series 2

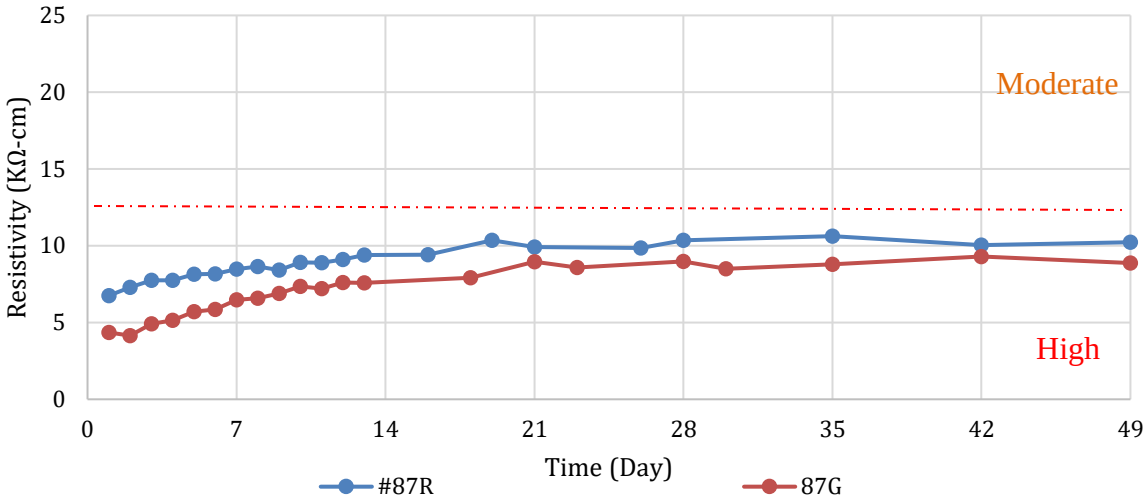

Figure 5.10: The average surface resistivity of MSA #87 to 49 days for Series 2

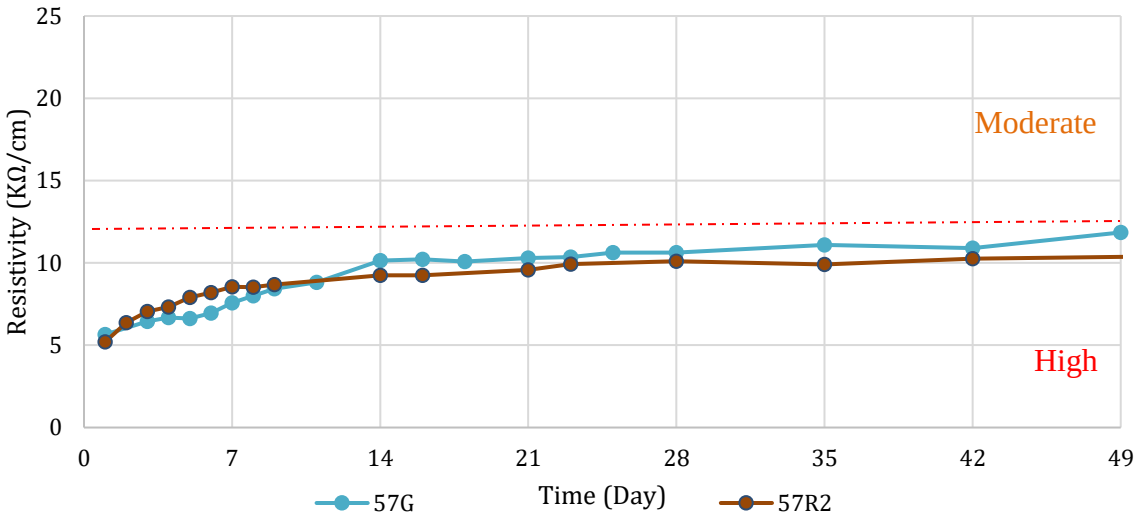

Figure 5.11: The average surface resistivity of MSA #57 to 49 days for Series 2

Figures 5.8 – 5.11 above show that, up to 49-days, most of the mixes had high permeability. All the mixes showed similar surface resistivity around 10 - 11 kΩ-cm. The #87 mixes in Series 2 was the only case where the RAC remained higher than the NAC at all testing dates.

Both #67-15FA and #67-15FRCA were measured up to 28 days then were measured at 91-day. The 91-day surface resistivity measurements were 8.2 kΩ-cm and 24.7 kΩ-cm for #67-15FRCA and #67-15FA, respectively. Mix #67-15FRCA underperformed all the other mixes by approximately 20%. However, due to the slower reacting pozzolanic reaction, #67-15FA had similar surface resistivity as #67R and #67G until 28 days when it was measured at moderate and then increased at 91-day to low permeability.

Surface resistivity and RCPT are both used to measure the permeability of concrete. As seen in Table 5.1, surface resistivity and RCPT often correlates well with each other. Based on previous studies, surface resistivity tends to be more conservative than RCPT [[70];[69]]. Figure 5.12 below show the plot of surface resistivity measurement to RCPT at 28-day.

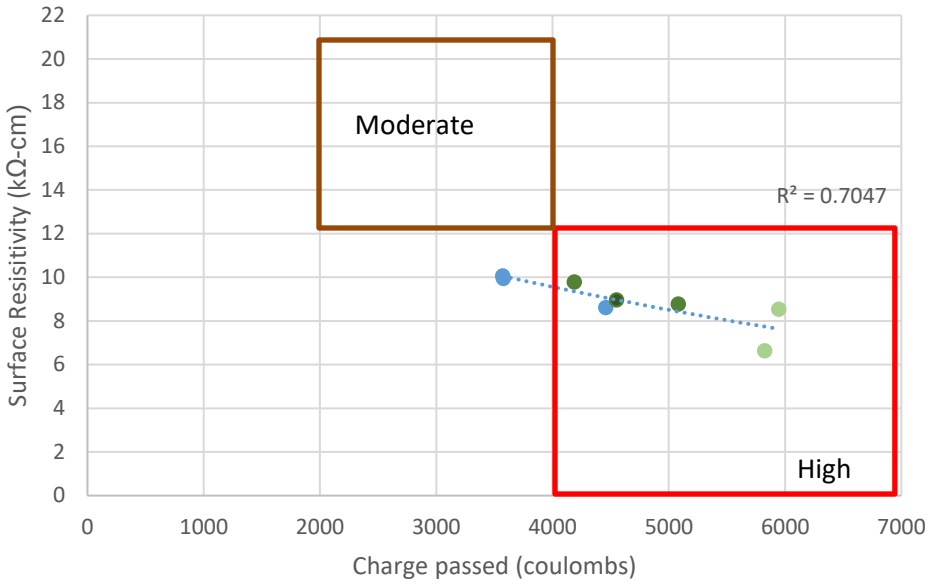

Figure 5.12: Surface resistivity verses RCPT for the average results for 28-day for Series 1

In general, the surface resistivity for these mixes had lower correlate with RCPT results then previous studies, with the R^2= 0.61 for all mixes and R^2= 0.70 for the average mixes per MSA. In Figures 5.12, the results agree with previous studies that surface resistivity is more conservative than RCPT as the data points fell below the boxes [69, 70]. Figure 5.13 compares the difference of aggregate type and time to correlation of surface resistivity and RCPT results.

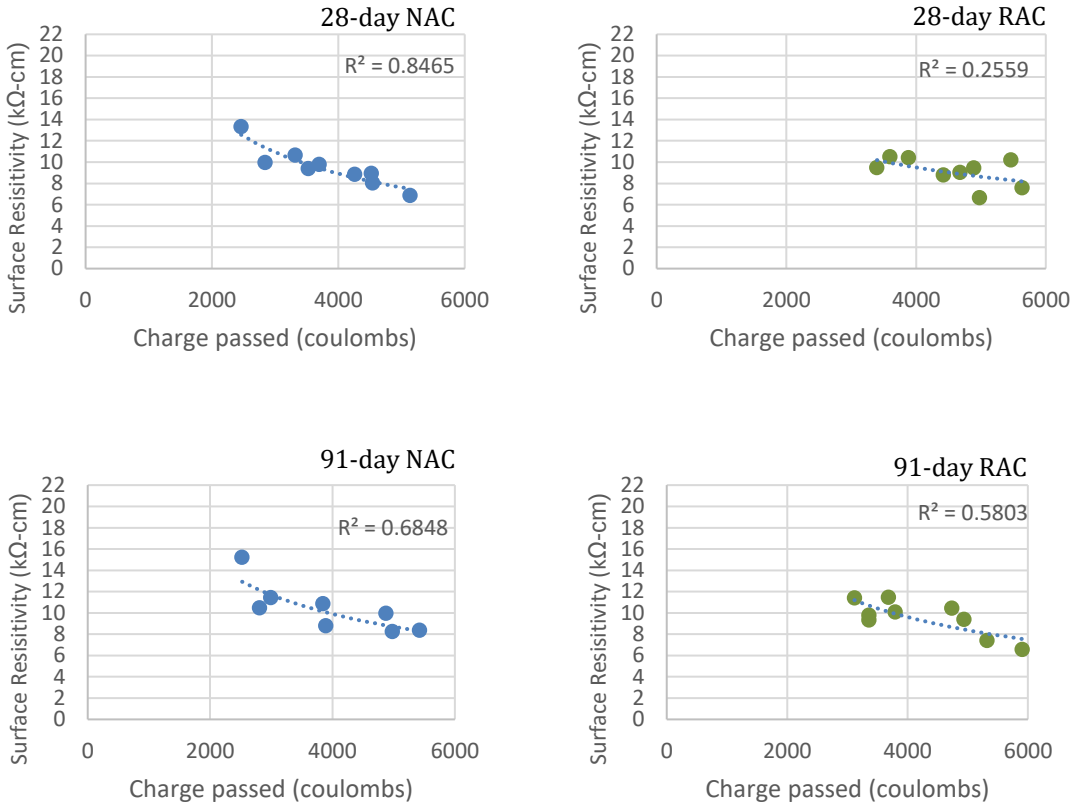

Figure 5.13: Surface resistivity versus RCPT results for 28-day and 91-day for Series 1 per aggregate type

In comparing of the aggregate type, NAC had higher correlation of surface resistivity to RCPT than RAC. However, at later age NAC correlation decreased from R^2= 0.85 to R^2=0.68. An opposite trend is seen for RAC. Similar trends as seen in Series 1 are seen in Series 2. Figure 5.14 below display the correlation of surface resistivity to the RCPT.

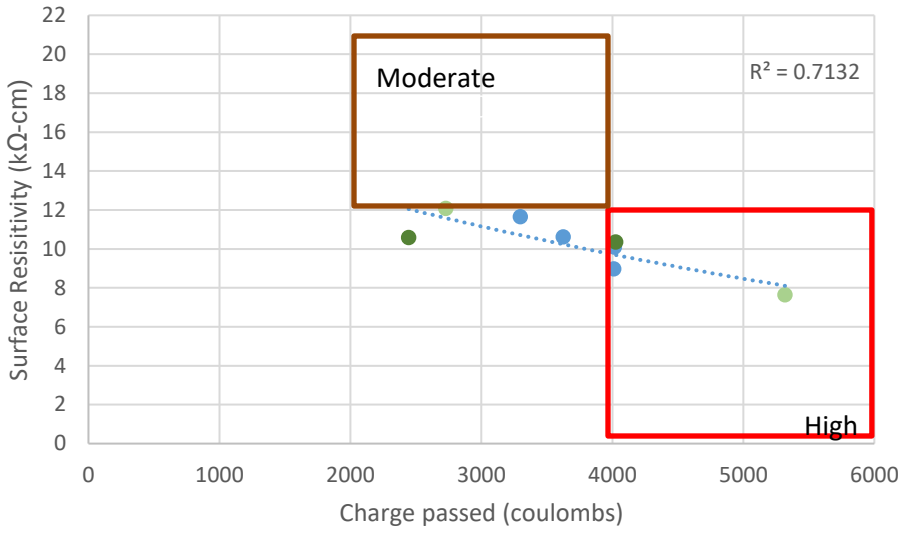

Figure 5.14: Surface resistivity verses RCPT results for 28-day for Series 2

The surface resistivity for these mixes adequate correlation with RCPT results, where R^2= 0.71. Both series had similar correlations of surface resistivity to RCPT results. The lower correlations are due to incorporation of RCA, potentially due to attached mortar and the internal porosity of RCA. As seen in the both Figure 5.13 and 5.15, RAC had lower correlations than NAC.

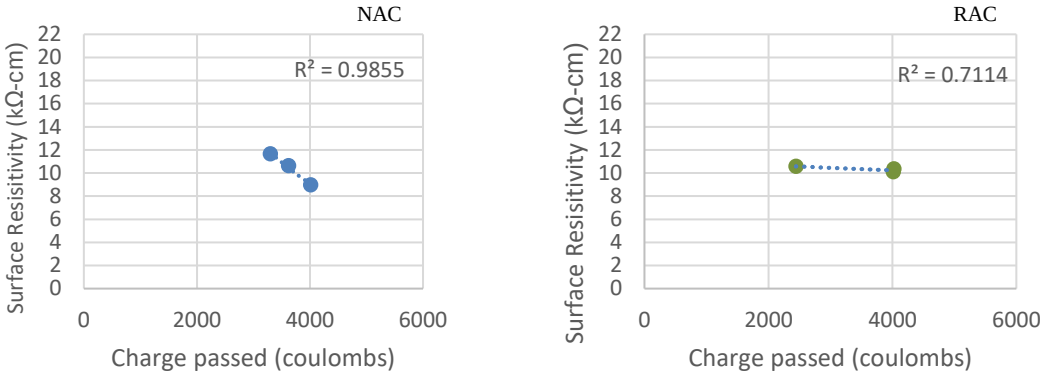

Figure 5.15: Surface resistivity verses RCPT results for 28-day for series 2 per aggregate type

In comparing the correlations of surface resistivity to RCPT of NAC and RAC separately as seen in Figure 5.15. NAC has high correlation of surface resistivity to RCPT agrees with previous studies [69, 70]. However, the RAC had low correlation. The lower correlation for RAC could be due to RAC attached residual mortar, which could be modifying of pore solution or internal porosity of RAC.

5.2 Alkali-Silica Reaction

Alkali-silica reaction is chemical reaction involving alkalis, hydroxyls ions and moisture as seen in the Figure 5.16. ASR causes expansion and cracking of the concrete as the result of formation of gels within the pores. As the ASR gel adsorbs water leads to more expansion and map cracking. Extensive cracking could lead to pops out and gel exudation.

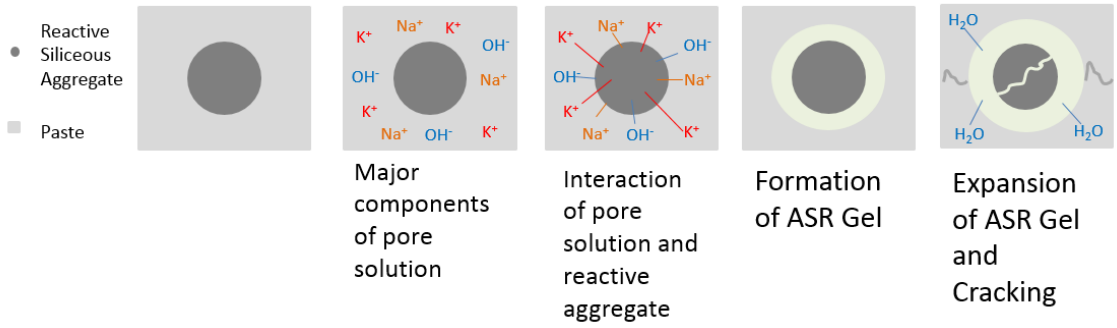

Figure 5.16: Formation of Alkali-Silica Reaction [71]

The formation of ASR gel depends on the amount of available alkalis and hydroxyls ions in the pores solution. The alkalis in the pore solution is from the of cement and the depends on chemical composition of the Portland cement. Increasing either the cement content or cement with higher than 0.6% of equivalent Na_2O can increase the likeliness of damage due to ASR [30]. Furthermore, the hydroxyls ions are ready available in the pore solution as the result of calcium hydroxide in the hydrated cement paste. The silica part of ASR is provided by minerals in reactive aggregate (RA), i.e., alkali-reactive aggregate. Their reactivity depends on several factors, including particle size, type and morphology of siliceous material, time and temperature [30]. All silica and silicate materials react with alkaline solutions at varying degrees, but many are insignificant [30]. The natural aggregate commonly used in Georgia is granitic gniss, which is classified as innocuous aggregate [30].

There are several methods to minimize/eliminate the potential risk of ASR are by limiting the availability of four major components of ASR: alkali, silica, hydroxyl ions, and water. The most common method to limit the use of reactive aggregate. Removing the reactive

aggregate from the system will remove the availability of reactive silica. A common test method to determine if aggregate is reactive is ASTM C1260 Standard Test Method for Potential Alkali Reactivity of Aggregates. ASTM C1260 is an accelerated testing method to determine the reactivity of aggregates and cement based on ASR [72]. Another method to change or reduce Portland cement content to limit the amount of available alkalis. Final common method is to use SCM to potentially limit the amount of both alkalis and hydroxyl ions. SCMs limit both alkalis and hydroxyl ions by a combination of effects; this approach reduces the amount of cement, densifies the matrix to reduce the ingress of harmful ions and moisture, and, if the SCM is pozzolanic consumes the calcium hydroxide to form secondary calcium silicate hydroxide (CSH). ASTM C1293 Concrete Prism Test, a common test to measure ASR in concrete, is uses to account for SCMs delayed reaction time. ASTM C1293 Concrete Prism Test is a long-term testing method, usually 1 to 2 years, that can be used to assess cement, SCM, and aggregate performance in regard to ASR [73]. ASTM C 1293 relays on wicking action of moisture and relates better to field performance.

In this study, four cases were considered in terms of ASR and RCA: (1) a control of 100% reactive aggregate, (2) 100% RCA, (3) 50% reactive aggregate and 50% RCA, and (4) 100% reactive aggregate with 20% replacement of cement with FRCA. The reactive aggregate was gravel from Nebraska. Both aggregates (i.e., reactive aggregate and RCA) were graded according to the ASTM C1260 grading requirement for mortar bars. ASR samples were cast and measured in accordance with ASTM C1260. Three mortar bars were cast for each case. Expansion was measured three times a week for 2 weeks. The expansion shown in Figure 5.17 was the average of the measure of each mortar bar.

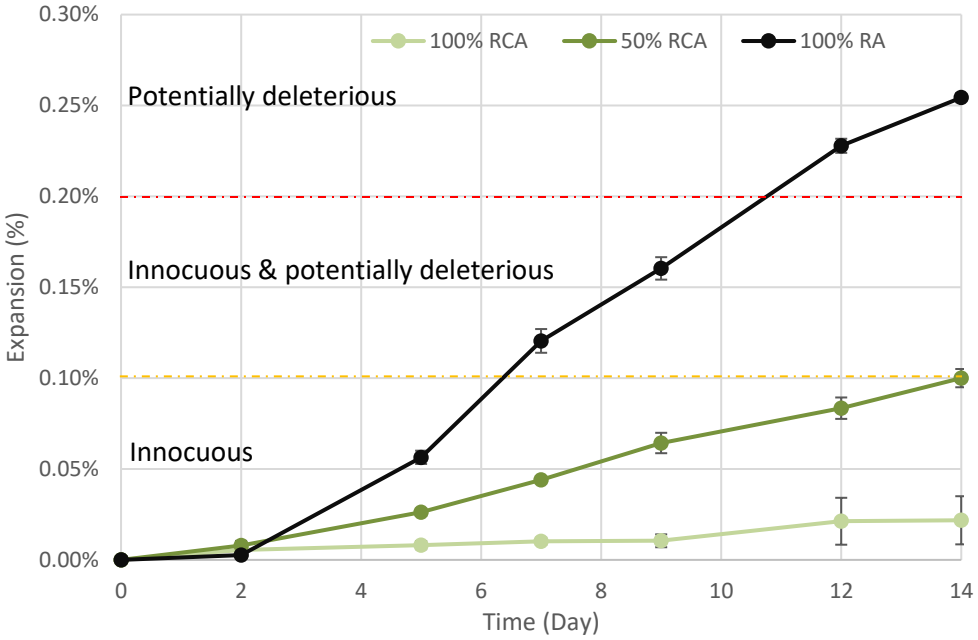

Figure 5.17: 14-day ASR expansion data

The ASTM C1260 expansion limits for equal or below 0.1% is innocuous, between 0.1% – 0.2% aggregate has tested as both innocuous and potentially deleterious, and above 0.2% aggregate is mostly potentially deleterious [72]. Figure 5.17 shows that both 50% RCA and 100% RCA are innocuous at 14 days, while the control of 100% RA was potentially deleterious. In comparison, the 50% of RCA and RA and control there was a 60% reduction in expansion. Potentially, the larger reduction of the 50% RCA could be due to absorption of the mix water in the RCA, therefore lowering the water–cement ratio.

Figure 5.18 show the expansion of control of (1) the control of 100% reactive aggregate, (2) 100% of reactive aggregate and 20% replacement of Portland cement with FRCA. The 20% replacement of FRCA shown a decrease in reactivity of the mortar bars compared to the control.

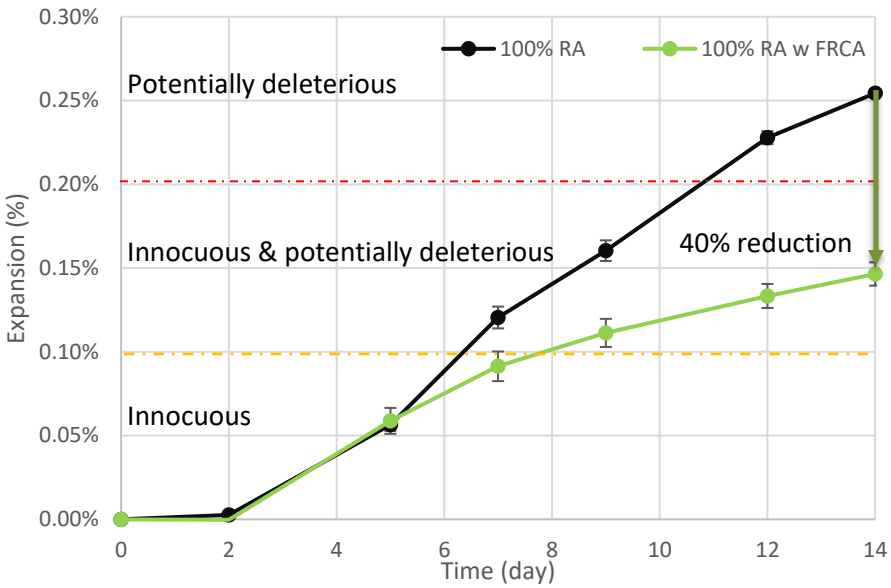

Figure 5.18: 14-day ASR expansion data with recycled concrete fines

The 20% replacement of Portland cement with FRCA lowered the expansion from potentially deleterious zone to the innocuous and potentially deleterious zone. The expansion of RA with fine recycled concrete had a 40% reduction compared to the control. Its expansion had a 40% reduction compared to the control. The large reduction could be caused by densifying of the microstructure of the mortar bar by the filler effect and overall lowering of the water–cement ratio due to the higher water absorption of FRCA [74].

5.3 Service Life Modelling

Service life modelling is representation of potential longevity of concrete as it is exposed to of chloride ingress. Chloride ingress causes cracking and potential corrosion of reinforcement in the concrete, therefore lowering the durability on the concrete. The ingress of chloride ions used to predict initiation period of corrosion of reinforcement is govern by Fick's second law assuming diffusion is dominating mechanism. Fick's second

law equation is given in Equation 5.1, where C is chloride content, D_a is apparent diffusion coefficient, x is depth of exposed surface, and t is time [75].

$$\frac{dC}{dt} = D_a \frac{d^2 C}{dx^2} \tag{5.1}$$

The initiation period of corrosion of reinforcement is often defined as the time it takes the chlorides to reach or exceed the concrete cover depth to reinforcement layer. As seen in Equation 5.1, service life is depended on the apparent diffusivity coefficient, D_a, as well as temperature and availability of chlorides. The apparent diffusivity coefficient is measure of diffusion of ionic species through a porous medium [76]. A simplified version of Nernst-Einstein equation shown as Equation 5.2, where K_i is a constant based on temperature of the porous medium and charge and concentration of the species *i*, and σ_i is conductivity of charged species *i* through the porous material.

$$D_{a,i} = K_i \sigma_i \tag{5.2}$$

The service life of concrete often estimated by considering water-cement ratio, and supplementary cementitious materials. These factors are used to approximate the permeability of the concrete. However, this does not provide sufficient information when using nontraditional materials such as RCA. At high replacements greater than 30% of NA with RCA, the resulting concrete permeability is often modified [30, 32, 33]. Therefore, an approximate calculation of service life is using RCPT results. Considering Equation 5.2, the apparent diffusion coefficient is defined using RPCT results are shown in Equation 5.3, where Q_t is total charge passed in coulombs as D_a is given in the unit of in^2/s.

$$D_a \approx 2.87 \times 10^{-12} Q_t \quad (5.3)$$

This equation is derived assuming RPCT is only the movement of chlorides through concrete as well as considering geometric measurement of specimens and testing conditions defined by ASTM C1202 [76].

Life-365 was used to calculate the service life. Life-365 is a service life prediction model for reinforced concrete exposed to chlorides. Life-365 uses a modified apparent diffusion coefficient to calculate initiation period of uncracked concrete specimen by considering supplementary cementitious materials, such as fly ash or silica content, as well as temperature, as seen in Equation 5.4, where T is absolute temperature, U is activation energy of the diffusion process, R is a gas constant, D_{ref} is the apparent diffusion coefficient at reference time and temperature, and D(T) is apparent diffusion coefficient at time and temperature [75].

$$D(T) = D_{ref} * \exp\left[\frac{U}{R} * \left(\frac{1}{T_{ref}} - \frac{1}{T}\right)\right] \quad (5.4)$$

The temperature is defined by users defined geographic location. In considering equation 5.1, the chloride content in the model is defined by type of structure, type of exposure and geographic location [75].

Four cases were considered to calculate the estimated service life of the concrete mixes for both Series 1 and Series 2: (1) 1-D wall/slab in Atlanta, Georgia, urban road; (2) 2-D beam/column in Atlanta, Georgia, urban road; (3) 1-D wall/slab in Savannah, Georgia, marine tidal zone; and (4) 1-D wall/slab in Richmond, Virginia, urban road. Richmond,

Virginia, was selected as being similar to Georgia as it is a top-five granite aggregate producer in the U.S., and because of the colder temperatures. Savannah, Georgia, was selected based on its location near the ocean. The worst-case scenario was the marine tidal zone and the best-case scenario was the Atlanta, Georgia, urban road. Figure 5.19 shows the temperature profiles of Atlanta, Savannah, and Richmond [75].

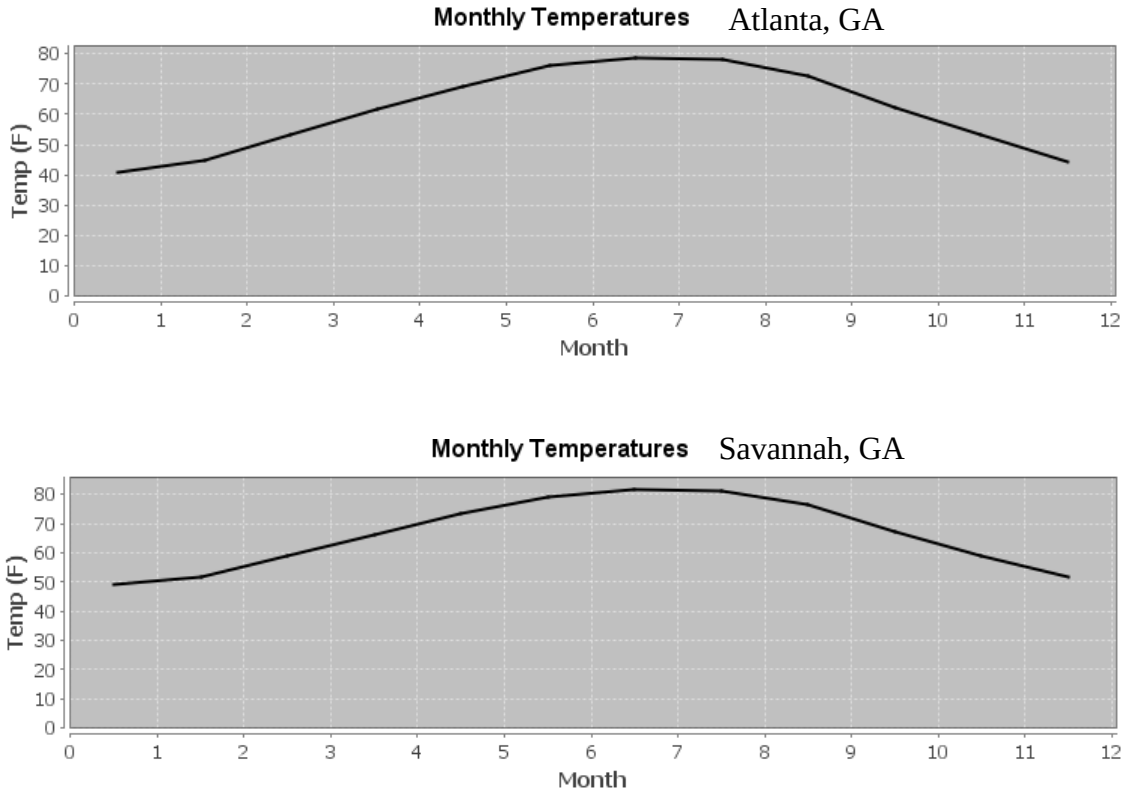

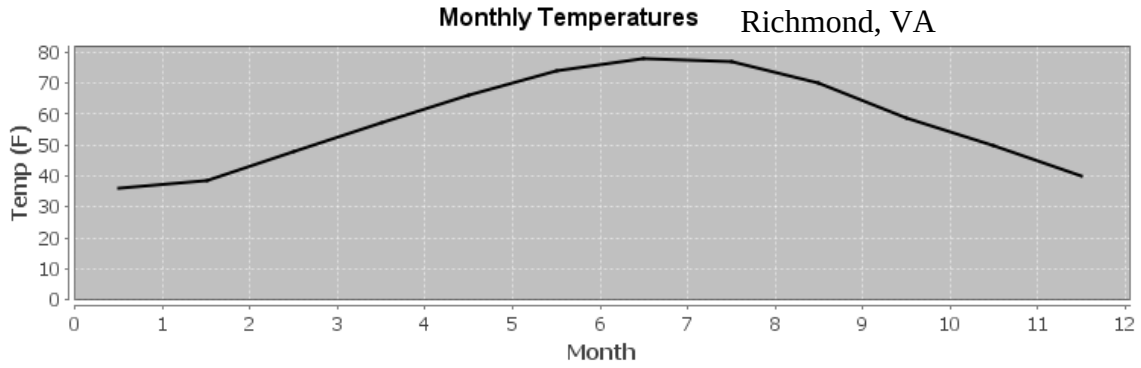

Figure 5.19: Average monthly temperature profiles per city [75]

Based on Figure 5.19, Savannah and Atlanta had similar temperature profiles, except for Atlanta has slight colder winter and summer months. Richmond had overall lower temperature profile in comparison to Savannah and Atlanta. Figure 5.20 shows surface concentrations of chloride exposure for different structure types.

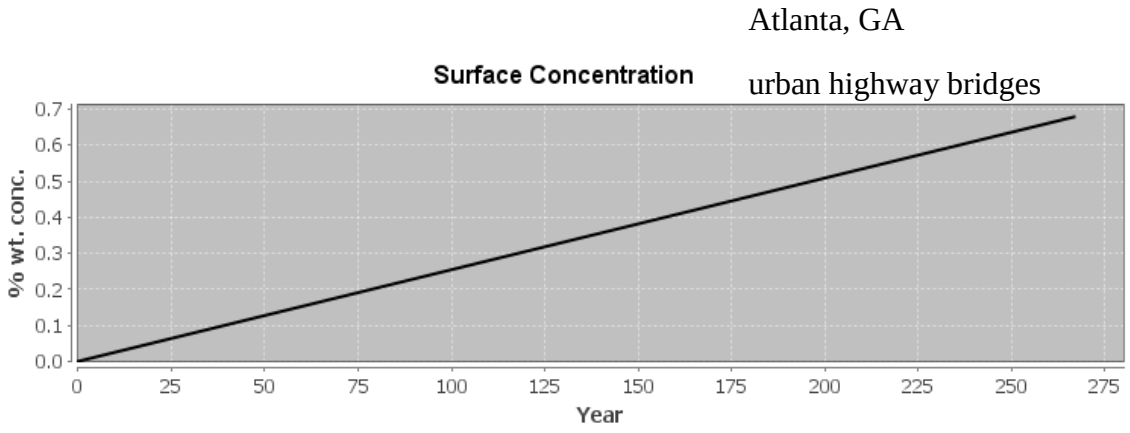

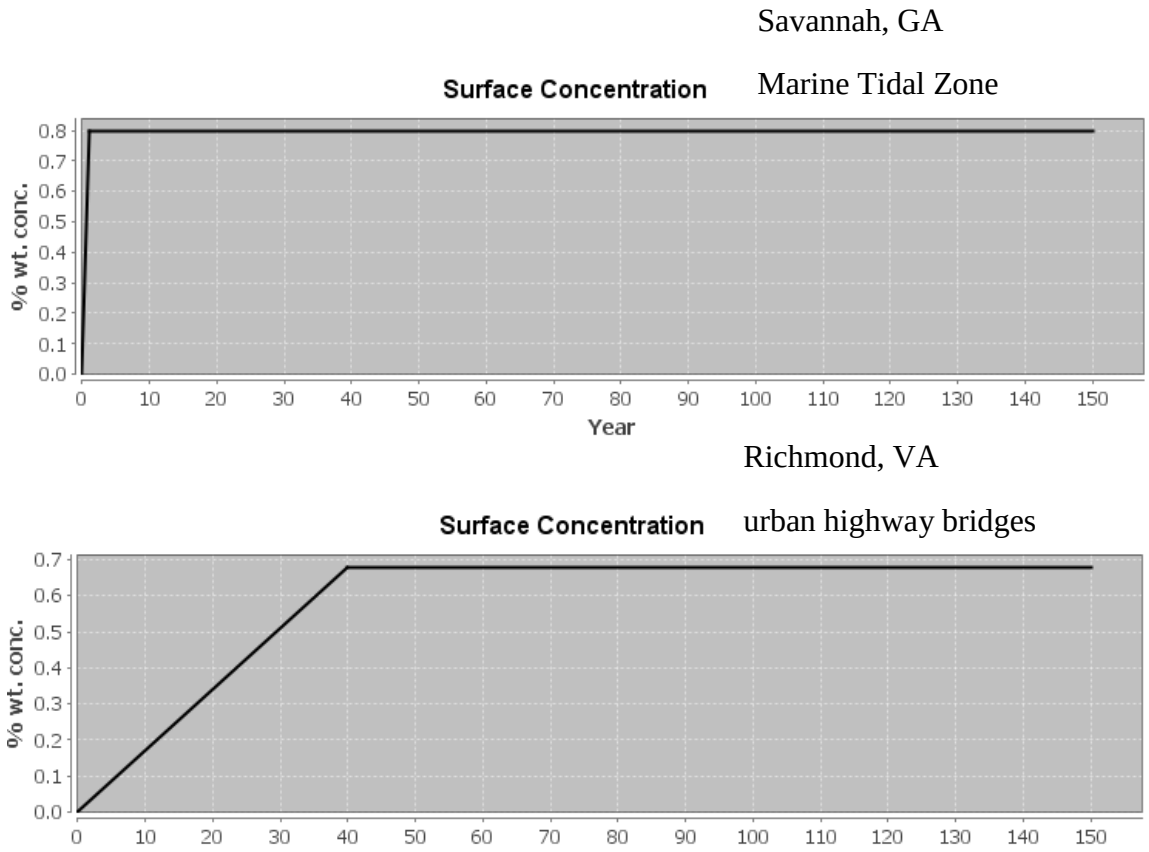

Figure 5.20: Surface Concentration per structure type and city [75]

As seen in Figure 5.20, Atlanta's urban highways had the lowest chlorides exposure compared to other two locations. The second-highest chloride exposure was in Richmond, and highest chloride exposure was for the Savannah marine spray zone. These cases were selected to determine the limitation of uses for RCA in terms of structure types and geographic locations.

The service life was estimated based on a user defined apparent diffusion coefficient from Equation 5.3. Since the apparent diffusion coefficient is directly proportional to RCPT results, the service life approximations had a similar trend as the RCPT results. Figures 5.21 – 5.22 shows a comparison of Case 1 as 28-day and 91-day for Series 1 and Series 2, respectively.

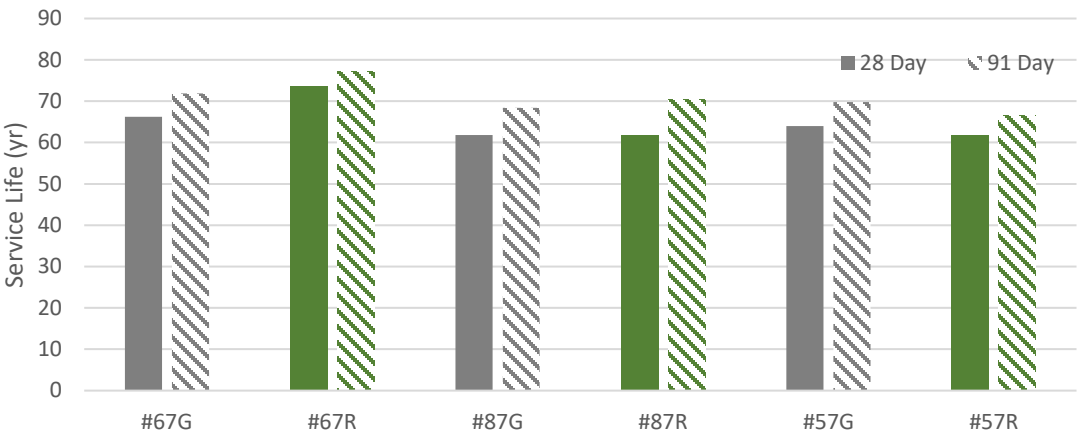

Figure 5.21: Service life at 28-day and 91-day for Case 1 Series 1

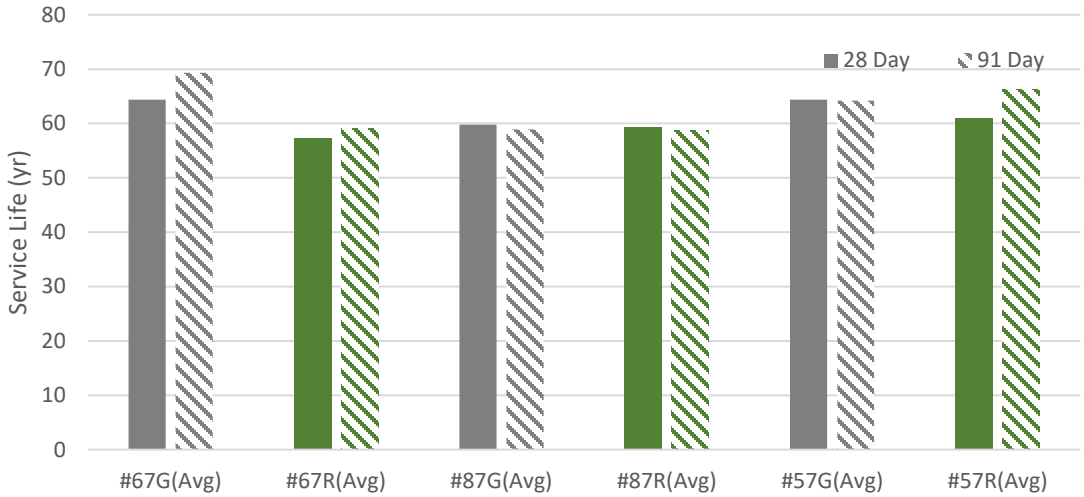

Figure 5.22: Service life at 28-day and 91-day for Case 1 Series 2

For Case 1, as seen in Figure 5.21 and Figure 5.22, the average service life was around 61 years for Series 1 and 65 years for Series 2 for 28-day, and 62 and 68 years for 91-day, respectively. In most cases, there was a positive correlation between concrete age and service life; however, there are a few cases where there were minor reductions in service life.

Figure 5.23 shows the average service life of #67 with inclusion of FRCA and fly ash for Series 1 and 2.

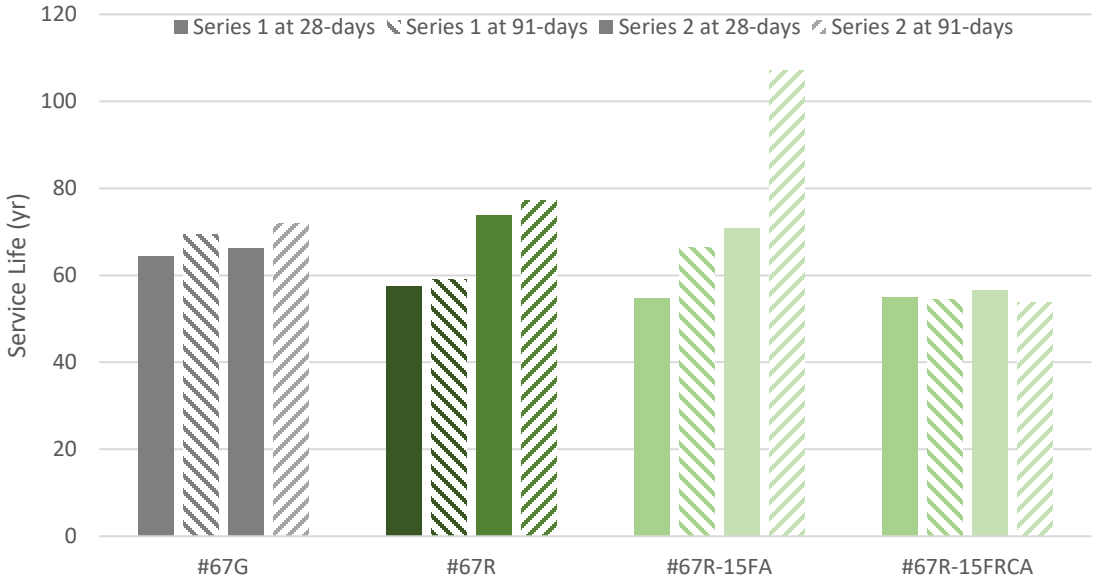

Figure 5.23: Service life at 28-day and 91-day for #67 with/without fines Case 1 Series 1 & 2

In comparison of Series 1 and Series 2, Series 2 seen a high increase of 36 years of service life for inclusion of fly ash, as compared to the low reactivity in Series 1 with an increase

of only 15 years in comparing 28-day results to 91-day. In contrast to concrete with fly ash, concrete with FRCA show a minor reduction of service life in both parts.

These similar trends in Case 1 are observed in the other three cases, as shown in Figure 5.24.

Figure 5.24: Service Life Estimates for at 28-day and 91-day for Case 1- 4 Series 1 & 2

As to be expected, Case 1 had the longest service life and Case 3, which had the severest chloride exposure, had the lowest service life. The average service life for each of the cases for Series 2 at 28-days are 65, 49, 10, and 27 for Case 1 – 4, respectively. In all cases, RCA

had performed similarly to NA. Therefore, RCA can be used in all cases, although SCMs are recommended for structures with high exposure to chlorides, similar to Case 3 and 4.

CHAPTER 6. UTILIZATION OF RECYCLED CONCRETE AGGREGRATE FINES

This chapter focused on the use of RCA fines as a filler or supplementary cementitious material. FRCA are defined in this study as the particles that majority passed the #325 sieve, 45 μm. Previous studies have shown FRCA without treatment have minimum to none reactivity and exhibit a filler effect at smaller replacement ratios [49, 50]. Furthermore, dehydrated cement paste with heat treatment are shown to be potential SCMs [51], although the presents of sand and other foreign particles can hinder the performance of FRCA [51, 52]. Therefore, this study of FRCA focused on the characterizing the material and then observing the hydration and reactivity of FRCA.

6.1 Material Characterization

FRCA is considered a combination of residue cement paste, unhydrated cement particles, sand and other foreign particles. The proportions of these components depend on the source of the original concrete, as well as storage of RCA. The potential reactivity of FRCA as terms of alternative SCM would be attributed to the contribution of residue cement paste and unhydrated cement particles. These effects are often reduced by percentage of sand and other foreign particles.

Similarly, fillers can be range of inert or reactive. Inert fillers such as quartz doesn't chemically react with hydration kinetics, whereas reactive fillers such as limestone does chemically react with hydration kinetics. Fillers act as partial replacement of cement and have two major impacts on cement systems: dilution and nucleation sites for hydration

products. Dilution is caused by the deceasing the cement content, which increases the overall water-to-cement ratio. The dilution effect can cause acceleration of cement hydration due increase of water available for reacting with unhydrated cement particles. Fillers also provide nucleation site for hydration, depending on the surface area of the fillers. Fillers often provide improve particle packing, since fillers are often smaller than cement particles. The filler effect is often controlled by the fineness and surface area of the particles [77, 78]. The following sections presents results of the treatment methods, particle size analysis, and composition of FRCA.

6.1.1 Treatment Methods

Previous studies shown that FRCA has minimum to no reactivity due to combination of factors [49-51]. However, additional studies have shown heat treatment increase reactivity of dehydrated cement paste. Therefore, this study considers a range of treatment methods to increase the reactivity of FRCA, including ball-milling and calcining.

Ball-milling is a common method in the cement industry to reduce the particle size of materials including but not limited to cement and natural admixtures [79]. Ball-milling utilize a combination grinding mediums, such as 8 mm steel balls and rotational motion, to grind the materials to finer sizes. This method uses a combination of frictional and impact forces that is used to reduce the size of material. Due to the grinding process, heat is generated. This heat could lead to phase transition of materials [79]. Therefore, the phase transition could result in a chemimechnical activation of the FRCA.

The ball-mill used for these studies are Retsch PM 100 and grinding medium was 8 mm steel balls, as shown in Figure 6.1.

Figure 6.1: (a) Photo of Ball-mill and (b) grinding medium

The FRCA was filled to half the sample holder container, enough to over the grinding medium. FRCA were ball-milled at 230 rpm for four different time intervals 15, 30, 45, 60 minutes. To enhance the effects of chemimechnical activation, the FRCA were ball-milled continuously for each time interval. The influence of increasing the time intervals of ball-milling should result in decrease in particle size and potentially increase chemimechnical activation. Ball-mill samples will be denoted as FRCA_BMXX, where XX represents the time interval. For example, FRCA_BM30 is samples that was ball-milled at 230 rpm for 30 minutes.

Calcining is the traditional method to modify physical and chemical properties due to high temperatures. The process of calcining often removes volatile impurities and oxidizing the material. The phase transformation of a solid material due the treatment of high heat could result in increased reactivity [80]. Calcining is commonly used in increasing the reactivity of clays by breaking down the crystal structure to form an amorphous structure [80]. The FRCA were calcined, potentially increasing the reactivity by removing impurities and

modifying crystalline structures. The FRCA were calcined in the Nabertherm furnace, as shown Figure 6.2.

Figure 6.2: Photo of Nabertherm furnace

The calcining procedure was as follows: The FRCA was heated at a constant rate of 20°C per minute until the target temperature was reached, then was held at the target temperature, T_T for 1 hour, followed by air cooling to room temperature, as seen in Figure 6.3.

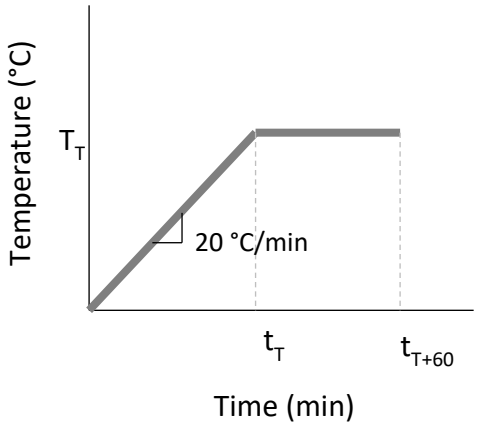

Figure 6.3: Calcining heating schematic

Four target temperatures, 750°C, 800°C, 850°C and 1000°C, was selected based on previous studies observed the optimum temperature range to enhance recycled cement paste was around 700 – 900°C [50, 51]. The FRCA were calcined at these temperatures to study the influence of increasing the temperature on reactivity of FRCA in hydrated cement systems. Calcined samples will be denoted as FRCA_CALXXX, where XXX represents the temperature. For example, FRCA_CAL750 is samples that was calcined at 750°C for an hour.

6.1.2 Particle Size Analysis

As stated previously, filler interaction with cement hydration kinetics are dependent on the both the surface area and the fineness of material. Thus, fineness of the FRCA was approximated using particle size analysis by laser diffraction. The particle size analyzer used in this experiment was Malvern PANalytical Mastersizer 3000E. Due to potential reactivity of the FRCA, ethanol was used as a dispersant while measuring particle size distribution (PSD). The reflective index used to approximate the particle size distribution

was 1.33 for FRCA, density was 2.54 measured using ASTM C188 and absorption using approximation of 0.1. In order to get a relative comparison, the FRCA were compared against quartz, an inert filler, quartz, dispersed in distilled water. The Mastersizer database was used to assign values for quartz, ethanol, and distilled water. The procedure for measuring the particle size distribution was as follows: The material was placed into dispersant to approximately 10% by volume, sonicated for 1 minute, then mixed for additional 2 minutes at rate of 840 rpm, and sampled for five times to measure PSD.

The averages of the five sampling are presented in Table 6.1. Table 6.1 shows mass division diameters in terms of 10, 50, and 90 and specific surface area (SSA). Mass division diameter as denoted as D##, represents that ## of the mass is smaller than the specified diameter. D50 is often representative of median diameter and will be used as approximate particle size.

Table 6.1: Mass Division Diameters and specific surface area of FRCA and quartz

Sample	D10 (μm)	D50 (μm)	D90 (μm)	SSA (m^2/kg)
FRCA_345	2.135	24.35	52.35	371.0
FRCA_500	1.39	14.45	31.1	491.5
FRCA_BM15	1.435	17.25	42.55	473.0
FRCA_BM30	1.32	14.8	39.4	530.5

FRCA_BM45	1.27	13.25	38.8	563.1
FRCA_BM60	1.195	11.05	37.15	625.8
FRCA_CAL750	1.43	18.45	44.8	457.6
FRCA_CAL800	2.275	25.3	56.0	357.3
QP_BP30	3.01	10.5	23.2	355.2

As seen in Table 6.1, the median particle size for FRCA was measures as 24.4 μm and SSA of 371 m^2/kg. Typical median particle size of cement is around 10.4 μm and SSA of 282 m^2/kg [76]. As a result, the median particle size of FRCA is larger than cement, therefore, FRCA as a filler will primarily have a dilution effect. Furthermore, most of additional treatment to FRCA decreased the particle size and increased the specific surface, with the expectation of calcining. As to be expected, increasing the ball milled time decreased the fineness and increased the surface area. In comparison to FRCA, QP_BP30 was finer PSD but similar SSA as represented in Figure 6.4 and Table 6.1. Figure 6.4 shows the PSD of the materials.

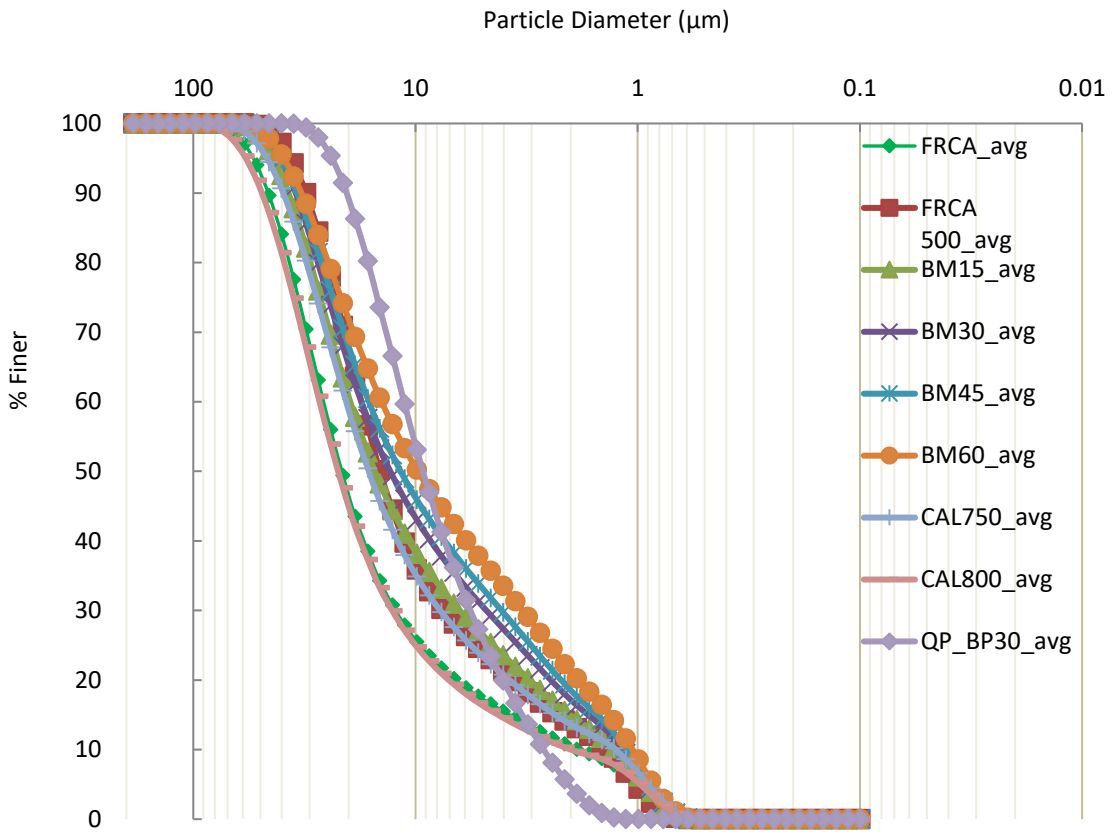

Figure 6.4: Particle size distribution of FRCA and quartz

Figure 6.4 shows that FRCA and FRCA_CAL800 had similar PSD. The quartz powder had a finer PSD; it median particle size aligned well with treated FRCA. Furthermore, increased bill-milling shifted the right and upwards. A close-up of the changes due to ball-mining can is shown in Figure 6.5.

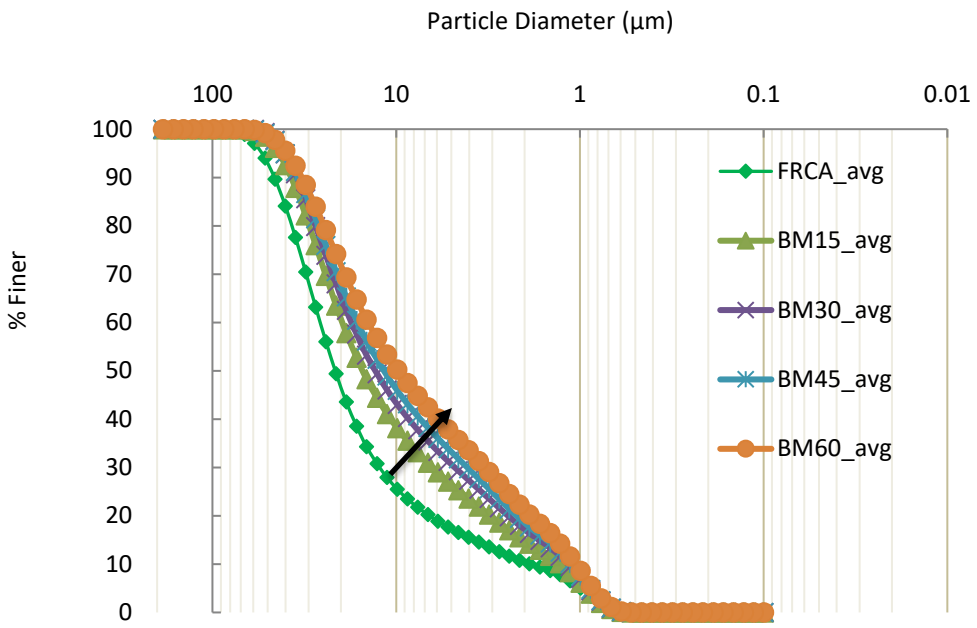

Figure 6.5: The effect of grinding FRCA in terms of PSD

As seen in Figure 6.5, grinding for 15 minutes resulted in a large shift in the PSD of FRCA. In addition, the differences in PSD was negligible between BM30 and BM45.

6.1.3 X-ray Powder Diffraction

X-ray Powder Diffraction (XRD) was used to measure the crystalline composition of the FRCA. XRD is a laboratory technique using scattering of x-rays to identify crystal atoms based on the diffraction pattern. Studies have shown that FRCA is a combination of quartz, calcite, ettringite, and a combination of feldspar materials [[50]; [81]]. Similar to other studies, XRD showed that the FRCA were a combination of quartz, calcite, plagioclase and alkali feldspar, and trace amounts of other minerals, as shown in Figure 6.6. Figure 6.6 shows the diffraction pattern on FRCA that passed #345 without any additional treatment.

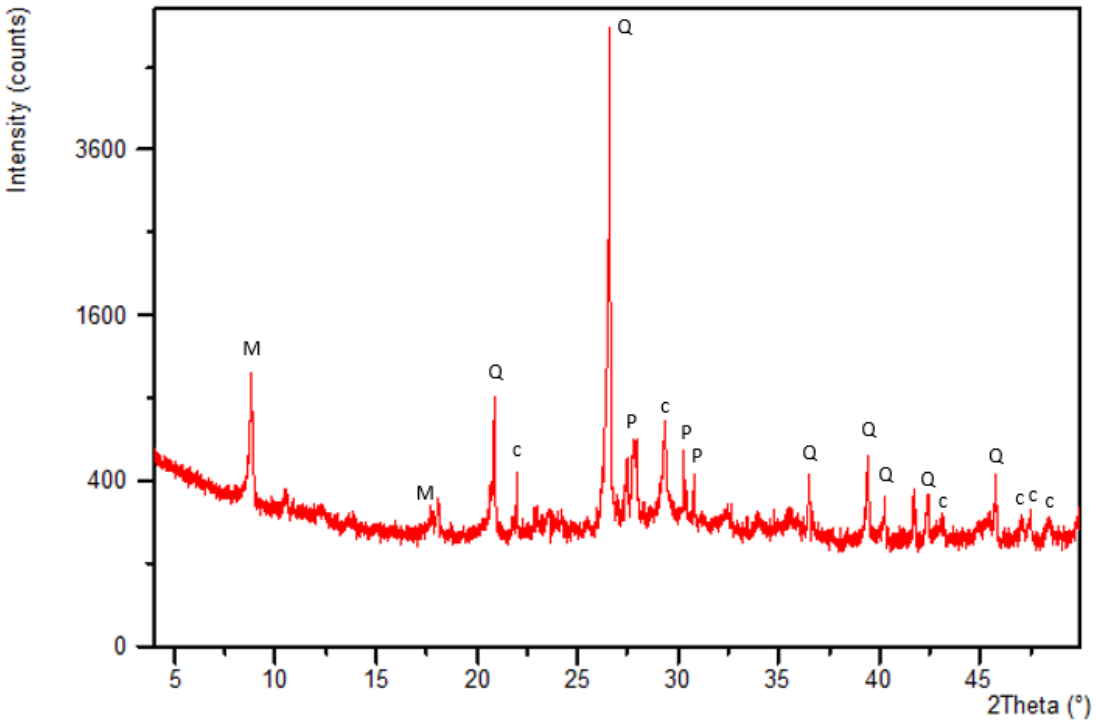

Figure 6.6: XRD diffraction pattern of FRCA without additional treatment

Figure 6.6 shows the composition of crystalline material FRCA without additional treatment, where M is mica, Q is quartz, c is calcite, and P is plagioclase feldspar. The presence of amorphous material was evident in the diffraction pattern as the result of humps, i.e., non-defined broad peaks, in the line. The majority of the crystalline composition of the FRCA was determined by PANalytical's HighScore Plus. Table 6.2 displays the crystalline composition of the FRCA.

Table 6.2: Crystalline Composition of FRCA

Sample	Quartz (%)			Calcite (%)	Plagioclase Feldspar (%)	Alkali Feldspar (%)	Mica (%)	Other (%)
	Quartz	Coesite	Cristobalite					
FRCA_345	✓✓	-	-	✓	✓	-	✓	✓
FRCA_500	✓	✓	-	✓	✓✓	-	✓	-
FRCA_800	✓	✓	-	✓	✓✓	-	✓	✓
FRCA_BM15	✓	-	-	✓	✓✓	✓	✓	-
FRCA_BM30	✓	✓	-	✓	✓✓	✓✓	✓	✓
FRCA_BM45	✓	-	✓	✓	✓✓	-	✓	-
FRCA_BM60	✓	-	-	✓	✓✓	-	✓	-
FRCA_CAL750	✓✓	-	-	-	✓	-	✓	✓
FRCA_CAL800	✓✓	-	✓	-	✓	-	✓	✓
FRCA_CAL850	✓✓	-	-	-	✓	-	✓	✓
FRCA_CAL1000	✓	-	-	-	✓✓	-	✓	✓

Table 6.2 shows that additional treatment modified the crystalline structure of the FRCA, where one check mark denotes presents of crystalline material and double check mark denotes major crystalline material. The modifications included phase transfer of quartz and plagioclase feldspar minerals due to either high temperatures and pressure, or high temperature. The phase transfer to more reactive crystalline phases of both quartz and plagioclase feldspar. In addition, calcining resulted in the presence of other minor

crystalline materials and decomposition of calcite to lime. The presence of calcite was reduced by deduction of fineness and ball-milling.

The FRCA were characterized by PSD and XRD, and these material characterization techniques are important to understand the effects the FRCA has on hydration and reactivity in cement paste and mortar system. The next section will discuss the effects of additional treatment on FRCA in terms of hydration of cement paste.

6.2 Hydration Kinetics

Hydration kinetics is study of cement hydration in terms of percentage of hydrated cement in a cement system. The percentage of hydrated cement is depended on several factors, including water-cement ratio, admixtures, SCMs, cement type, etc. There are numerous ways to measure hydration kinetics of cement, but this chapter focuses on the use of isothermal calorimetry. Isothermal calorimetry is measurement of heat production rate at isothermal conditions [82, 83]. Isothermal calorimetry can be used to approximate initial and final set times as well as strength, although there are no direct correlations [82, 84]. The heat evolution curve obtained by isothermal calorimetry can be broken down into six key points, as shown in Figure 6.7.

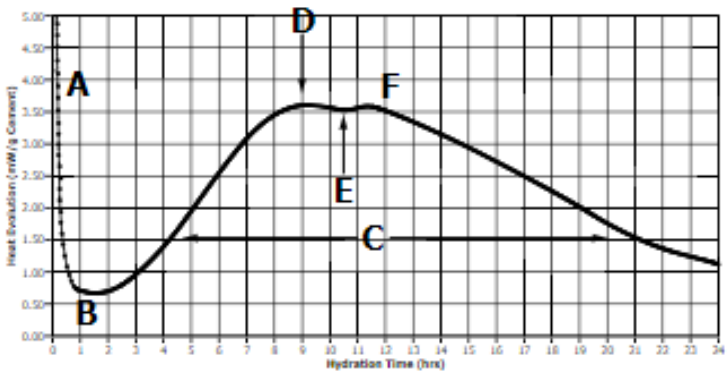

Figure 6.7: Sample heat evolution curve with key points labeled [83]

The six key points are: A – dissolution and initial hydration of cement, B – dormant period, C - main hydration peak, D – maximum peak, E – sulfate depletion, and F – calcium aluminate activity [82, 83]. These key components will be used to compare the influence of FRCA on cement paste hydration at 20% replacement.

The Thermometrics TAM AIR calorimeter was used to measures the heat evolution of the samples at constant water bath of 23°C. The samples were prepared in the standardize mixing procedure, as follows: Hand mix cement and other binders together for 30 seconds, then add a measured amount of water, hand mix for an additional 30 seconds, immediately mix with a hand blender on low for 1 minute and increase the speed to medium for an additional 1 minute, scrape down the sides of the container and stir to incorporate the material on the sides, and finally place the measured amount of the sample into ampules. Immediately after mixing, the samples were placed into the calorimeter. The time was recorded at regular intervals, including start of recording on the calorimeter, start of mixing of each sample, and placement of each sample into the calorimeter. This procedure was

followed for all the cases studied. The first case studied was the influence of w/cm ratio on hydration.

Due to the high water absorption of the FRCA, the effect of w/cm ratios was studied. Figure 6.8 shows the heat evolution of six samples at 0.45, 0.5, and 0.55 w/cm ratios. Figure 6.8 was normalized to mW per g of cement because of the dilution effect of 20% replacement of cement with FRCA. The effects of replacement of cement with FRCA was compared against ordinary portland cement (OPC).

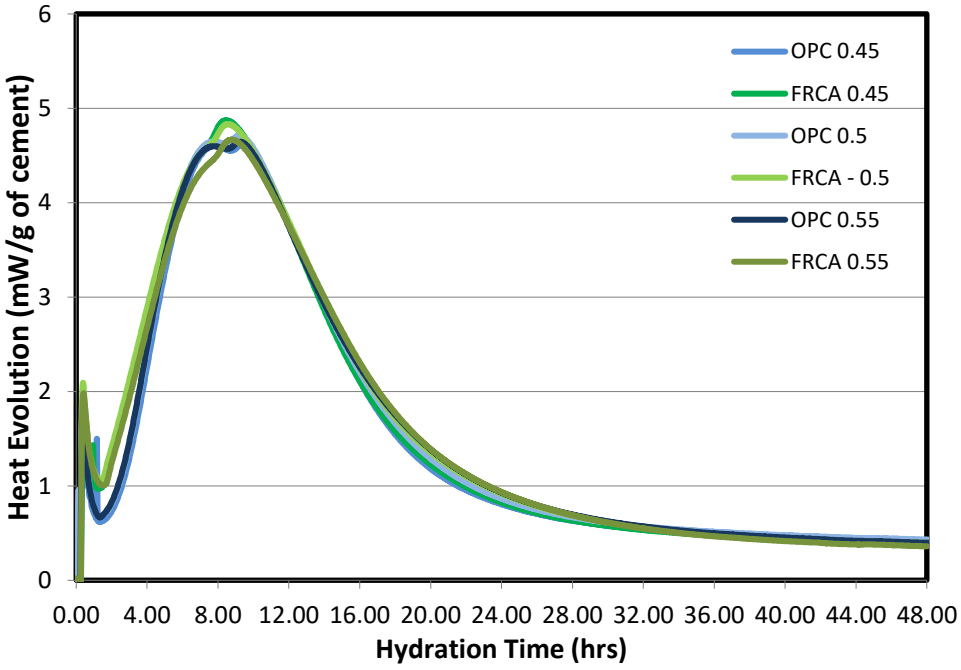

Figure 6.8: Heat evolution of cement paste with and without 20% replacement of FRCA at different w/cm ratios

In comparison, the FRCA mixes had acceleration in hydration and increase in reactivity as indicated by curves slight shift to the left and up. These effects might be contributed to the filler effect or just the dilution effect as a result of an increase of alkalis in the pore solution,

since FRCA have smaller particle size than the cement particles. Cement paste with 20% replacement of FRCA had comparable result at 0.45 and 0.5 w/cm ratios. Therefore, the 0.5 w/cm ratio was used for the subsequent tests for the ease of mixing and developing homogenous samples. The following cases studied the influence of treated FRCA.

To enhance the reactivity of FRCA, the study looked at three types of treatments: fineness, calcining, and ball-milling. Figures 6.9 – 6.14 show the cumulative heat and heat evolution curves for each of these cases.

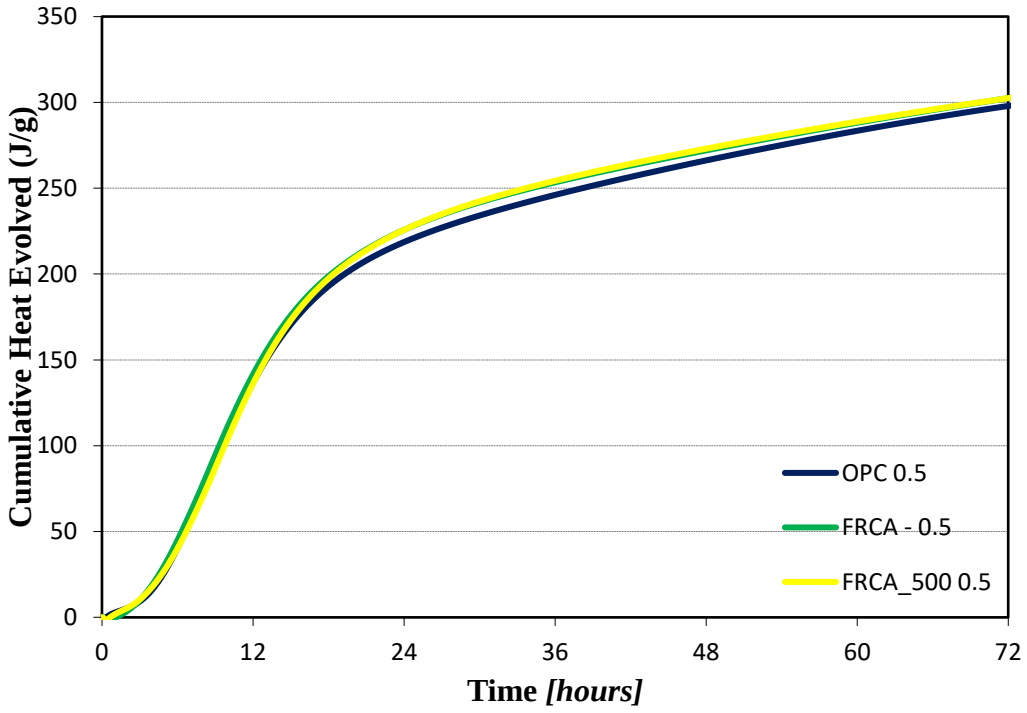

Figure 6.9: The effect of fineness of FRCA passing #325 and #500 sieve on cumulative heat evolved

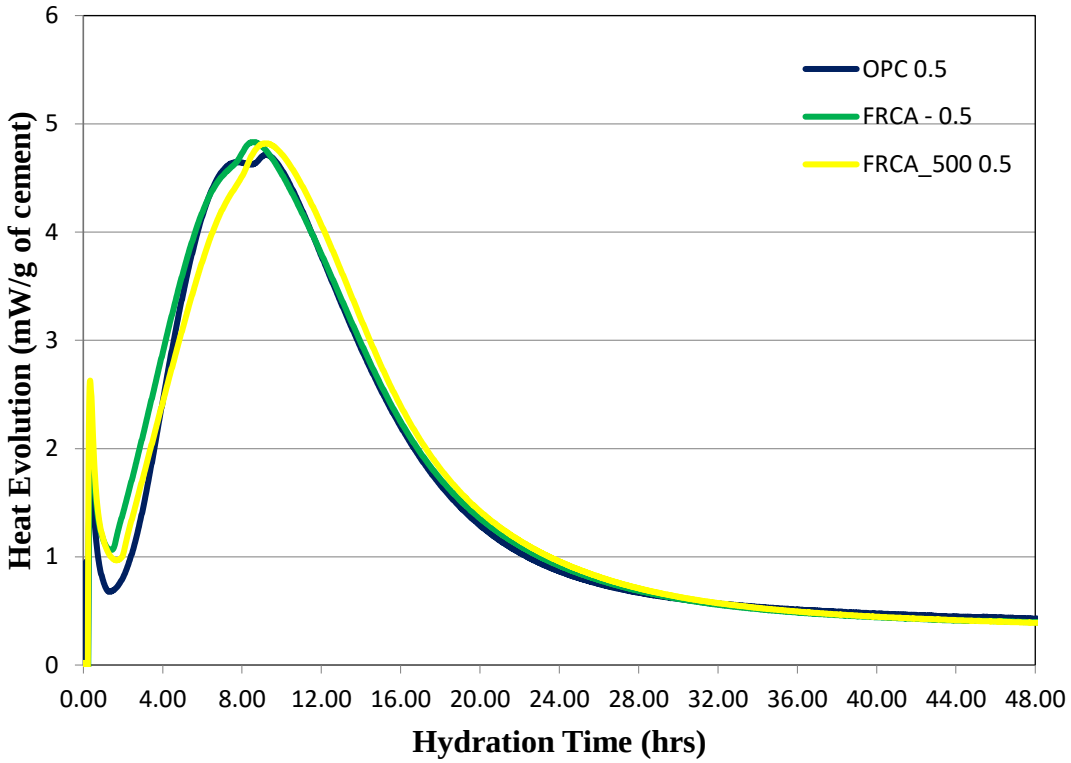

Figure 6.10: The effect of fineness of FRCA passing #325 and #500 sieve on heat evolution

The #325 sieve has 45 µm openings compared to #500 sieve with 25µm openings. Based on previous studies, 10 µm was the optimum size to enhance the filler effect [76]. Therefore, #500 sieve was selected due to commercial availability and since samples could be obtained with minimal processing. The majority of the FRCA_500 was obtain from sieving, but a minority of sample was ball milled at 15-minute intervals until FRCA_500 was obtained. For the effect of fineness, there was overall increase of cumulative heat evolution and retarded in hydration. The retardation in hydration maybe due to impurities in FRCA, such as clay. However, it had similar height of the calcium aluminate peaks.

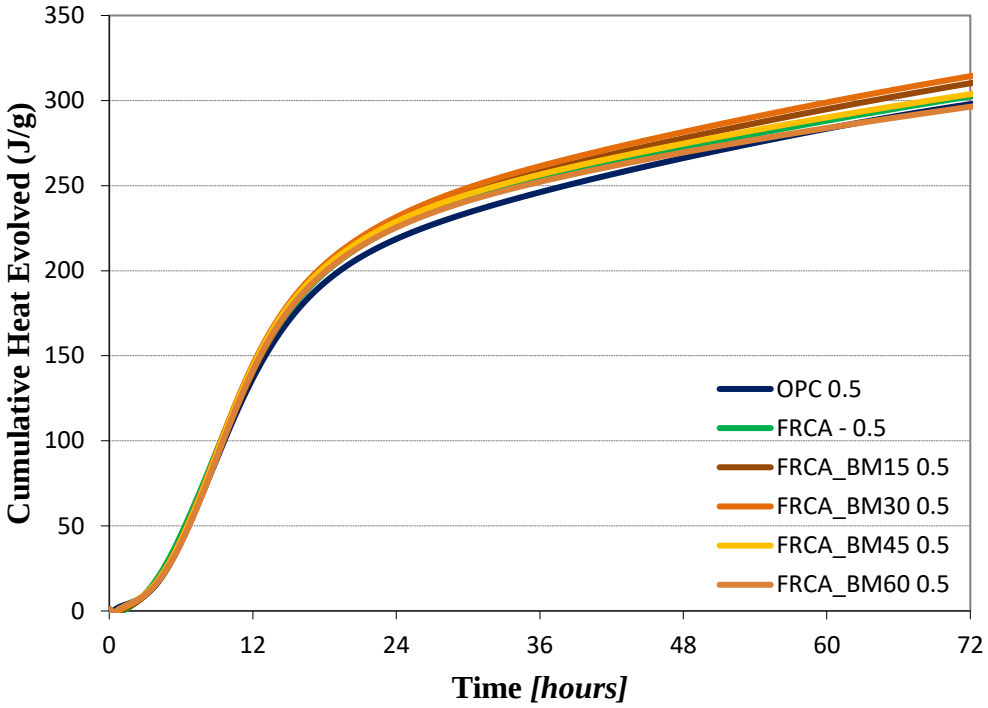

Figure 6.11: The effect of ball-milling FRCA on cumulative heat evolved

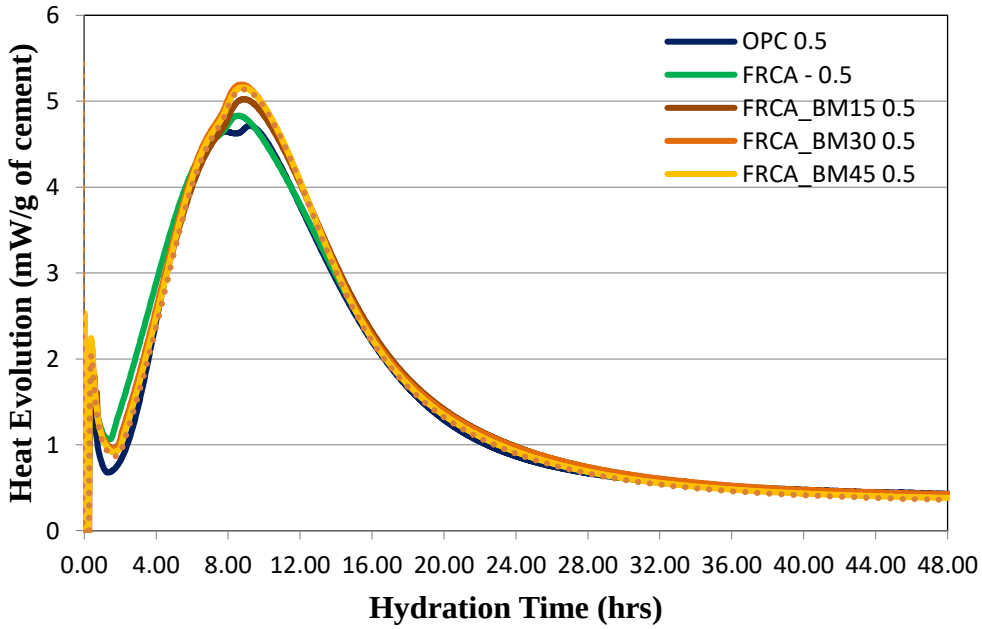

Figure 6.12: The effect of ball-milling FRCA on heat evolution

For effect of ball-milling case, the FRCA were studied at four different time intervals of ball-milling: 15, 30, 45, 60 minutes. Ball-milling decreased the particle size by 7.1, 9.55, 11.1, and 13.3 μm, respectively. In addition, ball-milling slightly modified the crystalline composition of FRCA, as discussed in Section 6.1.3. Overall, ball-milling increased hydration over cement paste and plain FRCA, except for FRCA_BM_60. FRCA BM_60 shown overall decrease in cumulative heat evolved, although it had a higher calcium aluminate peak then both cement and FRCA. However, there was an optimum level of ball-milling around 30–45 minutes.

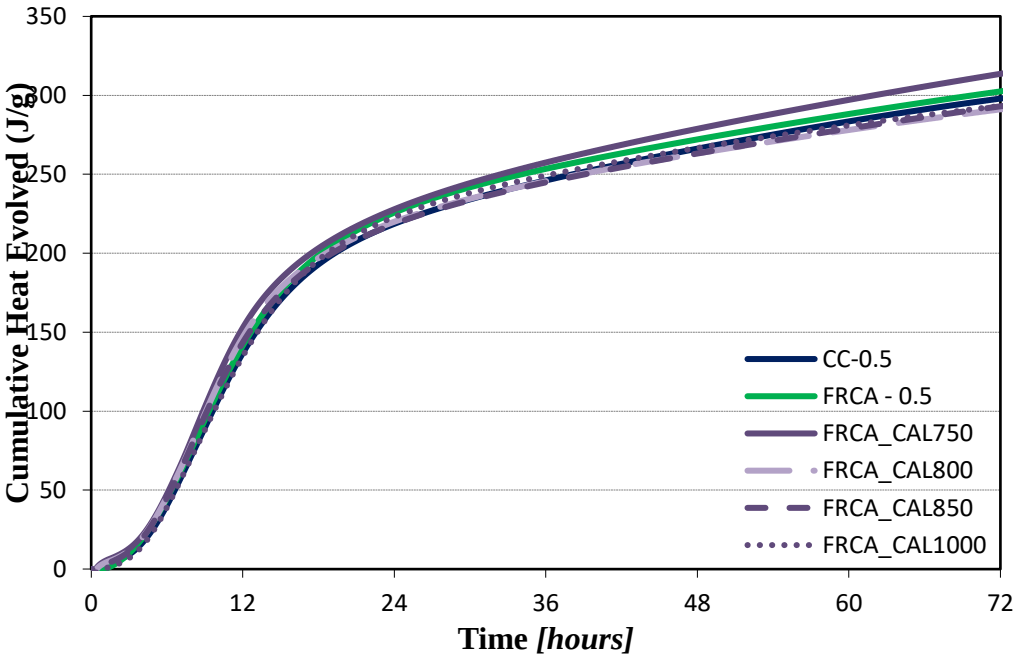

Figure 6.13: The effect of calcining FRCA on cumulative heat evolved

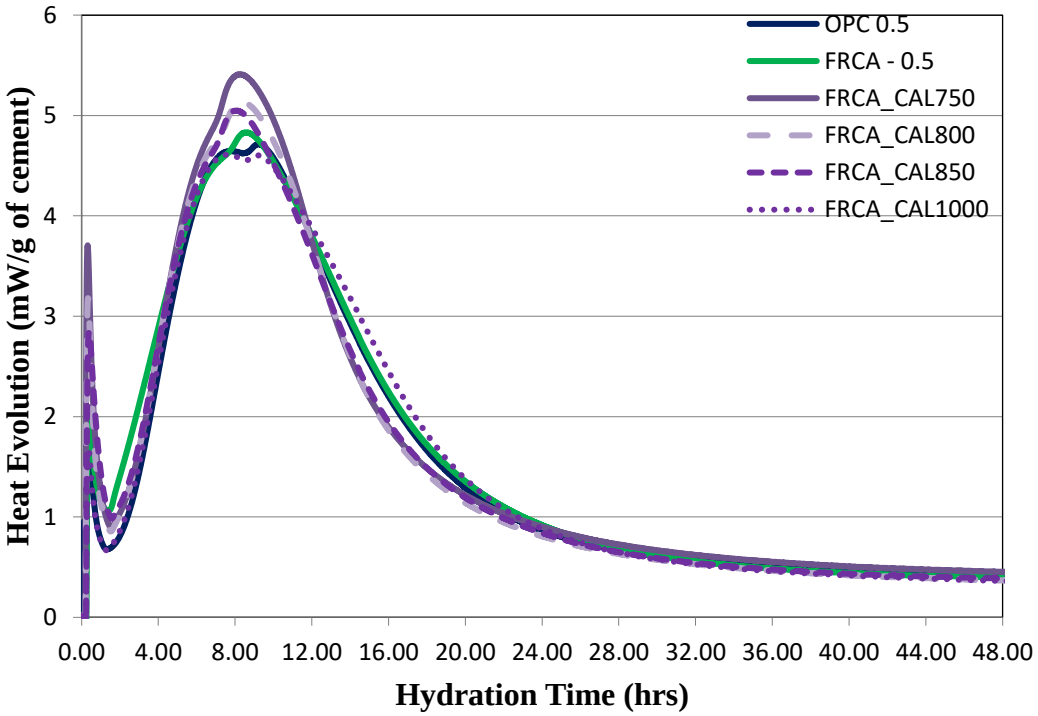

Figure 6.14: The effect of calcining FRCA on heat evolution

For the calcining case, the FRCA was studied at four temperatures: 750ºC, 800ºC, 850ºC and 1000ºC. Calcining resulted in modifications to the crystalline composition of FRCA. In comparing, calcining above 750ºC had a detrimental effect cumulative heat evolved and overall hydration of paste, while temperatures of 750ºC, 800ºC and 850ºC showed an increase of calcium aluminate peak compared to both cement and FRCA in the heat evolution plot. A temperature of 1000°C had a slight detrimental effect on hydration. As a result, the optimum calcining temperature was 750ºC, which agrees with previous studies the found the optimum temperature to enhance recycled cement paste was around 700–900ºC [50, 51].

To understand the influence the FRCA have on cement paste, this study used quartz, an inert filler, to compare with FRCA at the same 20% by mass replacement of cement. Figure 6.15 shows the cumulative heat evolved plot of FRCA and quartz.

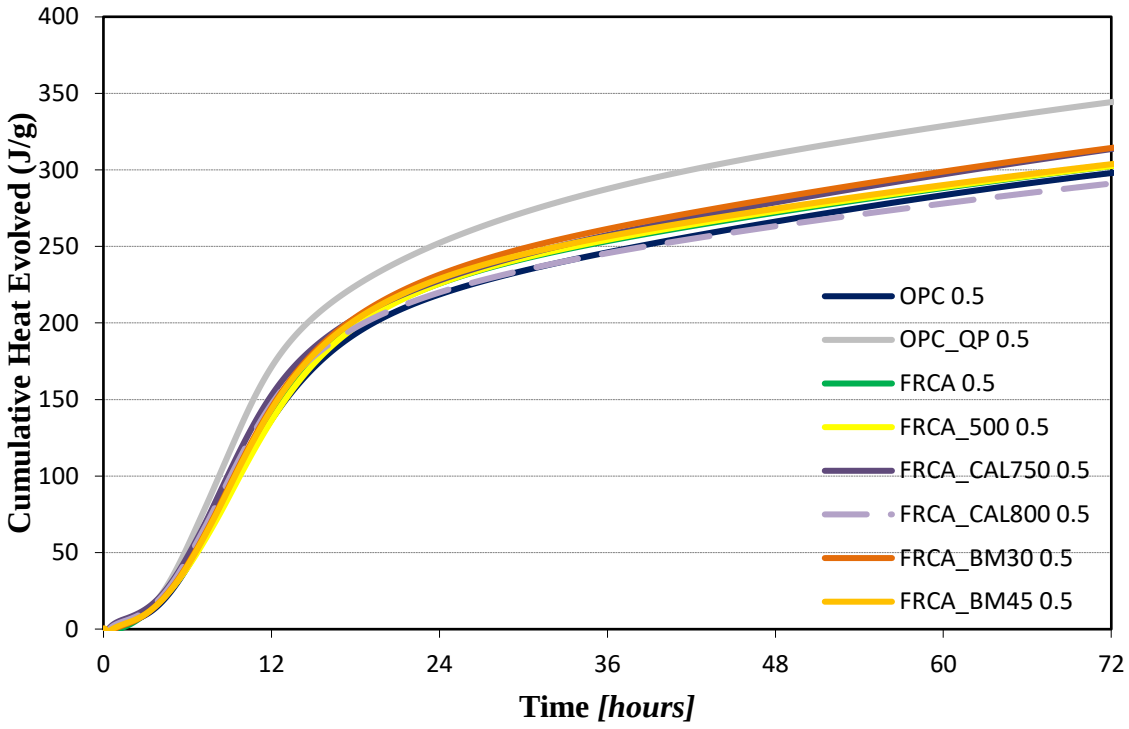

Figure 6.15: Study of FRCA verses quartz on cumulative heat evolved

Figure 6.15 shows that quartz had a greater impact overall hydration than the FRCA and the treated FRCA. Quartz powder had a finer particle size about 10 μm, which is the optimum size for fillers as found in previous literature [76]. The finer particle size in all likihood enhanced the available surface area for nucleation sites for hydrate phases [76, 82]. Table 6.3 shows the hydration kinetics of FRCA and Quartz. Equation 6.1 calculates the approximate hydration of anhydrous cement based on measured cumulative heat of hydration [77].

$$\alpha_t = \frac{Q_t}{Q_\infty} \tag{6.1}$$

The approximate hydration of anhydrous cement is α_t, Q_t is cumulative heat of hydration at time t, and Q_∞ is the cumulative heat of hydration at 100% hydration. Q_∞ is estimated based on the chemical composition of Type I/II Portland Cement and boque equations. Based on the composition of Type I/II Portland Cement, Q_∞ is approximately equal to 450 J/g of cement.

Table 6.3: Hydration kinetics by isothermal calorimetry for FRCA and quartz

Sample	**Heat Evolution (mW/ g of cement)**		**Peak of Heat Evolution Curve (hr)**		**Cumulative Heat @ 72 hr (J/ g of cement)**	**Hydration (%)**
OPC	4.65	4.71	7.73	9.25	297.92	66.2
OPC_QP	5.02	5.82	6.9	8.3	344.26	76.5
FRCA	-	4.83	-	8.6	302.45	67.2
FRCA_500	-	4.82	-	9.15	302.47	67.2
FRCA_CAL750	-	5.41	-	8.32	313.58	69.7
FRCA_CAL 800	-	5.14	-	8.33	219.1	48.7
FRCA_BM 30	-	5.19	-	8.75	310.4	69.0
FRCA_BM 45	-	5.16	-	8.82	303.7	67.5

Quartz had the largest impact on hydration kinetic by increasing hydration by 10%. The next best FRCA_CAL750, which improved hydration by 3%. Based on these results, it seems that the FRCA acted as a weak filler or SCM, although the FRCA are not inert like quartz, since it changed the calcium aluminate peak in the heat evolution curves. FRCA acts as a potential weak filler due to the large particle size when compared to cement particles. The large particle size lowers FRCA ability to attribute to nucleation site for cement particles; therefore, FRCA primarily influences the dilution effect for fillers. To

further study influences of the FRCA on cement systems, the next section explores the reactivity of the FRCA.

6.3 Reactivity

To study the reactivity of the FRCA, a basic understanding of how SCMs react with cement systems are important. The SCM are mineral-based materials that have pozzolanic, hydraulic or a combination of both pozzolanic and hydraulic reactivity. Pozzolanic reactions occur with both calcium hydroxide and water, whereas hydraulic reactions only react with water to form compounds with cementing properties, as shown in Equation 6.2 and 6.3 [85].

$$\text{Pozzolanic reaction: } \begin{matrix} SiO_2 \\ Al_2O_3 \end{matrix} + H + CH \rightarrow C\text{-}S\text{-}H \quad (6.2)$$

$$\text{Hydraulic reaction: } \begin{matrix} SiO_2 \\ Al_2O_3 \\ CaO \end{matrix} + H \rightarrow C\text{-}S\text{-}H \quad (6.3)$$

Replacing a percentage of cement with SCMs is increasingly becoming an industry standard due to the potential improvement in durability, strength, and workability in concrete structures. Attributable to the partial replacement of cement, SMCs lower the CO^2 emissions, energy consumption, and cost of concrete. There are two types of SCMs: natural and processed. Natural SCMs are produced by natural minerals, such as volcanic ash. Some natural SCMs require heat retreatment to enhance the reactivity. Processed SCMs are often byproducts of manufacturing, such as fly ash and silica fume. Fly ash is the most widely used SCM and often is used as the basis for comparison of SCMs [85]. Therefore, if the FRCA are an alternative SCM, they should either react with calcium hydroxide and/or water to produce additional C-S-H, the primary compound in cement systems.

6.3.1 Compressive Strength of Mortar Cubes

The reactivity of the FRCA was measured with both compressive strength and thermogravimetric Analysis (TGA) at 20% replacement ratio on cement mortar cubes and cement paste, respectively. The mortar cubes were mixed and casted according to ASTM C109. The compressive strength of the mortar cubes was measured at 28 and 56 days. The results of the compressive strength test are shown in Figure 6.16.

Day	Sample	OPC (ksi)	FRCA (ksi)
28	1	6.97	6.60
	2	6.71	6.84
	3	6.16	7.40
	Avg	*6.61*	*6.95*
	SI	100%	**105%**
	StdDev	0.336	0.338
56	1	7.36	8.26
	2	7.19	7.19
	3	7.03	7.49
	Avg	*7.19*	*7.65*
	SI	100%	**106%**
	StdDev	0.136	0.450

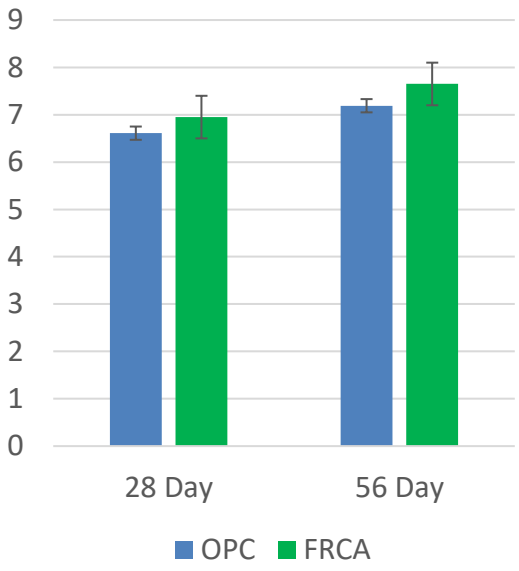

Figure 6.16: Mortar cube compressive strength at 28 and 56 day

The results showed that 5% and 6% increase in compressive strength at 28 and 56 day, respectively. The increase in strength was most likely due to filler effect as an increase particle packing and reduction of porosity due to decreased specific gravity of FRCA. Additional mortar cubes were casted of with 100% FRCA and water at w/cm ratio of 0.46. The mortar cubes exhibited little to none compressive strength and often crumbed while

handling. Therefore, it is to be assumed that FRCA has little to none hydraulic reactivity. Whether the FRCA exhibit pozzolanic reactivity was studied by performing TGA.

6.3.2 Thermogravimetric Analysis of Cement Paste

Themogravimetric analysis continuously measures changes in mass of the sample due to increasing temperature. The TGA machine has a sample pan supported on a cantilever balance that resides in a furnace that increases temperature at a constant rate. The sample environment is controlled by a purge gas of nitrogen. The mass loss is due to chemical reactions, including but not limited to combustion, dehydration, and decomposition [86]. The use of TGA for cement is often to study the cement hydration by measuring the degree of reactions [82, 87]. It also has been used to assess the bound water content and analysis effects of waste, additions, and pozzolanic materials on cement paste and mortars [82, 87]. A common range of temperatures for chemical reactions of cement paste is shown in Table 6.4 and Figure 6.17. These temperature ranges vary due to a variety of reasons, including sample preparation, testing environment, heat rate, and amount of sample.

Table 6.4: Chemical reactions in cement paste with temperature [88]

Temperature (ºC)	Chemical Reactions
30–105	The evaporable water and a part of the bound water escapes. It is generally considered that the evaporable water is completely eliminated at 120 °C
110– 170	The decomposition of gypsum (with a double endothermal reaction), the decomposition of ettringite and the loss of water from part of the carboaluminate hydrates take place
180 –300	The loss of bound water from the decomposition of the C-S-H and carboaluminate hydrates undergoes
450 –550	Dehydroxylation of the portlandite (calcium hydroxide)
700– 900	Decarbonation of calcium carbonate

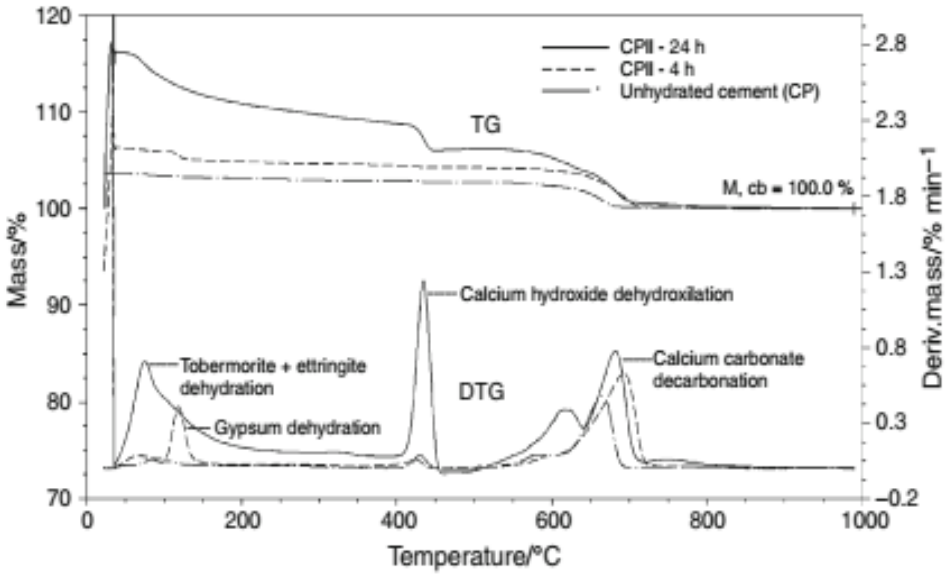

Figure 6.17: DTG/TG of unhydrated cement and hydrated cement paste [87]

The decomposition of calcium hydroxide (CH) is calculated by using the following equation proposed by Chris Shearer [82, 89].

$$CH = \frac{W_{400} - W_{470}}{W_{800}} * \frac{M[Ca(OH)_2]}{M[H_2O]} \quad (6.4)$$

In addition, carbonation was also considered. Carbonation depends on the porosity and moisture content of cement paste. Carbonation is calculated by measuring the amount of decomposition of calcium carbonate shown in Equation 6.5.

$$CaCO_3 = \frac{W_{470} - W_{750}}{W_{800}} * \frac{M[CaCO_3]}{M[CO_2]} \quad (6.5)$$

The molecular weight of $CaCO_3$ is 100 g/mol and CO_2 is 44 g/mol. Carbonation is caused by CH reacting with CO_2 in air. The estimated amount of CH consumed due to carbonation was added to the initial decomposition of CH to get to the estimated total CH available in the cement paste, as in Equation 6.6.

$$CH_{Total} = CH + CaCO_3 * \frac{M[Ca(OH)_2]}{M[CaCO_3]} \quad (6.6)$$

The CH is used to compare against the control OPC to measure the relative pozzolan reactivity of the FRCA. This is based on the pozzolan reactivity shown in Equation 6.2, therefore there is less available CH to decompose. As a result, seven specimens were selected: three controls (OPC, QP, and FRCA) and four treated FRCA (FRCA_BM30, FRCA_BM45, FRCA_CAL750, and FRCA_CAL800) based on optimum performance of hydration kinetics to calculate the total CH content based on Equation 6.6.

The cement paste samples are at constant 20% replacement of Portland cement at a w/cm ratio of 0.50. The mix design is shown in Table 6.5. The amount of each samples varied slightly due to limited availability of the FRCA fines.

Table 6.5: Mix design for TGA specimens

Material (g):	**OPC**	**FRCA**	**FRCA_ BM30**	**FRCA_ BM45**	**FRCA_ CAL 750**	**FRCA_ CAL 800**	**QP**
Cement	*50*	*40*	*40*	*32*	*28*	*40*	*40*
FRCA	-	*10*	*10*	*8*	*7*	*10*	*10*
Treatment	-	-	*BM 30 min*	*BM 45 min*	*CAL 750°C*	*CAL 750°C*	-
Quartz	-	-	-	-	-	-	*20*
Water	*25*	*25*	*25*	*20*	*17.5*	*25*	*25*

The samples were prepared in the standardized method by hand mixing cement and other binders together for 30 seconds, then adding water, hand mixing for an additional 30 seconds, followed by mixing with a hand blender on low for 1 minute and increasing the speed to medium for an additional 1 minute, scraping down the sides of the container, stirring to incorporate the material on the sides, and finally placing measured samples into a small plastic zip bag for 24 hours to cure. After the 24 hours, the specimens were removed from the bags and placed into an air-tight container to cure in a moist environment at room temperature for a designated time of 1, 7, 28, 56, 91, and 180 days. Once the designated

age was reached, a part of the cast specimens was removed and then crushed (using a hammer) into pieces with a maximum size of ¼ inch. Then, the crushed specimens were placed in isopropanol for 12 minutes to stop hydration and to minimize carbonation, followed by air drying for an additional 6 minutes to release isopropanol. Finally, the specimens were sealed in two zip bags until testing.

Prior to testing, the cement paste specimens were crushed (using mortar and pestle) into powder passing the #100 sieve. Then, a sample was weighed to 20 ± 5 mg on an open platinum pan for TGA. The pan was placed into an EXSTAR TG/DTA 7300 under a constant flow of nitrogen gas. The heating rate of the sample was 10°C/min until the temperature reached 105°C, then it was held for 45 minutes at 105°C to release free water, and then the temperature was increased at a rate of 10°C/min until the temperature reached 900°C [89]. Figures 6.18–6.20 show the results of the TGA.

To quantify the pozzolanic reactivity of the FRCA, a combination of factors was considered. The CH decomposition is usually measured just considering the portlandite phase. The basic CH decomposition is displayed in Figure 6.18.

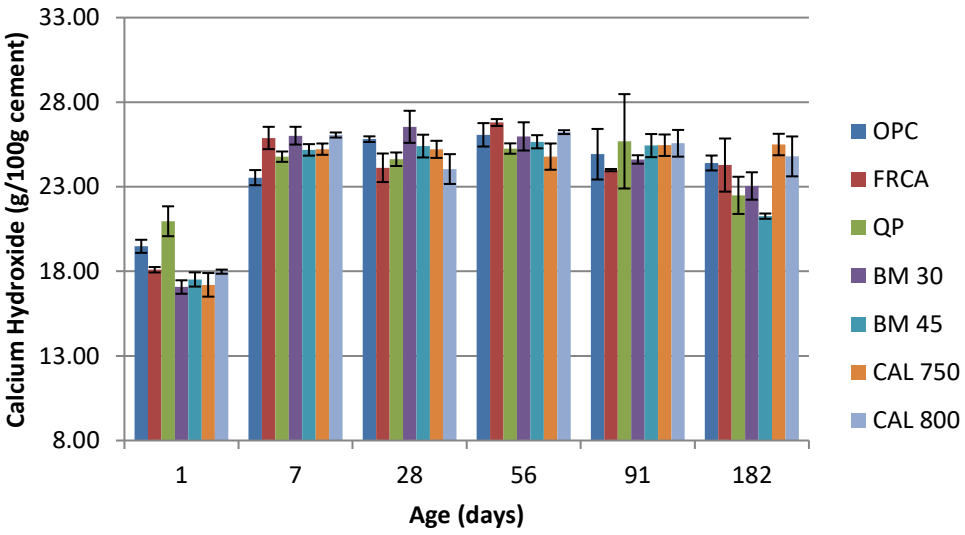

Figure 6.18: Decomposition of calcium hydroxide per cement content

In order to ignore the filler effects, the CH was plotted per percentage of cement. CH decomposition initially increased from Day 1 to Day 7 due to nucleation, then decreased, and all the FRCA showed a decreased amount of CH compared to the control, except for CAL 700 and CAL 800. Also, QP had the second lowest CH; however, this only partially describes the situation, since, as mentioned above, carbonation also decreases the amount of available free lime. Figure 6.19 shows the decomposition of calcium carbonate per cement content.

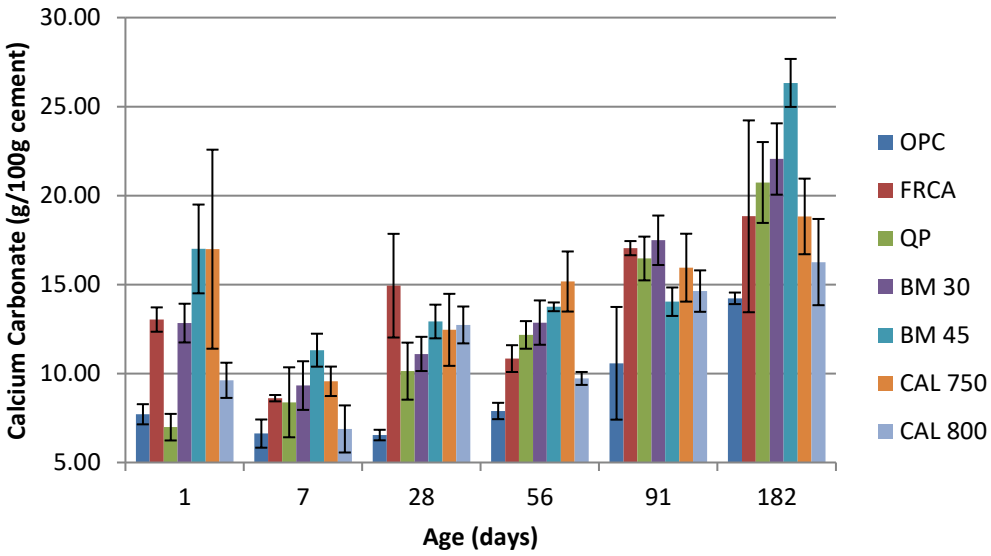

Figure 6.19: Decomposition of calcium carbonate per cement content

The calcium carbonate in general gradually increases with age, except at early and late age. The amount of carbonation was highest at 182 days for BM45, followed by BM30 and quartz. All samples were prepared using the same technique, and some of the carbonation could have been contributed to the organic solvent used to stop hydration, as well as storage times between stopping hydration and testing time. In addition, some of $CaCO_3$ decomposition perhaps also can be attributed to the material properties of the raw material. Therefore, Figure 6.20 shows the estimated available CH, including the effects of carbonation.

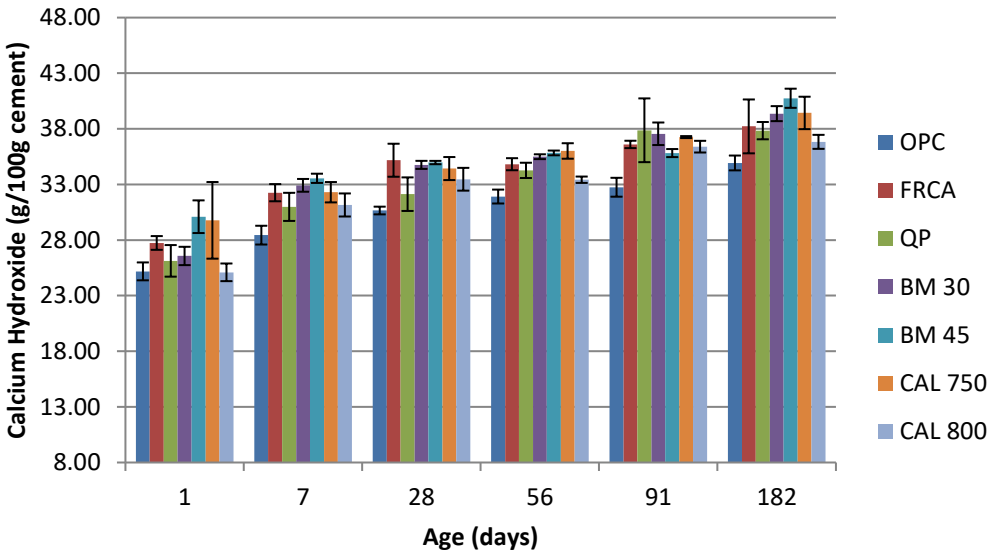

Figure 6.20: Estimate total calcium hydroxide per cement content

The estimated total available CH is based on total carbonation is due to consumption of free lime. OPC had the lowest CH. Therefore, it can be confirmed that FRCA is not SCM, as most like acts as a filler in cement systems.

CHAPTER 7. CONCLUSIONS AND RECOMMENDATIONS

This final chapter will provide main conclusions of this study, as well as recommendation to consider for use of RCA and suggestions further areas of study.

7.1 Conclusions

The focus of the study was to expand the reuse options for RCA. To accomplish this goal, the study was broken down into two main objectives: (1) the potential use of recycled coarse aggregates in structural concrete, and (2) the potential use of fines, resulting from crushing concrete coarse aggregate, as alternative supplementary cementitious material or filler.

Based on the literature review, minimum research has been done on the impacts of maximum size aggregate on mechanical performance and durability of RAC or on the use of RCA fines for partial replacement of cement. To develop a further understanding of RCA and its impacts on structural concrete, several aspects were studied, including material properties, design properties, and durability properties. Furthermore, the use of FRCA was studied by characterization, hydration kinetics, and reactivity.

7.1.1 Designed properties of RAC

The aggregates (NA and RCA) used in the study are locally available and commonly used in Atlanta, Georgia. Therefore, the assumption was that the majority of the original coarse in the RCA was the same as the NA that was tested. The primary difference between the RCA and the NA is the residual mortar. The residual mortar accounts for two ITZs in RAC;

these boundary layers are weaker zones and more porous regions in the aggregate. The residual mortar modifies the material properties of the coarse aggregate, depending on the amount of residual mortar. This RCA had residual mortar accounting for 15%–40% by weight of the RCA. As a result, the bulk density was lower for the RCA than for the NA by 7%–12%, the absorption capacity is 3–5 times greater for the RCA than for the NA, and the bulk specific gravity at SSD for the RCA is 8%–12% lower than for the NA. Due to the lower bulk density, the amount of coarse aggregate by mass in a mix of the RAC is greater than the amount in the NAC. To minimize the effect of changing the maximum size aggregate in terms of the aggregate gradation, a modified mix design was used to keep the percentages of both mortar fraction (66%) and coarse aggregate (34%) constant.

Throughout this study, the RAC was proven to provide adequate strength compared to the NAC at 100% of coarse aggregate at w/cm of 0.45.

- The compressive strength of all mixes (NAC and RAC) met the basic requirement of 5.5 ksi specified by the mix design. The difference of RAC to the NAC in compressive strength varied form 4%–20% due to variability of RAC. In addition, RAC as seen in Series 2 had greater strength gain with maturity than NAC due to potential internal curing as the slow release of additional water absorbed during mixing.
- The cracking pattern for RAC and NAC are similar, starting with small flexure cracking and developing large shear cracking that extend to top and bottom of the beam. The RAC shear short beams deflected more than the NAC and failed at lower strengths. In general, the RAC shear strength increase with a decrease of MSA,

however this trend does not hold true for NAC. The RAC shear beams have higher energy absorption than NAC.

- The flexural strength of RAC had equivalent to NAC. Flexural strength had positive correlation to compressive strength for both NAC and RAC.
- The measured static modulus of elasticity ranged from 3.11 – 4.43 x 10^6 psi. The RAC had a higher E then the NAC, potentially due to enhanced bond of RCA to cement matrix.

7.1.2 Durability

Durability was measured in terms of permeability, resistance to chloride penetration of concrete, and alkali-silica reaction. In general, RAC had comparable durability performance as NAC at 100% of coarse aggregate replacement.

- In both series, the RAC had comparable performance to the NAC in terms of charge passed for the rapid chloride penetration test. The performance level of the RAC and the NAC ranged from high to moderate permeability levels. In Series 1, the RAC had greater charge passed than NAC; however, this observation was not seen in Series 2.
- All mixes had a similar performance measured by surface resistivity. The difference between RAC and NAC in negligible. The average surface resistivity was around 10-11 kΩ-cm. Surface resistivity for these mixes had low correlation with the RCPT results with the RAC having lower correlations than the NAC. The lower correlation of the RAC could be due to the attached residual mortar, which could

be modifying the pore solution or internal porosity of the RAC. However, the results agree that surface resistivity is more conservative than the RCPT.

- In terms of ASR, samples of 50% RCA and 100% RCA were innocuous at 14 days, while the control of 100% reactive aggregate was potentially deleterious. In comparison, the 50% of RCA and 50% RA, and the control had a 60% reduction in expansion, potentially due lower w/cm ratio as a result of absorption of the mix water in the RCA.
- In all cases, the RAC had similar service life to the NAC. Therefore, the RAC can be used in all cases, although SCMs and/or lower w/cm are recommended for structures with high exposure to chlorides, similar to Case 3 and 4.

7.1.3 Recycled Concrete Fines

FRCA are a combination of residue cement paste, unhydrated cement particles, sand, and other foreign particles. The potential reactivity of FRCA in terms of alternative SCM would be attributed to the contribution of residue cement paste and unhydrated cement particles. On the other hand, filler interactions with cement hydration kinetics are dependent on both the surface area and the fineness of the material. Due to the low reactivity of the FRCA, three treatment methods were considered: reducing particle size, ball-milling, and calcining. The FRCA studied at 20% replacement of cement were studied in terms of material characterization, hydration kinetics, and reactivity.

- The median particle size for FRCA was measures as 24.4 μm and SSA of 371 m^2/kg. Furthermore, most additional treatment to the FRCA, with the exception of calcining, decreased the particle size and increased the specific surface.

- X-ray powder diffraction showed that the FRCA were a combination of quartz, calcite, plagioclase and alkali feldspar with trace amounts of other minerals. Some of the crystalline phases were amorphous. Additional treatment modified the crystalline structure of FRCA by phase transfer of quartz and plagioclase feldspar minerals, as well as deduction of calcite.
- Quartz had a greater impact overall hydration than the FRCA and treated FRCA. Based on these results, the assumption was that the FRCA acts a filler or SCMs. However, the FRCA are not inert like quartz, since they changed calcium aluminate peak.
- In mortar system, the FRCA showed an increase of compressive strength at 28 and 56-day. However, 100% FRCA had negligible strength gain. Therefore, hydraulic reaction was eliminated as potential strength gain mechanics for SCMs.
- TGA shown that cement had to lowest availability of total calcium hydroxide when considering effects of carbonation. As a result, FRCA were eliminated as alternative SCM.

Since testing has proven that FRCA acts as filler, it explains the minimum effect 15% replacement of FRCA in concrete, as seen in this study, as compared to fly ash.

- In terms of ASR, 20% replacement of Portland cement with the FRCA lower the expansion from potentially deleterious zone to the innocuous and potentially deleterious zone. The 40% reduction can be due to densifying the microstructure of the mortar bar by the filler effect and the overall lowering the w/cm ratio due to higher absorption of FRCA, and reducing the amount of available alkalis.

7.2 Recommendations for uses of Recycled Concrete Aggregate and Limitations

Based on the results of this study, this RCA manufactured from a quality and regulated manufacturer that meets local and national coarse aggregate standards can be used in structural concrete for normal weight and strength concrete applications. However, concrete producers need RCA limitations in mind including:

- RCA has high water absorption and need to account for additional water demand during mixing. Otherwise, it will alter the w/cm ratio and lower workability of concrete.
- RAC performs adequately in compressive and shear strength for high quality RCA at w/cm of 0.45. Potential lower strengths should be accounted for when designing structures controlled by either compressive and shear. If high strength is required, it is recommended to use SCMs or lower replacement percentages of RCA.
- Compared to NAC, RAC has potentially enhanced bond due to additional internal curing due to slightly higher E and flexural strength.
- In chloride-rich environments, RAC performed similarly to NAC at 0.45 w/cm. If used in aggressive environments, it is recommended to use SCMs and lower w/cm ratio.

7.3 Recommendations for Future Work

This study focused on the comparison of testing of RAC to NAC in terms of MSA; however, there are further areas that should be studied.

- This study only focused on the use of local materials; however, different types of RCA including various types of manufacturing, types natural aggregate's rocks and minerals, and shapes of RCA, should be testing to develop standards or best practices in regard to the use of RCA in structural concrete.
- Due to RCA effects on concrete, various preventative methods have been recommended, including multistep mixing procedures using SCMs and EMV. A study should compare the best methods to use based on available resources and type of RCA
- Properties of RCA are controlled by two main components: residual mortar and natural aggregate. These components affect both the inner and outer ITZ. Additional studies should look at the effect of ITZs based on the amount of residual mortar and type of RCA. As well as determine upper limits on amount on residual mortar for use in new concrete.
- In this study, there are potential signs of internal curing. Therefore, a study should quantify the amount of internal curing and the relationship of internal curing to amount of residual mortar.
- Shear strength depends on three main interactions with one of those being aggregate interlock. A future study could measure aggregate interlock of RAC, as well as the effects of residual mortar on aggregate interlock.
- FRCA acts as weak filler; however, FRCA has calcium carbonate that is attributed to residual mortar. Therefore, a study should look into the effect of FRCA in tertiary blends with other pozzolanic SCMs. The additional calcium carbonate can potentially accelerate and enhance the performance of SCMs in cement systems.

APPENDIX A. RAW DATA FOR SERIES 1

Series 1 was a combination of three duplicate batches per mix. Therefore, Table A.1 and A2 following is results for individual batches.

Table A.1: Fresh Properties of Concrete Mixes for Shear Beams

Mix	Batch	Slump	Superplasticizer Amount (oz/100 lbs of cement)	Temperature (F)	Unit Weight lb/ft^3	Average	SD
67G	1	5		73	144.7		
67G	2	6		73	146.1		
67G	3	7.5		74	144.0	144.9	0.89
67R	1	5.5		69	146.1		
67R	2	8		86	143.3		
67R	3	7		77	140.8	143.4	2.18
67R-15FRCA	1	2			144.6		
67R-15FA	1	7		80	143.1		
87G	1	8.5		68	146.4		
87G	2	8	5.57	78	142.3		
87G	3	9.5		68	144.4	144.3	1.69
87R	1	8		69	142.3		
87R	2	7.5		77	144.1		
87R	3	9		68	142.1	142.8	0.90
57G	1	7		64	149.0		
57G	2	5.75	3.89		144.7		
57G	3	4	0.971	80	141.3	145.0	3.15
57R	1	5		80	143.6		
57R	2	4.5	3.89	74	142.3		
57R	3	4		79	147.0	144.3	1.96

Table A.2: Maximum deflection and shear strength

	Δ (inch)	Vu (psi)	Δ _stdev (inch)	Vu _stdev (psi)
#67G(1)	0.41	803.6	0.16	25.23
#67G(2)	0.80	842.9		
#67G(3)	0.66	864.6		
#67G(Avg)	0.63	837.0		
#67R(1)	0.26	538.2	0.28	156.2
#67R(2)	0.93	884.2		
#67R(3)	0.54	852.5		
#67R(Avg)	0.58	758.3		
#67R-15FRCA	0.63	827.4		
#67R-15FA	0.95	846.6		
#87G(1)	0.26	810.3	0.08	67.26
#87G(2)	0.35	695.7		
#87G(3)	0.46	855.5		
#87G(Avg)	0.35	787.2		
#87R(1)	0.44	814.9	0.09	20.64
#87R(2)	0.56	851.0		
#87R(3)	0.67	863.7		
#87R(Avg)	0.56	843.2		
#57G(1)	0.34	819.9	0.12	16.84
#57G(2)	0.53	812.5		
#57G(3)	0.62	851.4		

#57G(Avg)	0.50	827.9		
#57R(1)	0.66	841.1	0.09	123.7
#57R(2)	0.43	546.5		
#57R(3)	0.51	754.8		
#57R(Avg)	0.53	714.1		

APPENDIX B. METRO GREEN RECYCLING

The following sections are the transcript of phone interview and site visit with Metro Green Recycling.

B.1 Phone Interview on February 2016

- **Is the Recycled Concrete GAB/Crusher Run only recycled concrete or is it a combination of recycled concrete and dirt?**

  Some trace of dirt, it is mainly screened out.

- **What do you do with the fines?**

  Fines go into GAB… The site doesn't produce the half inch minus anymore. All the sizes are produced at the same time.

- **What the general size of the surge?**

  Mid-stage product, only goes though one crusher. It is based on product of get a rock correy. There is no sizing or screening, size range from fist to melon size.

- **I heard you have high quality recycled aggregate, what types of crushers do you use?**

  Jaw crusher (1^{st} step), cone crusher (2^{nd} step)

- **How it be possible to set up a tour of your facilities?**

  Pleasantdale Road (main site and accepts all C&D waste), altanta site is smaller and only accepts few C&D waste. Welcome to tour both…

B.2 Site Visit in May 2016

- **What are your typical customers?**

  Their primary customers are pipeline and construction fill contractors because the RCA is 15% lighter than the NA and possesses additional compacting properties beneficial in those applications

- **What limitations on there in availability of RCA?**

  The availability is limited due to a combination of factors, including illegal dumping of debris concrete, constructors opting to use on-site crushers, and local competitors

- **What is the benefit for recycling concrete?**

  Cheaper disposal due to lower tipping cost and lower cost of per ton for aggregate. Also, get more aggregate per ton due to RCA being 15% lighter than NA

REFERENCES

1. Agency, U.S.E.P., *Advancing Sustainable Materials Management: 2014 Fact Sheet*. 2016: epa.gov.

2. Development, W.B.C.f.S., *The Cement Sustainability Initiative: Recycling Concrete*. 2009: wbcsdcement.org. p. 42.

3. Adams, M., et al., *Applicability of the Accelerated Mortar Bar Test for Alkali-Silica Reactivity of Recycled Concrete Aggregates.* 2013.

4. Grübl, P., A. Nealen, and N. Schmidt, *Concrete made from recycled aggregate: experiences from the building project Waldspirale.* Darmst Concr Annu J, 1999. **14**.

5. Poon, C.-S. and D. Chan, *The use of recycled aggregate in concrete in Hong Kong.* Resources, Conservation and Recycling, 2007. **50**(3): p. 293-305.

6. Silva, R.V., J. de Brito, and R.K. Dhir, *Properties and composition of recycled aggregates from construction and demolition waste suitable for concrete production.* Construction and Building Materials, 2014. **65**: p. 201-217.

7. Gonzalez, G. and H. Moo-Young, *Transportation applications of recycled concrete aggregate.* FHWA state of the Practice National Review, 2004.

8. Li, X., *Recycling and reuse of waste concrete in China.* Resources, Conservation and Recycling, 2008. **53**(1-2): p. 36-44.

9. McIntyre, J., Spatari, Sabrina, and MacLean, Heather L., *Energy and Greenhouse Gas Emissions Trade-offs of Recycled Concrete Aggregate Use in Nonstructural Concrete A North American Case study.* Journal of Infrastructure Systems, 2009. **15**(4): p. 361 - 370.

10. Black, M., *Site visit and Interview about Recycled Concrete*, L.S. Walker, Editor. 2016.

11. Topcu, I.B. and S. Şengel, *Properties of concretes produced with waste concrete aggregate.* Cement and concrete research, 2004. **34**(8): p. 1307-1312.

12. Kong, D., et al., *Effect and mechanism of surface-coating pozzalanics materials around aggregate on properties and ITZ microstructure of recycled aggregate concrete.* Construction and Building Materials, 2010. **24**(5): p. 701-708.

13. Padmini, A.K., K. Ramamurthy, and M.S. Mathews, *Influence of parent concrete on the properties of recycled aggregate concrete.* Construction and Building Materials, 2009. **23**(2): p. 829-836.

14. Javier Zega, C., A. Antonio Di Maio, and R. Luis Zerbino, *Influence of Natural Coarse Aggregate Type on the Transport Properties of Recycled Concrete.* Journal of Materials in Civil Engineering, 2014. **26**(6).

15. Manzi, S., C. Mazzotti, and M.C. Bignozzi, *Short and long-term behavior of structural concrete with recycled concrete aggregate.* Cement & Concrete Composites, 2013. **37**: p. 312-318.

16. McNeil, K. and T.H.-K. Kang, *Recycled concrete aggregates: A review.* International Journal of Concrete Structures and Materials, 2013. **7**(1): p. 61-69.

17. Shayan, A. and A. Xu, *Performance and properties of structural concrete made with recycled concrete aggregate.* ACI Materials Journal-American Concrete Institute, 2003. **100**(5): p. 371-380.

18. Levy, S.M. and P. Helene, *Durability of recycled aggregates concrete: a safe way to sustainable development.* Cement and concrete research, 2004. **34**(11): p. 1975-1980.

19. Rao, M.C., S. Bhattacharyya, and S. Barai, *Influence of field recycled coarse aggregate on properties of concrete.* Materials and Structures, 2011. **44**(1): p. 205-220.

20. Akbarnezhad, A., et al., *Effects of the Parent Concrete Properties and Crushing Procedure on the Properties of Coarse Recycled Concrete Aggregates.* Journal of Materials in Civil Engineering, 2013. **25**(12): p. 1795-1802.

21. Garcia-Gonzalez, J., et al., *Pre-Saturation Technique of the Recycled Aggregates: Solution to the Water Absorption Drawback in the Recycled Concrete Manufacture.* Materials, 2014. **7**(9): p. 6224-6236.

22. Ho, N.Y., et al., *Efficient utilization of recycled concrete aggregate in structural concrete.* Journal of Materials in Civil Engineering, 2013. **25**(3): p. 318-327.

23. Zhang, H. and Y. Zhao, *Integrated interface parameters of recycled aggregate concrete.* Construction and Building Materials, 2015. **101**: p. 861-877.

24. Bairagi, N., H. Vidyadhara, and K. Ravande, *Mix design procedure for recycled aggregate concrete.* Construction and Building Materials, 1990. **4**(4): p. 188-193.

25. Abbas, A., et al., *Durability of recycled aggregate concrete designed with equivalent mortar volume method.* Cement and concrete composites, 2009. **31**(8): p. 555-563.

26. Vazquez, E., et al., *Improvement of the durability of concrete with recycled aggregates in chloride exposed environment.* Construction and Building Materials, 2014. **67**: p. 61-67.

27. Knaack, A.M. and Y.C. Kurama, *Design of Concrete Mixtures with Recycled Concrete Aggregates.* Aci Materials Journal, 2013. **110**(5): p. 483-493.

28. Li, X., *Recycling and reuse of waste concrete in China.* Resources, Conservation and Recycling, 2009. **53**(3): p. 107-112.

29. Kwan, W.H., et al., *Influence of the amount of recycled coarse aggregate in concrete design and durability properties.* Construction and Building Materials, 2011.

30. Mehta, P.K.M., Paulo J. M., *Concrete: Microstructure, Properties, and Materials*. third ed. 2006: McGraw-Hill Publishing.

31. Xiao, J., et al., *Properties of interfacial transition zones in recycled aggregate concrete tested by nanoindentation.* Cement and Concrete Composites, 2013. **37**: p. 276-292.

32. Kou, S.-C., C.-S. Poon, and M. Etxeberria, *Influence of recycled aggregates on long term mechanical properties and pore size distribution of concrete.* Cement and Concrete Composites, 2011. **33**(2): p. 286-291.

33. García-González, J., et al., *Porosity and pore size distribution in recycled concrete.* Magazine of Concrete Research, 2015. **67**(22): p. 1214-1221.

34. Olorunsogo, F. and N. Padayachee, *Performance of recycled aggregate concrete monitored by durability indexes.* Cement and concrete research, 2002. **32**(2): p. 179-185.

35. Thomas, C., et al., *Durability of recycled aggregate concrete.* Construction and Building Materials, 2013. **40**: p. 1054-1065.

36. Yang, K.-H., H.-S. Chung, and A.F. Ashour, *Influence of Type and Replacement Level of Recycled Aggregates on Concrete Properties.* Aci Materials Journal, 2008. **105**(3): p. 289-296.

37. Etxeberria, M., et al., *Influence of amount of recycled coarse aggregates and production process on properties of recycled aggregate concrete.* Cement and concrete research, 2007. **37**(5): p. 735-742.

38. Xiao, J., et al., *An overview of study on recycled aggregate concrete in China (1996–2011).* Construction and Building Materials, 2012. **31**: p. 364-383.

39. Xiao, J., H. Xie, and Z. Yang, *Shear transfer across a crack in recycled aggregate concrete.* Cement and Concrete Research, 2012. **42**(5): p. 700-709.

40. Sherwood, E.G., E.C. Bentz, and M.P. Collins, *Effect of aggregate size on beam-shear strength of thick slabs.* ACI Structural Journal, 2007. **104**(2): p. 180-190.

41. Fathifazl, G., et al., *Shear capacity evaluation of steel reinforced recycled concrete (RRC) beams.* Engineering Structures, 2011. **33**(3): p. 1025-1033.

42. Domingo-Cabo, A., et al., *Creep and shrinkage of recycled aggregate concrete.* Construction and Building Materials, 2009. **23**(7): p. 2545-2553.

43. Shehata, M.H., et al., *Reactivity of reclaimed concrete aggregate produced from concrete affected by alkali–silica reaction.* Cement and Concrete Research, 2010. **40**(4): p. 575-582.

44. Debieb, F., et al., *Mechanical and durability properties of concrete using contaminated recycled aggregates.* Cement and Concrete Composites, 2010. **32**(6): p. 421-426.

45. Xiao, J., B. Lei, and C. Zhang, *On carbonation behavior of recycled aggregate concrete.* Science China Technological Sciences, 2012. **55**(9): p. 2609-2616.

46. Sagoe-Crentsil, K.K., T. Brown, and A.H. Taylor, *Performance of concrete made with commercially produced coarse recycled concrete aggregate.* Cement and concrete research, 2001. **31**(5): p. 707-712.

47. Knoeri, C., E. Sanye-Mengual, and H.-J. Althaus, *Comparative LCA of recycled and conventional concrete for structural applications.* International Journal of Life Cycle Assessment, 2013. **18**(5): p. 909-918.

48. Marinkovic, S., et al., *Comparative environmental assessment of natural and recycled aggregate concrete.* Waste Manag, 2010. **30**(11): p. 2255-64.

49. Kim, J., et al., *Evaluation of recementation reactivity of recycled concrete aggregate fines.* Transportation Research Record: Journal of the Transportation Research Board, 2014(2401): p. 44-51.

50. Florea, M., Z. Ning, and H. Brouwers, *Treatment and application of recycled concrete fines.* 2013.

51. Serpell, R. and M. Lopez, *Properties of mortars produced with reactivated cementitious materials.* Cement and Concrete Composites, 2015. **64**: p. 16-26.

52. Florea, M.V.A. and H.J.H. Brouwers, *Properties of various size fractions of crushed concrete related to process conditions and re-use.* Cement and Concrete Research, 2013. **52**: p. 11-21.

53. Black, M., *Re: Inquiry about ordering recycled concrete aggregate*, L.S. Walker, Editor. 2016.

54. *ASTM C136M-14 Standard Test Method for Sieve Analysis of Fine and Coarse Aggregates*. 2014, ASTM International: West Conshohocken, PA.

55. *ASTM C33M- 16e1 Standard Specification for Concrete Aggregates*. 2016, ASTM International: West Conshohocken, PA.

56. *ASTM C29M-16 Standard Test Method for Bulk Density ("Unit Weight") and Voids in Aggregate*. 2016, ASTM International: West Conshohocken, PA.

57. *ASTM C127-15 Standard Test Method for Relative Density (Specific Gravity) and Absorption of Coarse Aggregate*. 2015, ASTM International: West Conshohocken, PA.

58. Abbas, A., et al., *Proposed method for determining the residual mortar content of recycled concrete aggregates.* Journal of ASTM International, 2007. **5**(1): p. 1-12.

59. *211.1-91: Standard Practice for Selecting Proportions for Normal, Heavyweight, and Mass Concrete*. 2002, American Concrete Institute. p. 38.

60. *ASTM C192M-16a Standard Practice for Making and Curing Concrete Test Specimens in the Laboratory*. 2016, ASTM International: West Conshohocken, PA.

61. Association, N.R.M.C., *CIP 36-structural light weight concrete.* NRMCA, USA, 2003.

62. *ASTM C39M-16 Standard Test Method for Compressive Strength of Cylindrical Concrete Specimens*. 2016, ASTM International: West Conshohocken, PA.

63. Duan, Z.H. and C.S. Poon, *Properties of recycled aggregate concrete made with recycled aggregates with different amounts of old adhered mortars.* Materials & Design, 2014. **58**: p. 19-29.

64. *ASTM C469M-14 Standard Test Method for Static Modulus of Elasticity and Poisson's Ratio of Concrete in Compression*. 2014, ASTM International: West Conshohocken, PA.

65. *318-14: Building Code Requirements for Structural Concrete and Commentary*. 2011, American Concrete Institute.

66. *363R-10: Report on High-Strength Concrete*. 2010, American Concrete Institute. p. 65.

67. *ASTM C78M-16 Standard Test Method for Flexural Strength of Concrete (Using Simple Beam with Third-Point Loading)*. 2016, ASTM International: West Conshohocken, PA.

68. *ASTM C1202-12 Standard Test Method for Electrical Indication of Concrete's Ability to Resist Chloride Ion Penetration*. 2012, ASTM International: West Conshohocken, PA.

69. Nadelman, E.I. and K.E. Kurtis, *A resistivity-based approach to optimizing concrete performance.* Concrete international, 2014. **36**(5): p. 50-54.

70. AASHTO, T., *95-11 "Standard Method of Test for Surface Resistivity Indication of Concrete's Ability to Resist Chloride Ion Penetration.".* AASHTO Provisional Standards, 2011 Edition, 2011.

71. Thomas, M.D., et al., *The Use of Lithium to Prevent or Mitigate Alkali-Silica Reactions in Concrete Pavements and Structures*. 2007.

72. *ASTM C1260-14 Standard Test Method for Potential Alkali Reactivity of Aggregates (Mortar-Bar Method)*. 2014, ASTM International: West Conshohocken, PA.

73. *ASTM C1293-08b(2015) Standard Test Method for Determination of Length Change of Concrete Due to Alkali-Silica Reaction*. 2015, ASTM International: West Conshohocken, PA.

74. Delobel, F., et al., *Application of ASR tests to recycled concrete aggregates: Influence of water absorption.* Construction and Building Materials, 2016. **124**: p. 714-721.

75. Bentz, E.C. and M.D.A. Thomas, *Life-365 Service Life Prediction Model and Computer Program for Predicting the Service Life and Life-Cycle Cost of Reinforced Concrete Exposed to Chlorides*. 2014, Life-365 Consortium III.

76. Nadelman, E.I., *Hydration and Microstructural Development of Portland Limestone Cement-Based Materials*, in *School of Civil and Environmental Engineering*. 2016, Georgia Institute of Technology. p. 355.

77. Lawrence, P., M. Cyr, and E. Ringot, *Mineral admixtures in mortars: effect of inert materials on short-term hydration.* Cement and concrete research, 2003. **33**(12): p. 1939-1947.

78. Oey, T., et al., *The filler effect: the influence of filler content and surface area on cementitious reaction rates.* Journal of the American Ceramic Society, 2013. **96**(6): p. 1978-1990.

79. Sun, H., et al., *Jet mill grinding of portland cement, limestone, and fly ash: Impact on particle size, hydration rate, and strength.* Cement and Concrete Composites, 2013. **44**: p. 41-49.

80. Sabir, B., S. Wild, and J. Bai, *Metakaolin and calcined clays as pozzolans for concrete: a review.* Cement and concrete composites, 2001. **23**(6): p. 441-454.

81. Limbachiya, M.C., E. Marrocchino, and A. Koulouris, *Chemical-mineralogical characterisation of coarse recycled concrete aggregate.* Waste Manag, 2007. **27**(2): p. 201-8.

82. Scrivener, K., R. Snellings, and B. Lothenbach, *A practical guide to microstructural analysis of cementitious materials*. 2016: Crc Press.

83. *ASTM C1679-17 Standard Practice for Measuring Hydration Kinetics of Hydraulic Cementitious Mixtures Using Isothermal Calorimetry*. 2017, ASTM International: West Conshohocken, PA.

84. *ASTM C1702-17 Standard Test Method for Measurement of Heat of Hydration of Hydraulic Cementitious Materials Using Isothermal Conduction Calorimetry*. 2017, ASTM International: West Coshohocken, PA.

85. Kurtis, K., *Supplementary Cementing Materials*. 2015.

86. Borrachero, M.V., et al., *The use of thermogravimetric analysis technique for the characterization of construction materials.* Journal of Thermal Analysis and Calorimetry, 2008. **91**(2): p. 503-509.

87. Dweck, J., et al., *Importance of quantitative thermogravimetry on initial cement mass basis to evaluate the hydration of cement pastes and mortars.* Journal of Thermal Analysis and Calorimetry, 2013. **113**(3): p. 1481-1490.

88. Alarcon-Ruiz, L., et al., *The use of thermal analysis in assessing the effect of temperature on a cement paste.* Cement and Concrete Research, 2005. **35**(3): p. 609-613.

89. Shearer, C.R., *The productive reuse of coal, biomass and co-fired fly ash*. 2014, Georgia Institute of Technology.